In compliance with the
Canadian Privacy Legislation
some supporting forms
may have been removed from
this dissertation.

While these forms may be included
in the document page count,
their removal does not represent
any loss of content from the dissertation.

University of Alberta

Late Quaternary Glaciation, Relative Sea Level History and Recent Coastal Submergence of Northeast Melville Island, Nunavut

By

Michelle A. Hanson

A thesis submitted to the Faculty of Graduate Studies and Research in partial fulfillment of the requirements of Master of Science

Department of Earth and Atmospheric Sciences

Edmonton, Alberta
Fall 2003

National Library
of Canada

Acquisitions and
Bibliographic Services

395 Wellington Street
Ottawa ON K1A 0N4
Canada

Bibliothèque nationale
du Canada

Acquisisitons et
services bibliographiques

395, rue Wellington
Ottawa ON K1A 0N4
Canada

Your file Votre référence
ISBN: 0-612-87775-2
Our file Notre référence
ISBN: 0-612-87775-2

The author has granted a non-exclusive licence allowing the National Library of Canada to reproduce, loan, distribute or sell copies of this thesis in microform, paper or electronic formats.

The author retains ownership of the copyright in this thesis. Neither the thesis nor substantial extracts from it may be printed or otherwise reproduced without the author's permission.

L'auteur a accordé une licence non exclusive permettant à la Bibliothèque nationale du Canada de reproduire, prêter, distribuer ou vendre des copies de cette thèse sous la forme de microfiche/film, de reproduction sur papier ou sur format électronique.

L'auteur conserve la propriété du droit d'auteur qui protège cette thèse. Ni la thèse ni des extraits substantiels de celle-ci ne doivent être imprimés ou aturement reproduits sans son autorisation.

Canada

University of Alberta

Library Release Form

Name of Author: Michelle A. Hanson

Title of Thesis: Late Quaternary Glaciation, Relative Sea Level History and Recent Coastal Submergence of Northeast Melville Island, Nunavut

Degree: Master of Science

Year this Degree Granted: 2003

Permission is hereby granted to the University of Alberta Library to reproduce single copies of this thesis and to lend or sell such copies for private, scholarly or scientific research purposes only.

The author reserves all other publication and other rights in association with the copyright in the thesis, and except as herein before provided, neither the thesis nor any substantial portion thereof may be printed or otherwise reproduced in any material form whatever without the author's prior written permission.

Date: 16/06/2003

University of Alberta

Faculty of Graduate Studies and Research

The undersigned certify that they have read, and recommend to the Faculty of Graduate Studies and Research for acceptance, a thesis entitled "Late Quaternary Glaciation, Relative Sea Level History and Recent Coastal Submergence of Northeast Melville Island, Nunavut" submitted by Michelle A. Hanson in partial fulfillment of the requirements for the degree of Master of Science.

Date: 06/06/2003

Abstract

Melville Island is pivotal to the late Quaternary history of Arctic Canada, occupying the junction of three former ice masses: the NW Laurentide Ice Sheet, the SW Innuitian Ice Sheet, and local, island-based ice caps. The distribution of glacial and deglacial landforms mapped across NE Melville Island indicates that the area was occupied solely by local ice caps that coalesced during the last glaciation and advanced seaward of modern coastlines. Thirty-eight samples (predominantly molluscs) were collected from raised marine deposits and radiocarbon-dated. Glaciers retreated radially into the island's interior between 10.5 and 10.0 ka BP, when marine limit stood at 42 to 65 m asl. Three relative sea level curves display half-lives ranging from 1.5 to 2.1 ka. Together with postglacial isobases drawn on the 8.5 ka BP shoreline, these curves show progressively greater emergence to the ESE across the study area. This is attributed to a transition zone between the glacioisostatic unloading of the Laurentide and Innuitian ice sheets. Late Holocene submergence is a significant and ongoing characteristic of the western part of the study area. It is considered to record the ESE migration of a crustal forebulge across the western archipelago that has now reached E. Melville Island.

Acknowledgements

For initially introducing me to fieldwork in the Canadian Arctic, I thank Dr. Janis Dale, University of Regina. For providing me with a continuing opportunity to work in this milieu, I am grateful to my supervisor, Dr. John England. Thank you to John as well for good humour, endless pond-hockey games, thorough discussions, multiple rereads, and meticulous edits of my thesis. Thank you also goes to Dr. Patrick Lajeunesse for providing guidance during the field season, as well as good company, and for subsequently answering a never-ending stream of questions. Thank you as well to Nigel Atkinson for answering many last minute questions. Finally, thank you to the committee members, Drs. Catuneanu and Le Blanc for their valuable comments.

Financial support for this thesis was provided by the Natural Sciences and Engineering Research Council of Canada (NSERC; PGS A Scholarship to myself, and Grant #A6608 to J. England), the Canadian Circumpolar Institute (CBAR grant to P. Lajeunesse), and the University of Alberta (Harington Paleoenvironmental Scholarship, Walter H. Johns Graduate Fellowship, and University of Alberta Entrance Scholarship). Logistical support in the field was provided by the Polar Continental Shelf Project in Resolute Bay, Nunavut.

Table of Contents

Chapter	Page
1. INTRODUCTION AND RATIONALE	1
1.1 INTRODUCTION	1
1.2 GEOLOGY	1
1.3 PHYSIOGRAPHY AND FIELD SITES	3
1.4 CLIMATE	4
1.5 PREVIOUS RESEARCH	5
1.5.1 Glaciation	5
1.5.1.1 Laurentide Ice Sheet	5
1.5.1.2 Innuitian Ice Sheet	7
1.5.1.3 Local Melville Island Ice	8
1.5.2 Regional Deglaciation and Postglacial Emergence	9
1.5.2.1 Deglaciation	9
1.5.2.2 Postglacial Emergence	10
1.6 RATIONALE FOR STUDY	12
1.7 RESEARCH OBJECTIVES	12
2. METHODS	25
2.1 INTRODUCTION	25
2.2 RESEARCH METHODS	25
2.2.1 Surficial Geological Mapping	25
2.2.2 Establishing the Elevation and Age of Former Relative Sea Levels	27
3. LATE QUATERNARY ICE COVERAGE, DEGLACIATION AND RELATIVE SEA LEVEL HISTORY	32
3.1 INTRODUCTION	32
3.2 SURFICIAL MAPPING	32
3.2.1 Rock, Weathered Rock and Associated Landforms	32
3.2.2 Till and Associated Landforms	33
3.2.3 Raised Marine Sediments and Associated Landforms	34
3.2.4 Alluvium	36
3.2.5 Colluvium	37
3.3 ICE COVERAGE AND DEGLACIATION	37
3.3.1 Style	37
3.3.2 Elevation and Age of Marine Limit	40
3.4 RELATIVE SEA LEVEL HISTORY	43

3.4.1 S. Sabine Bay 44
3.4.2 E. Sabine Bay 45
3.4.3 Eldridge Bay 45
3.4.4 Sherard Bay 46

4. DISCUSSION, REGIONAL SYNTHESIS AND FUTURE RESEARCH 74

4.1 INTRODUCTION 74
4.2 DISCUSSION 74
4.2.1 Late Quaternary Ice Coverage 74
4.2.2 Deglaciation and the Profile of Marine Limit 76
4.2.3 Age of Marine Limit and Relative Sea Level Curves 79
4.2.3.1 S. Sabine Bay 81
4.2.3.2 E. Sabine Bay 82
4.2.3.3 Eldridge Bay 83
4.2.3.4 Synthesis 83
4.2.4 Isobases 86
4.3 REGIONAL IMPLICATIONS AND FUTURE RESEARCH 87
4.3.1 Last Glaciation 87
4.3.2 Deglaciation 87
4.3.3 Postglacial Emergence and Submergence 89
4.3.4 Conclusions and Future Research 90

REFERENCES 100

List of Tables

Table		Page
3.1	Radiocarbon dates associated with marine limit, NE Melville Island	64
3.2	Holocene radiocarbon dates, S. Sabine Bay	66
3.3	Holocene radiocarbon dates, E. Sabine Bay	69
3.4	Holocene radiocarbon dates, Eldridge Bay	71
3.5	Holocene radiocarbon date, Sherard Bay	73
4.1	Equations, emergence rates, and half-lives of RSL curves	96

List of Figures

Figures		Page
1.1a	Location map for Queen Elizabeth Islands	15
1.1b	Location map for Melville Island	16
1.2	Innuitian, Greenland, and Laurentide ice sheet coverage of the QEI	17
1.3a	Geological map of Melville Island	18
1.3b	Landsat 7 image of NE Melville Island	19
1.4	Geomorphic regions of the Canadian Arctic Archipelago	20
1.5	Field areas, NE Melville Island	21
1.6	Laurentide tills, central Melville Island	22
1.7	Last glaciation ice configuration, western Melville Island	23
1.8	Previously surveyed marine limits, Melville Island	24
2.1	Meltwater channels, E. Sabine Bay	31
3.1a	Distribution of surficial sediments and landforms, Sabine Bay	48
3.1b	Distribution of surficial sediments and landforms, central Sabine Peninsula	49
3.1c	Distribution of surficial sediments and landforms, northern Sabine Peninsula	50
3.2	Bedrock formations of NE Melville Island	51
3.3	Periglacial stripes in weathered Hecla Bay Fm	52
3.4	Morainal bank, proglacial meltwater channel, and ice-fed delta, E. Sabine Bay	53
3.5	Dissected delta, S. Sabine Bay	54
3.6	Telescoping finger delta, Chads Point, western Sabine Peninsula	55
3.7	Modern sandur, E. Sabine Bay	56
3.8	Gelifluction lobes on exposed Weatherall Fm	57
3.9	Mega-flutings, NW Sabine Peninsula	58
3.10	Proglacial meltwater channel, E. Sabine Bay	59
3.11	Sandstone erratics on morainal bank, E. Sabine Bay	60
3.12	Littoral fill, S. Sabine Bay	61
3.13	Ice-fed marine limit delta, E. Sabine Bay	62
3.14	Marine limits and associated radiocarbon-dated samples, NE Melville Island	63
3.15	Radiocarbon-dated samples, S. Sabine Bay	67
3.16	Erosion microcliff, S. Sabine Bay	68
3.17	Radiocarbon-dated samples, E. Sabine Bay	70
3.18	Radiocarbon-dated samples, Eldridge Bay	72
4.1	Previous and new marine limits, NE Melville Island	92
4.2	Relative sea level curve, S. Sabine Bay	93

4.3	Relative sea level curve, E. Sabine Bay	94
4.4	Relative sea level curve, Eldridge Bay	95
4.5	Three relative sea level curves, NE Melville Island	97
4.6	Three relative sea level curves and previously published curves	98
4.7	Isobases drawn on the 8.5 ka BP shoreline, NE Melville Island	99

CHAPTER 1: INTRODUCTION AND RATIONALE

1.1 INTRODUCTION

Quaternary research in the Canadian High Arctic has made rapid progress during the past decade concerning the extent and style of the last glaciation and its associated sea level adjustments. Most significantly, a consensus now favours coverage of the Queen Elizabeth Islands (QEI; Figure 1.1a) by the Innuitian Ice Sheet (IIS; Blake 1970, 1972) during the Late Wisconsinan (Figure 1.2; Bednarski 1998; Dyke 1998, 1999; England 1998, 1999; Ó Cofaigh 1999; Ó Cofaigh *et al.* 2000; Lamoureux & England 2000; EPILOG, Dyke *et al.* 2002). As originally proposed by Blake (1970), the IIS coalesced with the Greenland Ice Sheet to the east and the Laurentide Ice Sheet (LIS) to the south (Dyke *et al.* 2002). The geological evidence now accords with reconstructions based on a variety of models presented by Mayewski *et al.* (1981), Reeh (1984), Tushingham and Peltier (1991), Peltier (1994), Bishof and Darby (1999), and Marshall and Clarke (1999).

Despite this progress on the understanding of the IIS, its geometry and extent across the western part of the Canadian Arctic Archipelago remains undocumented. Consequently, fieldwork for this thesis is principally concerned with clarifying the style of the last glaciation and the chronology of Holocene sea level change on northeast Melville Island in the western Canadian Arctic (Figures 1.1a & b). This is an important area for Quaternary research as it is situated between the presently known limits of the northwestern LIS and the western extent of the IIS, whereas local ice caps on uplands of western Melville Island suggest the possibility of a third source of ice buildup in the past. This chapter presents the characteristics of the study area, an overview of both regional and local research, and presents the objectives of the thesis in this context.

1.2 GEOLOGY

The Franklinian mobile belt constitutes the oldest bedrock in the study area, surrounding the southern part of Hecla and Griper Bay (Figure 1.3a). It is composed of clastic sediments of Paleozoic age (Ordovician, Silurian, Devonian, and Pennsylvanian;

Tozer & Thorsteinsson 1964) and is characterised by shelf marginal and basinal sediments (sandstone, siltstone, and shale; Harrison 1993, 1994). These rocks were tightly folded by the mid to late Paleozoic Ellesmerian Orogeny and exhibit a prominent WNW-ESE structural trend (Figure 1.3b; Hodgson *et al.* 1984).

Lying unconformably over the Franklinian mobile belt, and occupying the majority of Sabine Peninsula, are the clastic sediments of the Sverdrup Basin (Figure 1.3a). The Sverdrup Basin is characterised by an alternating series of non-marine and marine sandstone, siltstone and shale ranging in age from Middle Pennsylvanian to early Tertiary (Tozer & Thorsteinsson 1964). The Sverdrup Basin was deformed during the Eurekan Deformation (late Cretaceous to early Tertiary) into shallow folds, which culminated in thrust-faulting during the mid-Tertiary (Thorsteinsson & Tozer 1964; Kerr 1981). Sands characterise the margin of the former basin, which outcrops near southern Sabine Peninsula, whereas shales and siltstones correspond to the axial part of the basin, which runs across the northern tip of the peninsula (Figure 1.3a; Tozer & Thorsteinsson 1964). Here, two circular piercement domes, the Barrow and Cape Colquhoun domes (Figure 1.3a), are characteristic of the axis of the Sverdrup Basin. These domes are composed of Pennsylvanian or Permian gypsum and anhydrite, with lesser limestone and gabbroic intrusive rock (Tozer & Thorsteinsson 1964; Harrison 1995). Both domes form conspicuous physiographic features on Sabine Peninsula, rising to $\geq$ 200 m above sea level (asl).

On southern Melville Island, isolated patches of unlithified gravel, sand, and some silt, commonly containing uncompressed wood fragments and logs, overlie the Franklinian mobile belt (Craig & Fyles 1960; Fyles 1965). Lithologically, these sediments are composed of sandstone, quartzite, chert and resistant fine clastic rocks (Fyles 1990). These deposits represent the remnants of a thin fluvial cover that may be as old as late Tertiary (Hodgson *et al.* 1984). These sediments are commonly attributed to the Beaufort Formation, which was deposited across the archipelago by braided streams en route to the Arctic Ocean prior to the regional block faulting that terminated this drainage system (Craig & Fyles 1960; Fyles 1965; Kerr 1981; England 1987; Fyles 1990; Dyke *et al.* 1992).

The abrupt boundary between the Franklinian mobile belt and the Sverdrup Basin occurs within the study area and juxtaposes two regional geological provinces. The advantage of this is that the advance of former ice sheets from the south (either of Laurentide or local origin) or the advance of former ice sheets from the north (either of Innuitian or local origin) would serve to transport easily recognizable erratics from one geological province to the other. Furthermore, any advance of Laurentide ice from the south would have carried conspicuous Precambrian igneous erratics from Victoria Island or mainland Canada. Thus, the geology of the study area favours the mapping of past ice sheet activity.

In Byam Martin Channel, off the eastern coast of Sabine Peninsula, a swarm of earthquake epicentres (extending from Weatherall Bay, north-northeast to Lougheed Island) runs roughly parallel to the trend of diapiric structures and dykes extending from northern Sabine Peninsula to the northeast (Basham *et al.* 1977; Hasegawa 1977; Harrison 1995). Recorded earthquakes since the 1960s have all registered < 5.7 on the Richter scale, with the majority registering < 5.1 (Basham *et al.* 1977; Hasegawa 1977).

1.3 PHYSIOGRAPHY AND FIELD SITES

According to the classification of Dawes and Christie (1991), the study area falls within two geomorphic regions: Parry Upland, which extends across the majority of southern Melville Island (southern part of Hecla and Griper Bay); and Sverdrup Lowland, which encompasses most of Sabine Peninsula (Figure 1.4). Parry Upland consists of undulating topography and subdued ridges of low to moderate elevation (< 600 m asl) in which strong fold trends of the deformed lower Paleozoic strata are evident (Dawes & Christie 1991). Sverdrup Lowland forms a shallow topographic basin in the western Queen Elizabeth Islands, north and west of Parry Upland. It is a low-lying region (< 200 m asl) of irregular hills and scarps in which dissected gypsum domes form distinctive landmarks (Dawes & Christie 1991).

Three field areas were investigated and these are discussed in the order of their occupation. Progressing from south to north, these are: S. Sabine Bay; E. Sabine Bay; and Eldridge Bay (Figure 1.5). Areas farther afield were visited via helicopter and

included: St. Arnaud Hills, Weatherall Bay, Drake Point, and northwest Sabine Peninsula (Figure 1.5). The first two field areas (S. & E. Sabine Bay), and Weatherall Bay, fall within Parry Upland, whereas the third field area (Eldridge Bay), and the three remaining sites visited by helicopter, are situated within Sverdrup Lowland.

The S. Sabine Bay field area occupies approximately 375 km^2, and extends eastward from Nias Point (Northwest Territories; Figure 1.5) to Sabine River (Nunavut), which flows into the southeast corner of Sabine Bay. Collectively, this field area is incised by many small rivers flowing north into Sabine Bay, and consists mostly of low coastal plains of raised marine sediment abutting undulating terrain of Parry Upland. The E. Sabine Bay field area occupies approximately 270 km^2, and is crossed by two prominent ridges (> 200 m asl) and intervening parallel valleys trending NW-SE (Figure 1.5). This field area is bordered to the south by Sabine River and to the north by the St. Arnaud Hills (~ 160 m asl). The coastline consists of low plains of unconsolidated marine sediment, which, in their lower elevation (< 20 m asl), are dominated by a large outwash plain (sandur) fed by several braided streams. The Eldridge Bay field area occupies approximately 120 km^2, and includes the low isthmus (< 80 m asl) between Eldridge Bay to the west and Sherard Bay to the east (Figure 1.5). Many streams flow across the terrain into both bays, with a rather prominent stream flowing into Sherard Bay. This part of the field area is bordered to the south by the St. Arnaud Hills, whereas, to the north, Sabine Peninsula consists of plateaux and south- and southeast-facing cuestas. Offshore, in Sabine Bay, water depth is less than 200 m, whereas water depth in the centre of Hecla and Griper Bay is less than 500 m (Perry *et al.* 1987; Harrison 1995).

1.4 CLIMATE

Northeastern Melville Island is classified as a polar desert and falls into Maxwell's sub-region Ia: Western Parry Channel (Maxwell 1981). The mean January temperature ranges between - 35 and - 33°C, whereas the mean July temperature ranges between + 3 and + 5°C (Maxwell 1981). Annual precipitation ranges between 100 and 125 mm per year, with 35 – 40 % falling as rain (Maxwell 1981). In the summer, mean airflow favours excursions of cold air masses from the central Arctic Ocean into the

Queen Elizabeth Islands (from north to south across NE Melville Island; Bryson & Hare 1974; Maxwell 1981; Edlund & Alt 1989). There is no major relief to produce orographic uplift, affecting local climate (Maxwell 1981). As well, the sea-ice surrounding this part of the island favours climatic stability, as it is predominantly multi-year fast ice (Maxwell 1981). This persistent sea-ice cover reduces the maritime effect of the cold polar sea on the atmosphere, resulting in a relatively high mean annual temperature range of ~ 40°C (Maxwell 1981). Extensive meltwater on the surface of the sea-ice during the summer months contributes to the presence of frequent low stratus and stratocumulus clouds with mean cloud cover in July reaching ~ 80 % (Edlund & Alt 1989). The terrain within the field area is currently unglaciated as the highest land (< 300 m asl) falls well below the regional snowline of 500 - 600 m asl (Edlund 1985). However, four small ice caps occur on western Melville Island, ~ 120 km west Nias Point (Figure 1.1b).

1.5 PREVIOUS RESEARCH

1.5.1 Glaciation

There are three possible sources of ice that could have occupied all or part of NE Melville Island during the Last Glacial Maximum (LGM; 18 ka BP (thousand years before present)): the Laurentide Ice Sheet from the south, the Innuitian Ice Sheet from the northeast, and local island-based ice caps from the island's interior.

1.5.1.1 Laurentide Ice Sheet

Small patches of till on Sabine Peninsula composed of material from the Franklinian mobile belt, and sparse igneous erratics in the uplands of western Melville Island, as well as granite erratics of unknown provenance and age of emplacement on Prince Patrick Island to the northwest (Figure 1.1a) are all possible evidence of an early Pleistocene continental glaciation from mainland Canada that covered most of Melville Island (Tozer & Thorsteinsson 1964; Hodgson 1990). On southern Melville Island, Laurentide ice occupied Dundas Peninsula on at least three occasions, depositing three separate till sheets (Figure 1.6; Hodgson *et al.* 1984; Vincent 1984). The oldest known

ice advance to cross Viscount Melville Sound deposited Dundas Till and a belt of kame-like hills, ~ 20 km inland of the coast on central Dundas Peninsula (Hodgson *et al.* 1984; Vincent 1984). The absolute age of Dundas Till is unknown. However, the ice that deposited it extended to at least 300 m asl (Hodgson *et al.* 1984). Subsequently, ice of undetermined age flowed into Liddon Gulf (to the north of Dundas Peninsula) from M'Clure Strait depositing Liddon Till (Figure 1.6; Vincent 1984; Hodgson *et al.* 1984; Hodgson 1992). The upper elevation (< 100 m asl) and coastal distribution (across a distance of 30 km and extending 5 - 10 km inland of the modern shore) suggest that Liddon Till is the product of an ice shelf (Hodgson & Vincent 1984; Hodgson *et al.* 1984; Hodgson 1992). Liddon Till has a similar composition to Bolduc Till, which occurs at a comparable elevation on southern Dundas Peninsula, and to till deposited to the west at Bailey Point, and thus the three tills may be coeval (Vincent 1984; Hodgson *et al.* 1984; Hodgson 1992). If so, this would indicate that Laurentide ice wrapped around southern Dundas Peninsula while it occupied Viscount Melville Sound (Figure 1.6; Hodgson *et al.* 1984).

During the Late Wisconsinan, Laurentide ice again occupied low coastal elevations (< 120 m asl), as the Viscount Melville Sound Ice Shelf impinged upon the southeast flank of Dundas Peninsula, depositing Winter Harbour Till (Figure 1.6; Fyles 1967; Hodgson & Vincent 1984; Hodgson *et al.* 1984). Whether the earlier Liddon and Buldoc tills that lie distal to Winter Harbour Till are also Late Wisconsinan is undetermined. The absolute chronology of these events still remains to be clarified. Winter Harbour Till has been correlated with till on Byam Martin Island to the east and with ice thrust sediments and till on Banks and Victoria islands, respectively, to the south (Figure 1.1a; Hodgson & Vincent 1984; Vincent 1984). Hodgson and Vincent (1984) bracketed deposition of Winter Harbour Till between 10.3 and 9.6 ka BP. This was based on a date of 10.3 ka BP obtained on shells in marine sediments distal to Winter Harbour Till (assumed to pre-date the arrival of the Viscount Melville Sound Ice Shelf) and a date of 9.6 ka BP on Holocene marine limit (~ 35 m asl) on the proximal side of Winter Harbour Till (providing a minimum age for ice retreat; Hodgson & Vincent 1984). This chronology was subsequently contradicted by deglacial dates of 11.0 and 10.5 ka BP on shells and whalebone collected on Prince of Wales Island (Figure 1.1a), approximately

400 km up-ice (to the southeast) of Dundas Peninsula (Dyke 1987). The dates from Prince of Wales Island require that Laurentide ice had already retreated to that area by 11.0 ka BP (Dyke 1987). This information, along with a date of 11.3 ka BP on shells that stratigraphically underlie Winter Harbour Till (Hodgson & Vincent 1984), prompted Dyke (1987) to conclude that the Viscount Melville Sound Ice Shelf advanced and retreated from Melville Island between 11.3 and 11.0 ka BP (~ 1000 years earlier than the Hodgson *et al.* reconstruction). In the southern part of Byam Martin Channel (Figure 1.1a), east of Melville Island, glacial drift (5 - 50 m thick), deposited by a formerly grounded ice sheet, is recorded in seismic records (MacLean *et al.* 1989). It is presumed to be of Holocene age due to its thin cover (1 - 3 m) of marine sediments (MacLean *et al.* 1989). Evidence of a Late Wisconsinan glaciation beyond the till noted on southern Melville Island, and the glacial drift in Byam Martin Channel, has not been documented.

1.5.1.2 Innuitian Ice Sheet

The southwest margin of the IIS constitutes a second possible source of ice on NE Melville Island. The hypothesis that the QEI were completely occupied by the IIS during the LGM was first proposed by Blake (1970, 1972). During the past five years, the configuration and geometry of the IIS has been increasingly clarified in the eastern QEI (Bednarski 1998; England 1998, 1999; Dyke 1998, 1999; Ó Cofaigh 1999; Ó Cofaigh *et al.* 2000). The IIS consisted of both an alpine sector in the highlands of Axel Heiberg and Ellesmere islands, and a lowland sector in the central Arctic, principally north and west of Devon Island (Figure 1.1a). The thickest part of the IIS in the alpine sector coincided with the infilling of Eureka Sound from encircling highland ice divides (Figure 1.1a; England & Ó Cofaigh 1998; Ó Cofaigh 1999). Towards the south end of Eureka Sound, granite erratic trains indicate that the dispersal centre of the IIS was in the highlands of eastern Ellesmere Island, probably in the vicinity of the present-day Prince of Wales Icefield, which overlies the Precambrian Shield (Figure 1.1a; Bell 1992; England 1999; Ó Cofaigh 1999; Ó Cofaigh *et al.* 2000; England *et al.* 2000). Southward of Eureka Sound, the IIS extended across the lowlands of the central Arctic Archipelago where an ice divide, oriented east-west, occupied the marine channel north of Grinnell Peninsula, Devon Island (Figure 1.1a). Erratic dispersal trains and striae indicate that ice

flowed northward from this divide across Cornwall Island and through Massey Sound (Lamoureux & England 2000; Atkinson 2003), whereas striae and flutings suggests that ice flowed southward through Wellington Channel, west of Devon Island (Figure 1.1a; Dyke 1998, 1999). This ice divide extended an unknown distance to the west, in the direction of Melville Island (Dyke 1999). Thus, the southwestern limit of the IIS remains unknown, and previous research has not reported evidence for non-local ice reaching NE Melville Island (Henoch 1964; Tozer & Thorsteinsson 1964; McLaren & Barnett 1978). However, on Lougheed Island (Figure 1.1a), 100 km to the northeast of Melville Island, raised glaciomarine sediments have a minimum age of 10.5 ka BP and overlie till of unknown provenance (Hodgson 1981).

1.5.1.3 Local Melville Island Ice

Currently, four local ice caps occupy the western highlands of Melville Island (Figure 1.1b; Tozer & Thorsteinsson 1964; Edlund 1985; Hodgson 1992). These constitute the only ice caps in the western Arctic islands and coincide with the only terrain above 500 m asl in this region (Edlund 1985; Hodgson 1992). Based on lichen-free zones surrounding the present-day ice caps, Edlund (1985) proposed that during the Little Ice Age (LIA; 1600 - 1900 AD), these ice caps expanded to approximately seven times their present size, from 300 km^2 to 2200 km^2. Consequently, it is apparent that any other lowering of the regional snowline in the past would have permitted the expansion of local Melville Island ice, which could have advanced to coalesce with the LIS, the IIS, or both during the LGM (Hodgson 1992). Fyles (1965) attributed an esker several kilometers in length on western Melville Island (between Ibbett Bay and Hecla and Griper Bay; Figure 1.1b), and a group of subdued drumlinoid ridges on the northwest tip of Sabine Peninsula, to local ice during the Late Wisconsinan. Subsequently, Hodgson (1992) mapped the minimum extent of a local ice cap ($\geq$ 300 m thick in places) on western Melville Island, during the last glaciation (Figure 1.7). However, no landforms indicative of interaction between local and continental ice were noted (Hodgson 1992).

1.5.2 Regional Deglaciation and Postglacial Emergence

In addition to the style of past glaciations on NE Melville Island, this thesis investigates the subsequent record of relative sea level (RSL) change in order to clarify the timing of ice retreat and the nature of postglacial emergence. Emphasis is placed on the pattern of differential rebound, or shoreline delevelling, which serves as a proxy for former ice thickness (i.e., raised marine shorelines rise in the direction of greatest former ice thickness; Andrews 1970). The form of postglacial RSL curves is also documented, with particular focus on the status of modern sea level change. The current status of modern coastlines (emergence versus submergence) is relevant to the past ice load history and issues such as forebulge migration. To date, minimal work has been conducted on both the chronology of deglaciation and the subsequent postglacial emergence of NE Melville Island.

1.5.2.1 Deglaciation

Blake (1972) reported that the oldest radiocarbon dates on marine molluscs collected from raised shorelines record the progressive entry of the sea as the IIS retreated eastward across the QEI. The oldest documented incursion of the sea in the far west occurred at 11.7 ka BP on the south coast of Prince Patrick Island (Blake 1972; Hodgson *et al.* 1994). Somewhat younger dates (11.2 to 10.0 ka BP) were obtained on shells collected on the east coast of Prince Patrick Island, from the inlets of western and northern Melville Island, and from Fitzwilliam Owen and Brock islands (Figure 1.1a; Blake 1972). Thus by ~ 10 ka BP, deglaciation of the larger marine channels was essentially completed in the western part of the QEI (Blake 1972; Lowdon & Blake 1987; Dyke *et al.* 1996). These dates are similar to both hypotheses currently proposed for the final retreat of the LIS from southeastern Melville Island, i.e., the Viscount Melville Sound Ice Shelf either broke up sometime after 10.3 ka BP (Hodgson *et al.* 1984), or it had retreated off of the island prior to 11.0 ka BP (Dyke 1987).

Between 9.5 and 9.0 ka BP, the whole of Parry Channel opened up, while deglaciation extended throughout Eureka Sound by 9.2 ka BP, extending to most fiord heads by 8.0 ka BP (Figure 1.1a; Blake 1972; Dyke *et al.* 1996; Ó Cofaigh 1998). In Nares Strait (between Greenland and Ellesmere Island; Figure 1.1a), radiocarbon dates

associated with deglaciation indicate re-entry of the sea from the north and south at 10.0 and 9.0 ka BP, respectively, and by 7.5 ka BP the strait was open, reconnecting the Arctic Ocean to Baffin Bay (Figure 1.1a; England 1999).

1.5.2.2 Postglacial Emergence

The pattern and magnitude of postglacial emergence has been used to model the former ice configuration and thickness of the IIS throughout the QEI (Tushingham & Peltier 1991; Peltier 1994). Although minimal work has been conducted on the postglacial emergence of Melville Island, Henoch (1964) and McLaren and Barnett (1978) concluded that the island was covered with ice that was thicker in the region of Sabine Peninsula and Hecla and Griper Bay because they noted more emergence in that direction. For example, measurements of marine limit have reported a decrease in elevations from the east coast of the island toward the north, west, and south (Henoch 1964; Tozer & Thorsteinsson 1964; McLaren & Barnett 1978). Currently, the highest reported marine limit (101 m asl) was recorded on the east coast of the island (south of Towson Point; Figure 1.8; McLaren & Barnett 1978). To the north, on Sabine Peninsula, marine limit on the isthmus between Eldridge and Sherard bays has been reported to be greater than 61 m asl (Henoch 1964; Tozer & Thorsteinsson 1964; McLaren & Barnett 1978), whereas on northern Sabine Peninsula, marine limit elevations decrease to 55 m asl (Henoch 1964). To the west of Towson Point, along the south coast of Hecla and Griper Bay, the uppermost raised marine shorelines decline to between 55 and 43 m asl (Tozer & Thorsteinsson 1964; McLaren & Barnett 1978; Hodgson *et al.* 1984). To the south of Towson Point, raised marine shorelines have been recorded at 61 m asl (Nelson Griffiths Point; Figure 1.8; Henoch 1964; McLaren & Barnett 1978) and similar elevations have been noted along the west coast (Comfort Cove; Figure 1.8; Hodgson 1992).

Measurements of raised marine shorelines on Melville Island determined by different authors appear to be in agreement for all areas except in the vicinity of Winter Harbour Till on Dundas Peninsula. There, the majority of measurements place Holocene marine limit between 30 and 35 m asl as recorded by a prominent washing limit that runs discontinuously for 35 km along the southeast coast of Dundas Peninsula (Figure 1.8;

Henoch 1964; Tozer & Thorsteinsson 1964; Fyles 1967; Hodgson *et al.* 1984). Farther south, near the tip of Dundas Peninsula, the highest deltas reported are only 20 m asl (Figure 1.8; Hodgson *et al.* 1984). On the distal (inland) side of Winter Harbour Till, marine limit reaches at least 55 m asl, where shells date 10.3 ka BP (Hodgson *et al.* 1984). McLaren and Barnett (1978) suggest that marine limit along Winter Harbour Till occurs at 61 m asl.

Isobases drawn by Andrews (1969, 1989) on shorelines from the QEI, as well as the mainland, show no emergence of the westernmost islands over the last 6 - 7 ka. Similarly, Walcott (1972) shows the zero isobases for 7, 6, 4, and 2 ka BP trending northeast-southwest through western Melville Island, indicating submergence for all of the westernmost islands, and the west coast of Melville Island, since at least 7 ka BP. Although the isobases in the western Arctic are only estimates, these studies imply that the boundary separating submergence to the west and emergence to the east has been relatively stationary for the past 6 - 7 ka, which would not accord with the geophysical theory of a migrating forebulge. To the northwest of Melville Island, on western Prince Patrick Island, Hodgson *et al.* (1994) reported 10 m of net submergence (based on drowned estuaries, breached lakes, and coastal barriers) since ~ 2.9 ka BP, whereas they proposed that the eastern coast of the island is still emerging. If Hodgson *et al.* (1994) are correct, the modern zero isobase would have to pass through Prince Patrick Island and lie well to the west of where Andrews (1969, 1989) and Walcott (1972) have placed it from 7 ka BP to the present. Previous work on Melville Island has proposed very slow ongoing emergence along the northeast coast of the island during the past 2 ka (Henoch 1964; McLaren & Barnett 1978). This viewpoint has yet to be contradicted by reports of Holocene submergence anywhere on Melville Island, although a date of 1.7 ka BP on a Dorset site at 1.8 m asl in McCormick Inlet precludes an emergence of the site of > 1 m in the last 1.7 ka and raises the question of whether recent submergence has occurred at this site (Henoch 1964).

A preliminary RSL curve with dates ranging from 9.0 to 0.6 ka BP indicated that little, if any, net emergence has occurred on the island in the last 2 ka, suggesting that Melville Island is close to isostatic equilibrium (Henoch 1964). However, the lack of sufficient dating control for the curve between 7.5 and 1.7 ka BP renders this conclusion

speculative (Henoch 1964). The most significant subsequent study of postglacial emergence of the island provided two provisional RSL curves for the south and east coasts of Melville Island, along Viscount Melville Sound and Byam Martin Channel, respectively (Figure 1.1b; McLaren & Barnett 1978). McLaren and Barnett (1978) concluded that emergence along Winter Harbour Till was nearing completion, while the northeast coast (including Sabine Peninsula) was still recovering at a rate of ~ 0.35 cm/a. Therefore, like Henoch earlier (1964), they concluded that the former ice cover in the northeast was thicker than in the peripheral areas of the LIS, lending support for coverage by the IIS, or by thick local ice, in that direction.

1.6 RATIONALE FOR STUDY

Although a consensus has been reached supporting the existence of the IIS during the LGM, few details exist concerning the style of glaciation across the western QEI, including its maximum extent, ice surface geometry, flow patterns, and chronology (both during ice buildup and retreat). This thesis will address the record of glaciation and deglaciation on NE Melville Island, as well as the subsequent magnitude and pattern of postglacial emergence, especially related to the form of RSL curves. NE Melville Island is an important area because it lies between the known limit of the LIS to the south on Dundas Peninsula (Hodgson *et al.* 1984) and borders the undocumented western limit of the IIS that extended at least as far as Cornwall Island to the northeast (Lamoureux & England 2000) and possibly crossed Lougheed Island, less than 100 km to the north (Hodgson 1981). Furthermore, local ice in the western highlands of Melville Island indicates a possible third source of ice during the LGM (Hodgson 1992). The work of Henoch (1964), McLaren and Barnett (1978), Hodgson *et al.* (1984), and Hodgson (1992) are acknowledged as the foundation upon which the current fieldwork builds.

1.7 RESEARCH OBJECTIVES

This thesis has three objectives concerning the late Quaternary glacial and deglacial and RSL history of NE Melville Island.

1) To determine the style of glaciation and deglaciation of NE Melville Island with respect to three potential sources of ice (the LIS, the IIS, and local, island-based ice caps);
2) To determine the magnitude and timing of postglacial emergence across NE Melville Island with respect to these former ice masses, including the direction of dominant glacial unloading following the LGM; and,
3) To further clarify the form of the RSL curves from marine limit to modern sea level.

With respect to objective 1, previous work on Melville Island has concentrated on Dundas Peninsula where the LIS overrode the coastline from Viscount Melville Sound (Hodgson *et al.* 1984). However, studies of postglacial emergence have determined that there has been more uplift (net emergence) on the northeast part of the island (Henoch 1964; McLaren & Barnett 1978), lending support to the hypothesis that Melville Island was glacioisostatically dominated by the IIS, local ice, or both. The configuration of ice on NE Melville Island, and the relative contribution of local vs. regional ice sources will be determined by mapping glacial sediments and landforms, including the evidence for local vs. far-traveled erratics across the head of Hecla and Griper Bay, and on Sabine Peninsula.

Marine incursion along the margins of retreating ice masses is recorded by marine sediments, deltas, and shorelines, that commonly record the maximum limit of the sea (marine limit). The subsequent rebound of the crust in response to glacial unloading results in forced regression as postglacial emergence of the former sea floor progresses. With respect to objective 2, mapping the distribution of raised marine sediments and landforms, and surveying their elevations will determine spatial variations in postglacial emergence. Radiocarbon dating of driftwood, molluscs and organic material associated with surveyed raised shorelines will provide a chronology to document the pattern of differential postglacial emergence (shoreline delevelling). The coastline of Hecla and Griper Bay has the advantage of having two opposing trajectories (one trending north-south and the other east-west), which provides the best opportunity to measure the

maximum slope of differential postglacial emergence recorded by the delevelled shorelines (i.e., one or the other of these coastlines could be oriented at a steep angle to the regional isobases). Because delevelled shorelines rise toward the dominant former ice load, the isobase pattern drawn on them can be used to determine the direction of maximum former glacioisostatic loading and subsequent unloading. These isobases can be combined with other reconstructions (Dyke 1998; Ó Cofaigh 1999) and should help to determine whether the LIS, the IIS, or local ice isostatically dominated NE Melville Island. Reconstructing postglacial isobases in areas previously uninvestigated will allow the broader regional pattern to be better determined, contributing to improved geophysical modeling of the LIS, IIS, and local ice masses.

Finally, with respect to objective 3, radiocarbon dating of marine fauna, driftwood and organic material collected from surveyed shorelines extending from marine limit to modern high tide will provide a chronological framework for establishing RSL curves. The RSL curves will permit the determination of whether emergence is still occurring on NE Melville Island, or whether sections of the coastline have begun to submerge. If Holocene emergence has given way to recent submergence, the spatial and chronological progression of that submergence across the study area should provide a measure of forebulge migration (Walcott 1972). Forebulge migration recorded in other parts of glaciated North America (Belknap *et al.* 1986; Dyke & Prest 1987; Liverman 1994; Barnhardt *et al.* 1995) can be compared with the evidence from western Arctic Canada where this process remains undocumented. Documentation of modern submergence would also be relevant to the understanding of modern coastal processes in this region and would differentiate it from the eastern and central QEI where net emergence is ongoing.

Figure 1.1a. Location map for Queen Elizabeth Islands. Ice caps are highlighted and place names cited in text are shown.

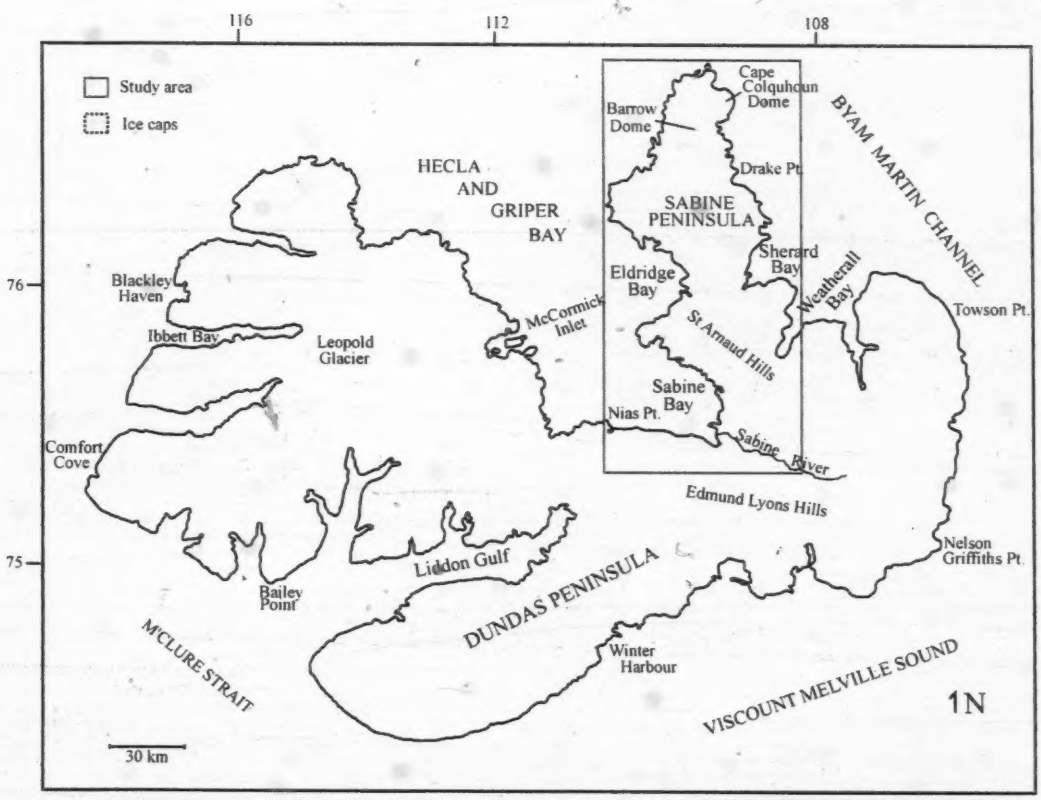

Figure 1.1b. Location map for Melville Island. Study area is highlighted in rectangle and place names cited in text are shown. Note ice caps on western Melville Island.

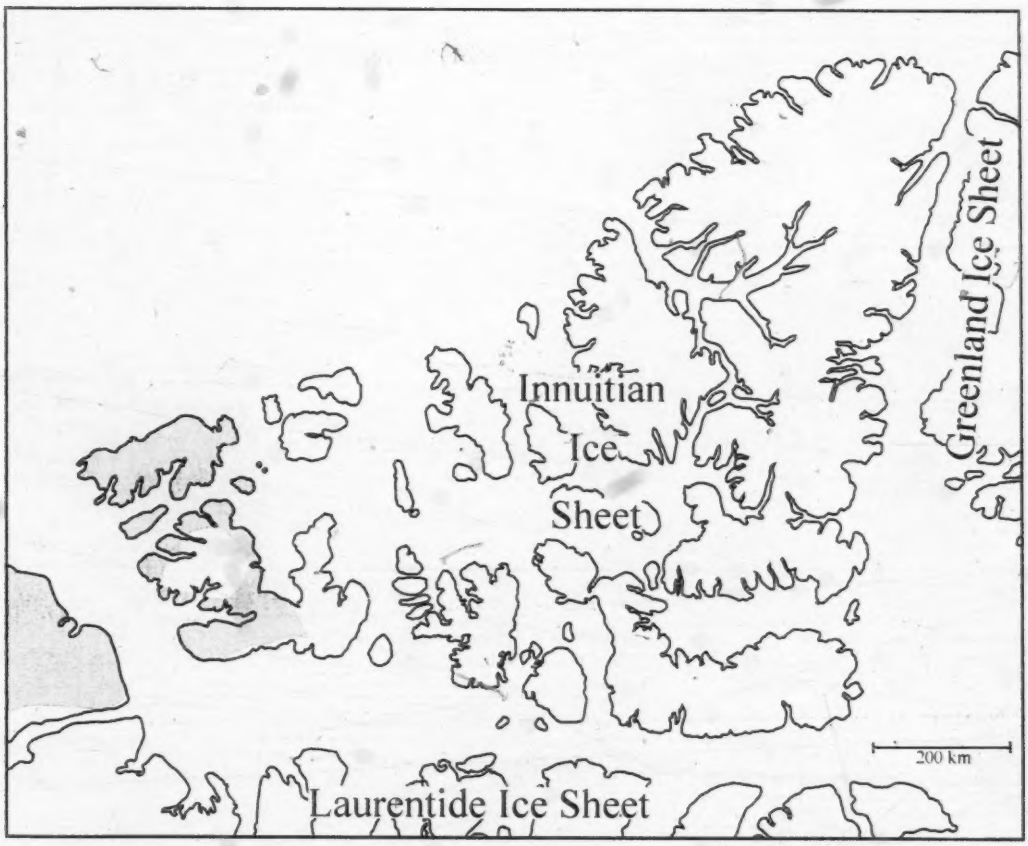

Figure 1.2. Coverage of the Canadian Arctic Archipelago by coalescing Innuitian, Greenland, and Laurentide ice sheets during the Late Wisconsinan. Note proposed Innuitian ice on northeast Melville Island (Sabine Peninsula), Laurentide ice along the southern coast and in Liddon Gulf, and local ice on western Melville Island. (Adapted from Dyke et al. 2002).

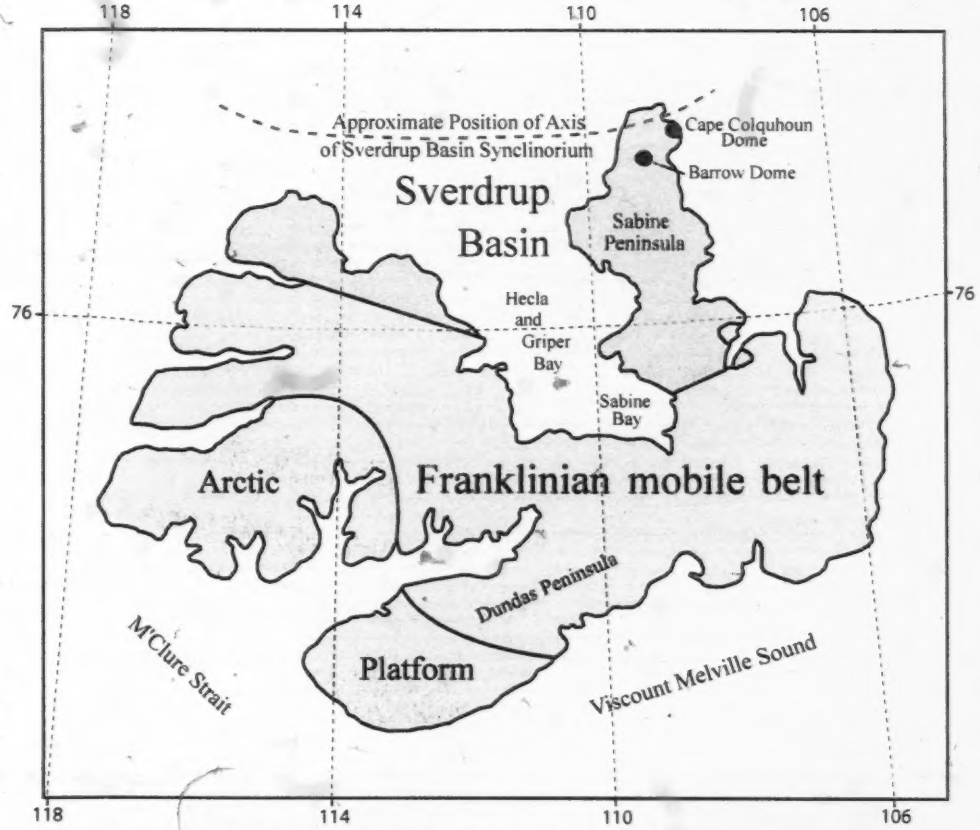

Figure 1.3a. Geological map of Melville Island denoting Franklinian mobile belt and Sverdrup Basin. Note approximate position of the axis of the Sverdrup Basin Synclinorium and the two piercement domes on northern Sabine Peninsula. (Adapted from Tozer & Thorsteinsson 1964).

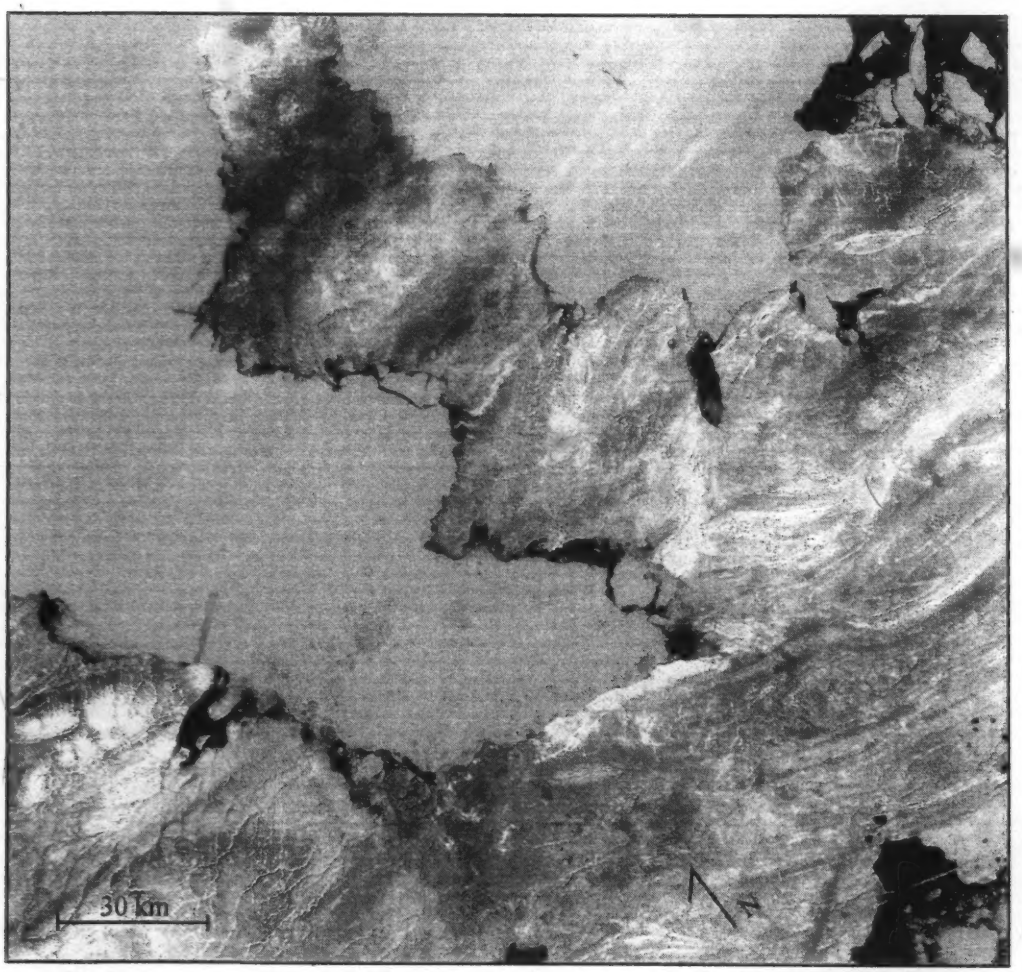

Figure 1.3b. Landsat 7 image of the study area. Note the WNW-ESE structural trend of the Franklinian mobile belt in the southern part of the study area (right third of image).

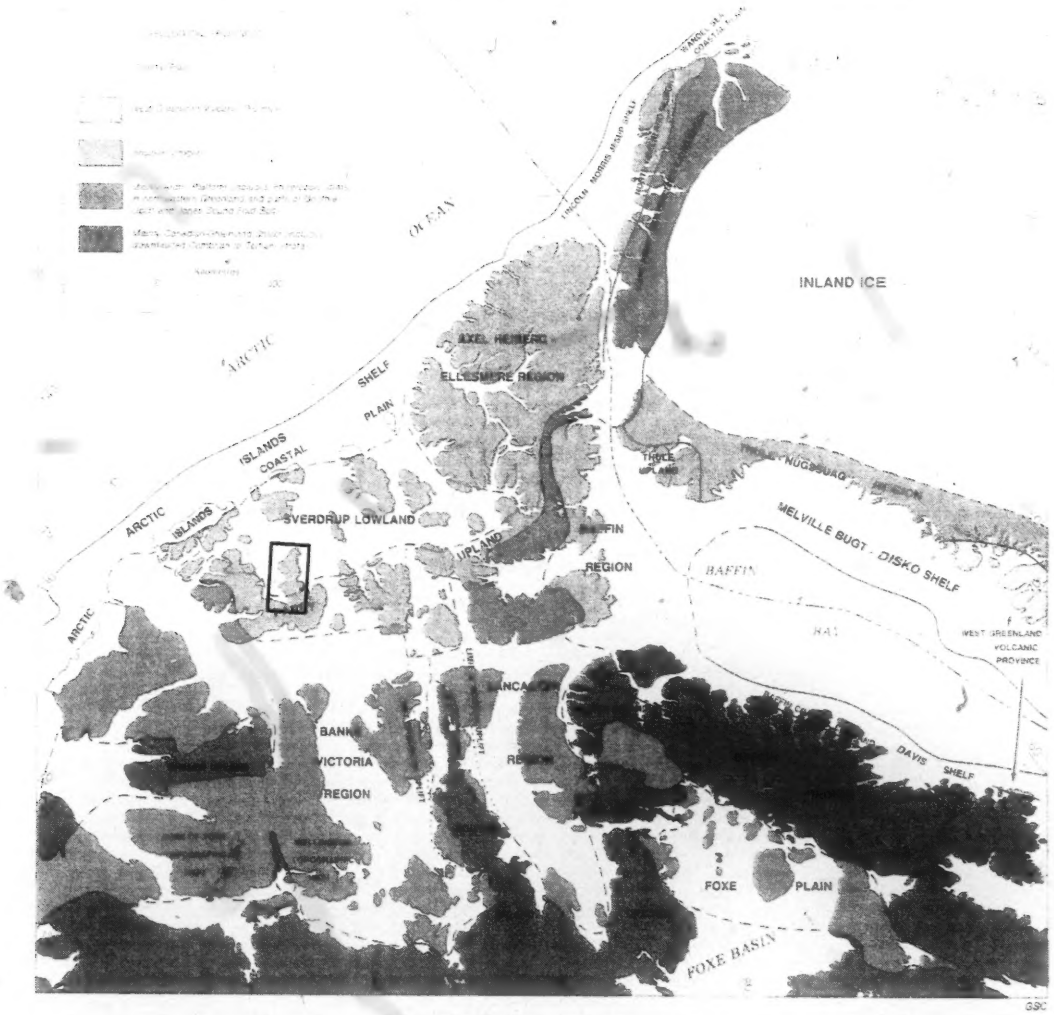

Figure 1.4. Geomorphic regions of the Canadian Arctic Archipelago. Study area is highlighted in rectangle. Note Parry Upland in southern part of study area, and Sverdrup Lowland in northern part of study area. (Source: Dawes and Christie 1991.)

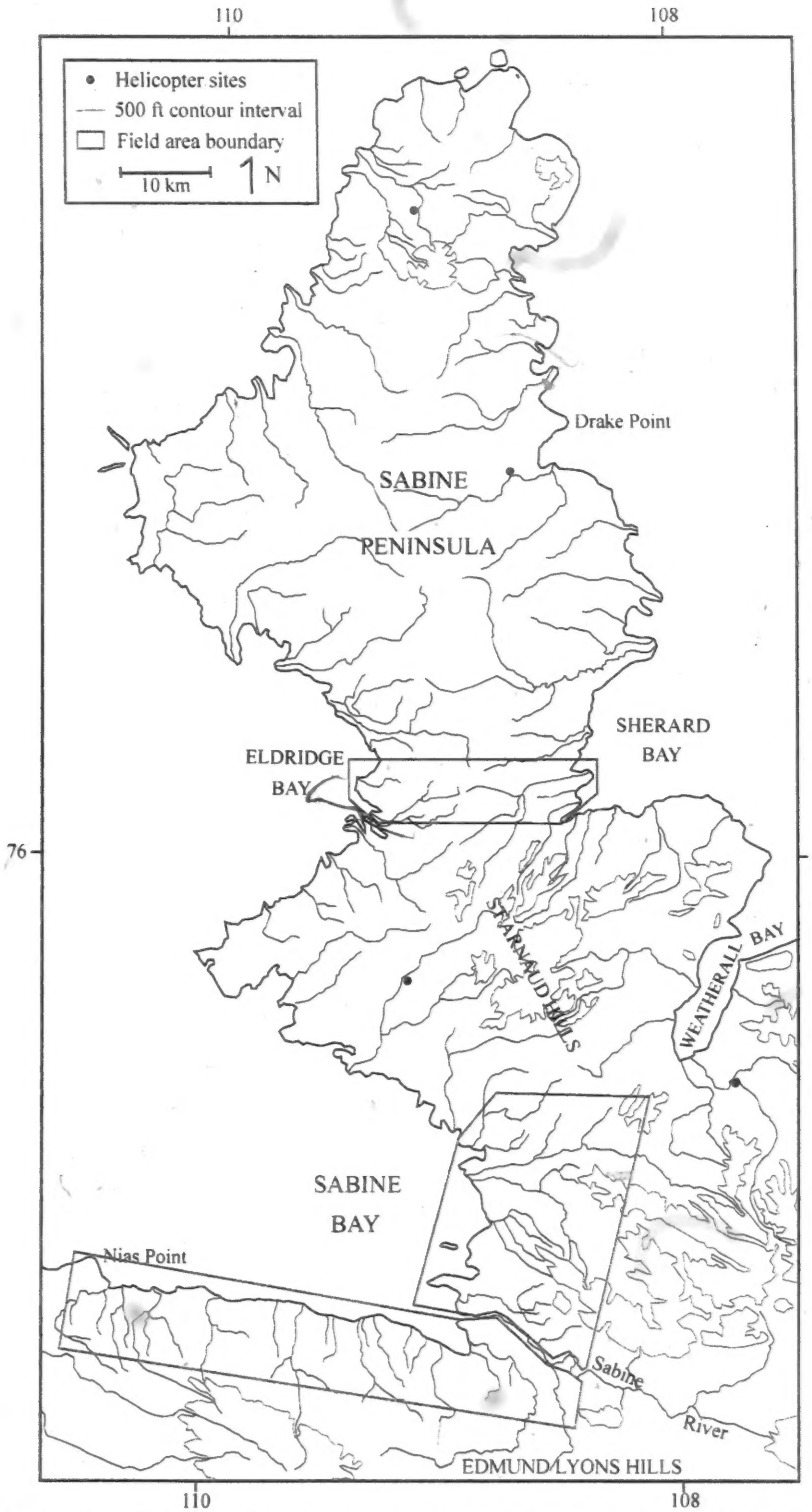

Figure 1.5. Northeast Melville Island, showing field areas and key sites visited by helicopter.

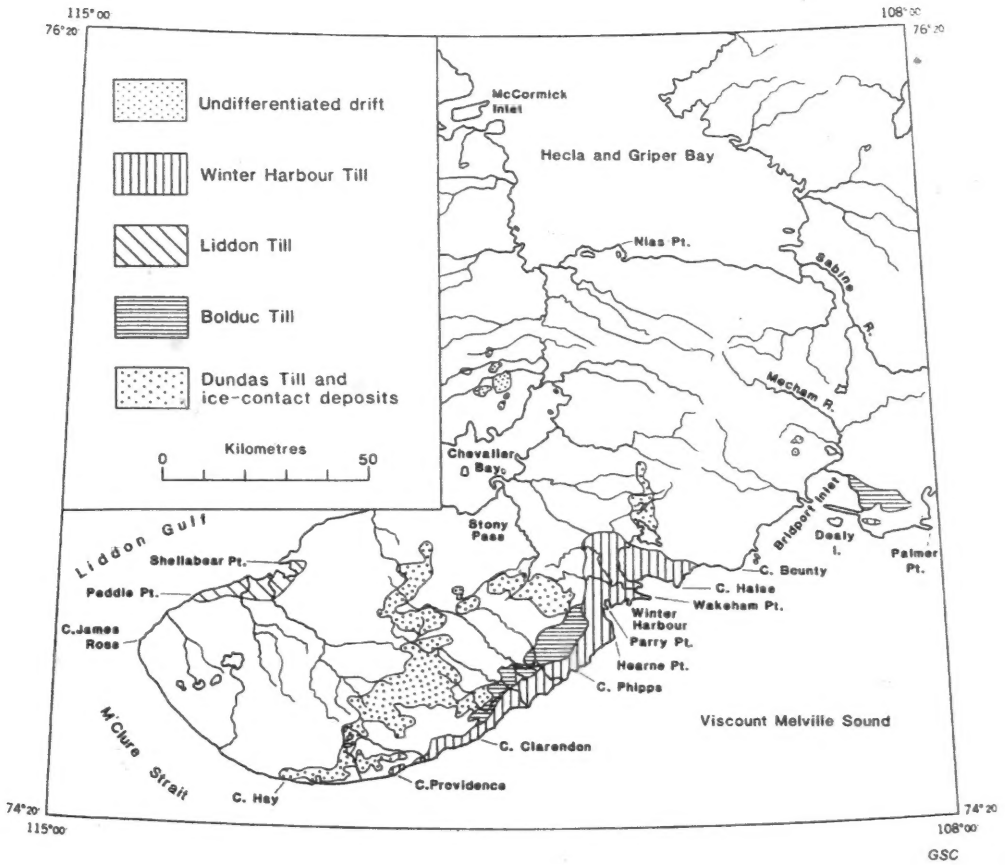

Figure 1.6. Central Melville Island showing Laurentide till units that mark the furthest documented extent of the Laurentide Ice Sheet. Note that none of the tills occur within the study area. (Source: Hodgson et al. 1984).

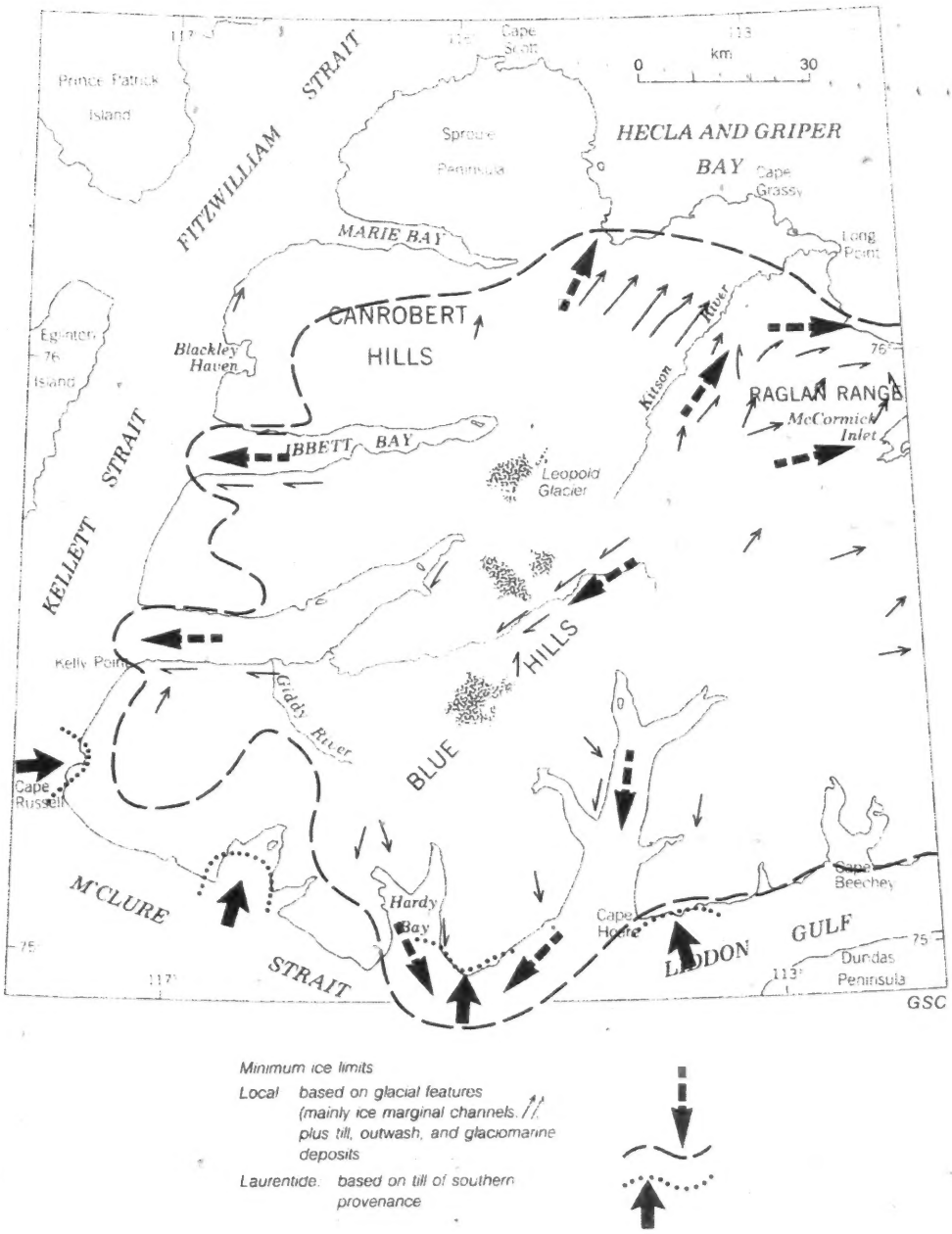

Figure 1.7. Minimum extent of local and Laurentide ice on western Melville Island during the last glaciation. (Source: Hodgson 1992).

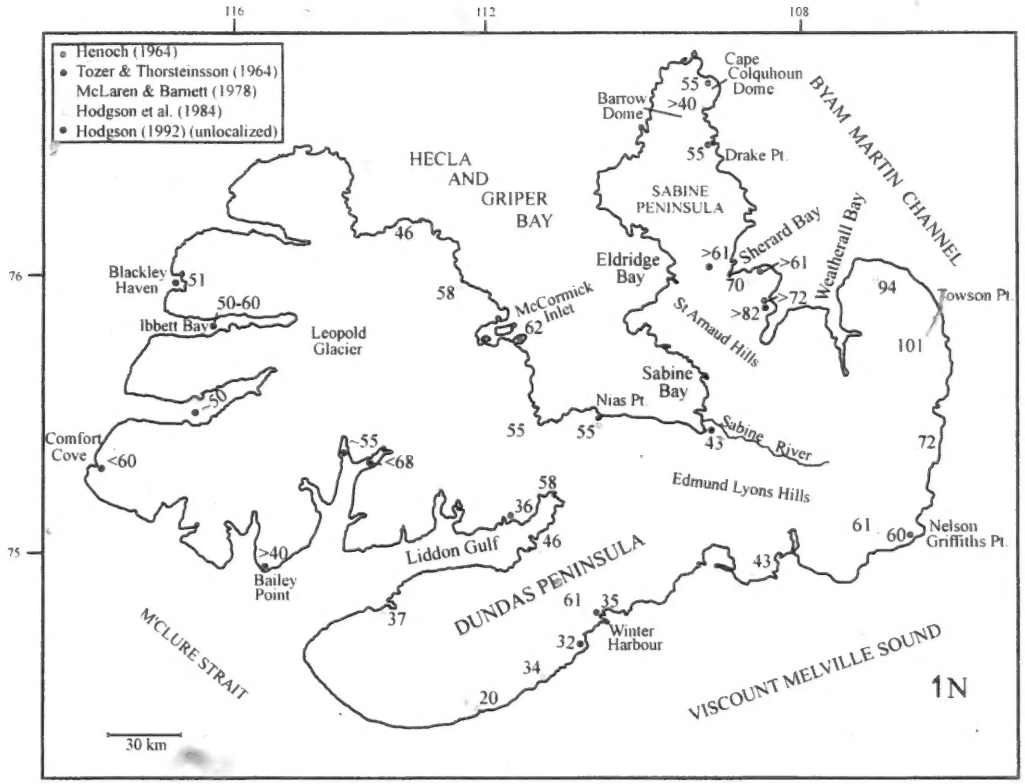

Figure 1.8. Previously surveyed marine limits on Melville Island (elevation in metres above sea level). Note general rise in marine limit elevations across Melville Island from southwest to northeast.

CHAPTER 2: METHODS

2.1 INTRODUCTION

The principal objective of this study was to reconstruct the deglacial and RSL history of NE Melville Island. This involved mapping the surficial geology and associated landforms, surveying marine limit and lower RSLs, and collecting and radiocarbon dating marine fauna, driftwood, and organic matter from the surveyed raised marine shorelines. Fieldwork was conducted from late June to early August, 2001, and mostly involved transects out of three camps conducted by all-terrain vehicle (ATV), supplemented by two days of helicopter survey along the south coast of Hecla and Griper Bay and around Sabine Peninsula.

2.2 RESEARCH METHODS

2.2.1 Surficial Geological Mapping

Prior to fieldwork, aerial photographs and a Landsat 7 image (Figure 1.3b) of the study area were studied and all pertinent sediments and landforms were mapped at a scale of 1:250,000. The mapping applied the standardised criteria used by the Geological Survey of Canada, which, for the Arctic Archipelago, predominantly includes: bedrock, weathered bedrock (felsenmeer and residuum), till (blankets and veneers), raised marine sediments, alluvium (active and inactive), and colluvium (cf., Dyke 1983). Landforms include mega-flutings, moraines, morainal banks, meltwater channels, raised deltas and beaches. The distribution of these sediments and landforms were used to identify the best camp locations and transects to meet the thesis objectives.

Exposures of bedrock and surficial units derived from *in situ* weathered bedrock were mapped as rock, felsenmeer, and residuum. Till is usually subdivided into two units: till blanket and till veneer (cf., Dyke 1983). A till blanket exceeds 2 m in thickness, and therefore obscures the underlying bedrock structure. Conversely, a till veneer is less than 2 m thick and therefore does not fully obscure the underlying bedrock structure evident on aerial photographs. Till veneer can also include sparse erratics

resting on, or admixed with, residuum. To distinguish till blankets from till veneers using aerial photographs, the distribution of ice-wedge polygons was used, as ice wedges are unable to form in sediments less than 2 m thick (Dyke 1983). Till was principally mapped from aerial photographs, although characteristics were further established by mapping throughout the three field areas (Figure 1.5). Raised marine sediments occur at and below marine limit and are categorised as deltaic, nearshore, or beach deposits. Deltaic deposits consist of gravel topsets, well-sorted sand and fine gravel foresets, and well-sorted bottomset silt and clay, all of which have often been incised by subsequent fluvial activity. Nearshore deposits consist of prodeltaic, lagoonal, and foreshore deposits composed of silt and sand that can be stratified to massive. These deposits often stand out as dark toned areas on aerial photographs because their fine texture and low topography combine to produce poor drainage and therefore wet meadow vegetation (Figure 3.4; Dyke 1983; Edlund 1993). The fine sand, silt and clay of these deposits are often characterised by ice-wedge polygons (Dyke 1983; Edlund 1993). In the field, stratigraphic sections exposed through raised marine sediments were sketched, measured and interpreted using standard stratigraphic techniques. Alluvial sand and gravel is divided into two types: deposits that flood annually (active), and those that do not (inactive). Active fluvial sediments often have channel-scarred surfaces that are unoxidised and unvegetated due to seasonal reworking during spring snowmelt (nival flood). Inactive fluvial sediments are separated from the contemporary floodplain by a distinct bluff greater than 1 m high and are commonly oxidised and vegetated. Colluvium is classified as weathered material transported downslope by mass movement. These sediments are mostly derived from residuum, which is often redeposited as gelifluction stripes and lobes (Figures 3.3 & 3.8). On steeper terrain, colluvium produces talus slopes or coalescent aprons.

Moraines in most parts of the High Arctic are rare, likely because much of the ice was cold-based and both eroded and deposited relatively little sediment. The most important landforms relating to former ice margins are lateral meltwater channels, which are widespread (Figure 2.1). These lateral meltwater channels are especially relevant because their distribution marks the pattern of retreat of former ice margins. Lateral meltwater channels are characteristic of cold ice margins (below the pressure melting

point) where surface meltwater and snowmelt from adjacent slopes is concentrated at the margins, eroding lateral channels into bedrock (cf., Dyke 1993). These channels can be distinguished from pre-Quaternary river channels because they are commonly orthogonal to slopes, converging on the valley floor in nested, subparallel patterns that mark successive stages of an ice lobe's retreat (cf., Dyke 1993). The lowermost channels along any coastline terminate at marine limit, commonly recorded by ice-contact or ice-fed deltas. As well, these channels are often larger than the channels of the postglacial drainage system. Lateral meltwater channels are also not controlled by bedrock and can crosscut interfluves at angles that can only be explained by the presence of a former ice margin.

2.2.2 Establishing the Elevation and Age of Former Relative Sea Levels

The presence of raised marine sediments and landforms throughout Arctic Canada, such as deltas and raised beaches, indicates the former occupancy of the sea from deglaciation to present. The maximum elevation of the sea along a glacioisostatically-depressed coastline is called marine limit (Andrews 1970). Marine limit is synchronous with deglaciation as the sea immediately crosses the glacioisostatically-depressed crust at the moment of ice retreat (Andrews 1970). Marine fauna within landforms or sediments marking marine limit therefore provide a minimum age for deglaciation and a measure of subsequent postglacial rebound. Marine limit is commonly marked by ice-contact or ice-fed deltas, the upper limit of littoral fill, a beach ridge, or a washing limit (Sim 1960; Andrews 1970). It can also be marked by the lowest glacial landform in the area such as the base of a meltwater channel or the lowermost occurrence of perched boulders (Andrews 1970). Another indicator of marine limit is the upper limit of *in situ* marine shells. However, because shells live in some depth of water (species specific) this must be a minimum measure of marine limit (Sim 1960). Preferably, a combination of the above criteria can be used to define marine limit for a specific stretch of coastline, and most often this elevation is based on multiple indicators that are all roughly accordant (± 2 m). The most useful of these indicators are ice-contact deltas, especially where they extend from the base of the lowermost meltwater channel. Well-developed ice-contact and ice-fed deltas occur only intermittently along most

coastlines, as do well-developed raised beaches. The primary constraints on their development at, and below, marine limit are: low sediment supply in this arid environment, and, in the case of raised beaches, pervasive (multi-year) landfast sea-ice that all but precludes wave action (Wadhams *et al.* 1986, 1988; Forbes & Taylor 1994). Preservation of marine limit can also be a problem, especially where active gelifluction has overridden and buried beaches with colluvium. Within the field area, marine limit was mapped and surveyed using multiple indicators wherever present. Where marine limit could not be conclusively identified, landforms providing a minimum estimate on its elevation were mapped and surveyed.

Once deglaciation has occurred, ongoing crustal rebound results in a forced regression as sea level falls from marine limit to its modern position. In most areas of Arctic Canada, sea level has fallen continuously since deglaciation and emergence remains ongoing. However, in areas closer to the former ice sheet margin, initial Holocene emergence has given way to recent and ongoing coastal submergence (cf., Hodgson *et al.* 1994). In some areas, such as the Mackenzie delta, RSL has been rising throughout the Holocene because there has been a net eustatic rise since deglaciation (Hill *et al.* 1985, 1993). Hence, depending on the location of a site in relation to a former ice sheet margin, there can be a range of possible RSL adjustments following deglaciation (Quinlan & Beaumont 1981). On NE Melville Island there has only been reported net emergence since deglaciation (Henoch 1964; McLaren & Barnett 1978). Within the field area, raised marine features below marine limit were mapped and surveyed in order to establish a history of RSL change.

Marine limit and subsequent lower shorelines were surveyed with a Wallace & Tiernan Surveying Altimeter and each measurement was corrected for variations in atmospheric pressure and temperature. Temperature was recorded with each altimeter reading and altimetry transects were closed as frequently as possible, using either the high tide mark or camp as datum, in order to determine the change in atmospheric pressure over the transect period. Corrections were subsequently applied to all measurements based on both the rate of pressure change throughout the transect period and the change in temperature (using standard temperature correction tables provided by the manufacturer). Multiple readings were made on key landforms and shorelines to

ensure consistency of the measurements. Elevations presented in this thesis are considered to be accurate to within ± 2 m on elevations up to 100 m asl and to within ± 0.5 m at elevations below 20 m asl. Key sites were fixed by a Global Positioning System (GPS).

To determine the age of a paleoshoreline and establish a chronology of ice retreat and RSL change, radiocarbon dating of marine fauna, driftwood, and organic material associated with specific marine landforms and sediments was undertaken. Dated shorelines at lower elevations were also surveyed in order to determine whether there was any discernible tilt across the study area, as this would record the direction of greatest former ice loading (i.e. shorelines of the same age rise toward areas of greatest glacioisostatic unloading, where ice was previously thicker). The most commonly observed marine fauna were the bivalves *Hiatella arctica*, although *Mya truncata*, *Macoma calcarea*, and *Astarte* species were also observed. Species such as *Portlandia arctica*, and *Serripes groenlandicus* were not observed. Paired valves in growth position can be accurately related to former sea levels when they occur in an unambiguous stratigraphic setting, such as within topset, foreset, or bottomset beds of Gilbert-type deltas (Andrews 1970). However, if molluscs are collected from undifferentiated marine sediments (deep water mud or rhythmites), it is more difficult to associate them with a former RSL because they once lived at an unknown water depth (which can range between 2 and 100 m, depending upon the species; Hillaire-Marcel 1980; Andrews 1986). Thus these samples can only provide a minimum estimate for a former (higher) paleoshoreline, and therefore, care was taken to select samples that could be stratigraphically linked to a specific former shoreline. Driftwood samples and organic material were also collected from marine deltas, and the most useful driftwood samples were collected from embedded positions in raised beaches, as these were less likely to have undergone downslope transportation.

The accuracy of radiocarbon analysis relies upon the quality of the material submitted and its absolute age. Most of the samples measured were done by accelerator mass spectrometry (AMS) and display standard errors of ~ ± 70 radiocarbon years. Paired valves are preferable for analysis as fragmented molluscs have been reworked and possibly moved an unknown distance downslope, or redeposited by retreating ice.

Fragmented shells can also contain a mixture of ages, which would not be apparent if a bulk sample was used for radiocarbon dating. Finally, surface shells can also be problematic if they exhibit encrustations of secondary calcite, or staining by lichen or algal growth, which would contaminate the sample's true age with younger carbon (cf., Dyke *et al.* 1991). Consequently, samples that were submitted for radiocarbon analysis were free of apparent redeposition and/or contamination. In order to remove all contaminants before submission for radiocarbon analysis, samples were cleaned in an ultrasonic bath containing deionised water for 20 minutes. They were subsequently air-dried and any remaining surface staining was removed using an electric grinder. All samples were also subjected to ≥ 20 % surface leaching to further ensure removal of any contaminants. In the field, driftwood samples were carefully selected and subsequently any visible lichen or algal growth was removed to expose clean inner wood for dating. If the sample was wet or damp, it was dried at room temperature and subsequently the surface layer was removed with a knife or an electric sander. Organic samples were filtered to remove as much sediment as possible and then dried at room temperature. All samples were subsequently weighed and put into sterile plastic sample bags. Larger samples of whole valves (> 27.0 g) and driftwood (> 30.0 g) were sent to Beta Analytic (Miami) for conventional radiocarbon analysis (beta counting), whereas individual valves and fragments (< 4.0 g), smaller driftwood samples (< 6.0 g), and organic samples (< 1.0 g) were sent to IsoTrace Laboratory (University of Toronto) for accelerator mass spectrometer (AMS) dating. Two small driftwood samples were also sent to Laval University C^{14} Laboratory for AMS dating. Because Isotrace Laboratory normalized its shell dates to $\delta^{13}C$ = - 25 ‰, these dates were subsequently corrected for a marine reservoir effect of – 410 years. The same correction was applied by Beta Analytic under their reported 'machine age', with an additional correction applied for $\delta^{13}C$ values that departed from - 25 ‰. IsoTrace does not measure or correct for $\delta^{13}C$. However this would not result in more than a few decades difference between IsoTrace and Beta Analytic, a difference well within the limits of their standard errors. Driftwood samples received no correction for the reservoir effect and are reported as received from the laboratory.

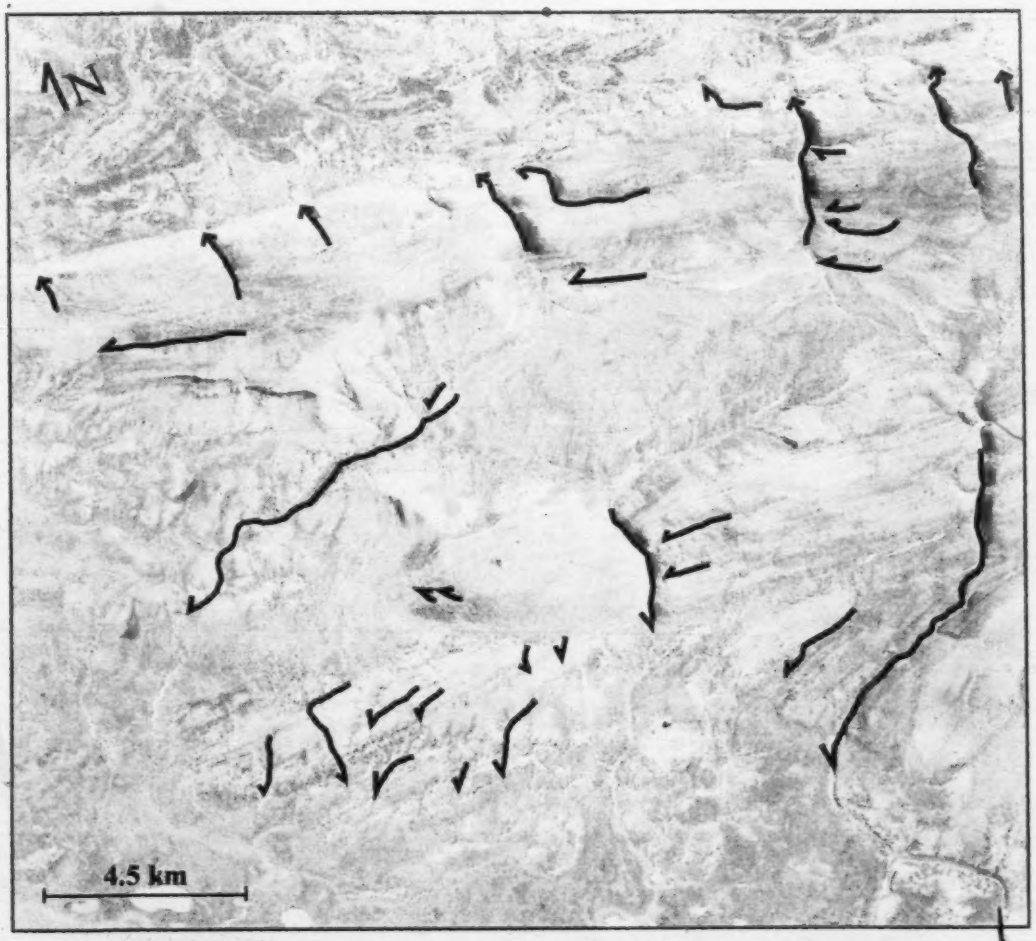

Figure 2.1. Lateral and proglacial meltwater channels, east coast of Sabine Bay, indicating pattern of retreat off of a local bedrock ridge both to the north and to the southeast. Note that lateral meltwater channels are often orthogonal to slopes, crosscut interfluves, and are often larger than the channels of the postglacial drainage system.

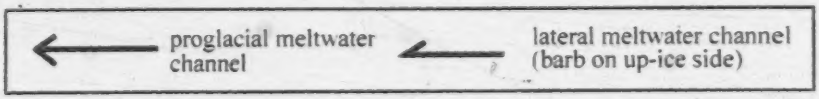

CHAPTER 3: LATE QUATERNARY ICE COVERAGE, DEGLACIATION, AND RELATIVE SEA LEVEL HISTORY

3.1 INTRODUCTION

This chapter presents surficial geology and geomorphology, which is used to reconstruct the style of ice coverage, pattern of deglaciation, and subsequent RSL adjustments across NE Melville Island. This information was derived from both aerial photograph and Landsat image interpretation and from fieldwork. The deglacial chronology and RSL history are based upon radiocarbon analysis of samples following return from the field. This chapter is divided into three sections, which pertain to surficial geology and geomorphology, deglaciation, and the RSL history of NE Melville Island.

3.2 SURFICIAL MAPPING

This section presents the surficial geology and geomorphology of NE Melville Island (Figures 3.1a, b, & c). Mapping followed criteria outlined by the Geological Survey of Canada (cf., Dyke 1983; Section 2.2.1). The entire study area was mapped from aerial photographs and a Landsat 7 image (Figure 1.3b) of the study area and was ground-truthed within each of the three field areas (Figure 1.5). The surficial units are presented in order, based upon their relative age, from oldest to youngest. The relevance of the surficial geology and geomorphology to the reconstruction of late Quaternary deglaciation and RSL of NE Melville Island is addressed in Sections 3.3, 3.4, and 4.2.

3.2.1 Rock, Weathered Rock and Associated Landforms

Rock and weathered rock constitute the most widespread surficial unit on NE Melville Island (Figures 3.1a, b, & c), with most of the bedrock having undergone frost shattering to produce widespread felsenmeer (blockfields) and residuum (granular overburden). These materials obscure the underlying bedrock structure in most of the study area. The bedrock formations of the Franklinian mobile belt are better lithified

than those of Sverdrup Basin (Figure 3.2) and therefore they are more resistant to erosion. The weathering characteristics of the Franklinian mobile belt sandstones along the south coast of Hecla and Griper Bay have been documented by Hodgson *et al.* (1984). Three formations underlie the study area: the Hecla Bay Fm (Middle Devonian), the Weatherall Fm (Middle Devonian), and the Griper Bay Fm (Upper Devonian). They consist mostly of fine- to medium-grained quartzose sandstone with layers of siltstone and shale (Hodgson *et al.* 1984). Weathering predominantly produces sandstone felsenmeer, but also produces minor amounts of sand, silt and clay (Hodgson *et al.* 1984). Hecla Bay Fm outcrops along the south coast of Hecla and Griper Bay where it produces felsenmeer characterised by periglacial stripes on hillsides (Figure 3.3; Hodgson *et al.* 1984). The weathering characteristics of the Sverdrup Basin have been documented both by Hodgson (1982) in the western Sverdrup Islands and by Barnett *et al.* (1977) on Sabine Peninsula. Weathering of the sixteen formations that underlie the study area on Sabine Peninsula (Figure 3.2) mainly produces residuum (ranging from coarse-grained sand to clay), but also produces minor amounts of felsenmeer. Weathering of the Kanguk Fm (Upper Cretaceous) is distinctive as it produces fissile shale fragments (Barnett *et al.* 1977; Hodgson 1982).

No evidence of glacial erosional landforms (e.g., striae, ice-moulded bedrock) was found in the study area, although deglacial landforms, such as lateral meltwater channels, are pervasive on much of the residuum, in particular on felsenmeer. The lack of glacial erosive features will be addressed in Section 4.2.1, and the lateral meltwater channels are discussed in Sections 3.3.1 and 4.2.2.

3.2.2 Till and Associated Landforms

Till blankets are uncommon in the study area and, where investigated, are comprised of local lithologies (predominantly sandstone) both on the Franklinian mobile belt and on the Sverdrup Basin rocks. Till blankets obscure the underlying bedrock (> 2 m thick; Dyke 1983), appear lighter in tone, and have a drainage pattern that is less incised than on the surrounding topography. They were mapped principally from aerial photographs based on nearly continuous networks of high-centred, ice-wedge polygons. Most of the till blankets occur on low plateaux along the south coast of Sabine Bay where

they cover ~ 36 km^2 and consist of polygons of ~ 30 - 60 m in diameter (Figure 3.1a). Approximately 8 km from the west coast of Sherard Bay (Figure 3.1b), till blankets were also noted mantling slightly higher topography than the surrounding area. Polygons reach ~ 100 m diameter on level ground and grade to sorted stripes on adjacent slopes. The large size of these polygons suggest that they may not be the product of thermal contraction cracking (normally < 50 m diameter) and hence they may record subsidence due to melt-out of underlying glacier ice (Dyke *et al.* 1992). Tozer and Thorsteinsson (1964) noted the occurrence of more till blankets on central Sabine Peninsula, but these were not observed during the course of this study.

Till veneer is common in the field area and occurs as scattered erratics resting on bedrock, felsenmeer, or residuum. However, till veneer was not distinguished from weathered rock in the study area because the two could not be separately identified on the air photos, and, in most cases, erratics are of local provenance (mostly sandstone; cf., Dyke 1983). Erratics along the south and east coasts of Sabine Bay consist of Franklinian mobile belt sandstones, whereas erratics on Sabine Peninsula consist predominantly of Sverdrup Basin sandstones. Glacial depositional landforms (e.g., end moraines, morainal banks, and mega-flutings) are rare within the study area and, as they pertain to the glacial and deglacial history of the area, they are discussed in Sections 3.3, 4.2.1, and 4.2.2.

3.2.3 Raised Marine Sediments and Associated Landforms

Most of the coast of the study area is mantled by raised marine sediments (Figures 3.1a, b, & c). Commensurate with deglaciation, the sea transgressed the glacioisostatically-depressed coastline, which temporarily received increased volumes of sediment-laden meltwater from the retreating ice margin. These sediments and landforms (deltas, beaches, deepwater rhythmites) have subsequently become exposed by postglacial emergence. The former limit of postglacial submergence ranges from 42 to 65 m asl, constituting Holocene marine limit across the field area. Because raised marine landforms directly record the deglacial and sea level history of NE Melville Island, their age and elevation are presented in Sections 3.3.2 and 3.4.

Examples of well-preserved deltas range in elevation from 7 to 65 m asl within the field area. In several cases, deltas extend from meltwater channels that terminate at Holocene marine limit (Figure 3.4). These deltas display topset sand and gravel, foreset sand and pebbly sand, and bottomset silt with minor clay (Figure 3.5). However, due to ongoing emergence and seaward progradation, the topset beds commonly truncate earlier foreset beds. Most deltas are fossiliferous and provide important age-control for deglaciation and the establishment of postglacial RSL curves. All raised deltas have been incised by fluvial activity during subsequent postglacial emergence; however, enough of the original delta surface has often been preserved to allow for the identification and surveying of former sea levels.

Deltaic sediments are prominent on Sabine Peninsula, many of which take the form of telescoping, finger deltas that record progradation during postglacial emergence (Figure 3.6). These deltas range from 1.0 to 1.5 km wide, and can extend up to 5 km inland of the modern coastline where they sometimes mark marine limit (cf., Henoch 1964; Barnett *et al.* 1977; Forbes & Taylor 1998). The deltas consist of a thin veneer of topset braided-channel sand and gravel, foreset sand and pebbly sand, underlain by marine silty clay and bottomset silt and muddy sand (Forbes & Taylor 1998). Delta surfaces often display ice-wedge polygons and can be dissected by snowmelt gullying (Figure 3.6; Barnett *et al.* 1977). The prominent, linear progradation of the deltas appears to be favoured by rapid incision of rivers into the Sverdrup Basin bedrock as emergence progresses. This entrenchment has minimised lateral migration of channels, and maintained a constant trajectory for seaward growth as emergence continues. Persistent multi-year sea-ice also dampens coastal erosion (Barnett 1972; Barnett *et al.* 1977; Forbes & Taylor 1998).

Fine-grained nearshore sediments mantle the majority of the coastal plain below marine limit. These sediments consist of prodeltaic accumulations of fine sand and silt, and record the deposition of suspended sediment from retreating ice margins, concomitant with marine transgression. Poor drainage created by the fine texture of nearshore sediments produces wet meadows (recognisable as dark-toned areas on aerial photographs), earth hummocks, and low-centre polygons, which sometimes contain small ponds and lakes (Figure 3.4; cf., Dyke 1983; Edlund 1993).

Raised beaches are rarely well preserved within the study area even though sand and coarser-grained material is readily available. This is attributed primarily to a lack of fetch caused by pervasive sea-ice, destruction by subsequent mass movement, or a combination of both (cf., Section 2.2.2). More beaches are preserved toward modern sea level, which may record increased opportunity for wave action as the rate of marine regression decreased through the Holocene (i.e., rate decreases exponentially following deglaciation). Raised beaches are best preserved along the south coast of Hecla and Griper Bay, although sparse beaches have also been noted along the east coast of Sabine Peninsula. Because these landforms have such a limited extent, they are not represented on Figures 3.1a, b, and c.

3.2.4 Alluvium

Active alluvium in the study area is confined to modern floodplains of major rivers and has not been illustrated at the scale of the surficial maps used in this study. All of the remaining alluvium mapped on Figures 3.1a, b, & c is inactive, forming terraces left by the incision of former floodplains. Most of the inactive alluvium mapped in the study area flanks the modern sandurs along the east coast of Sabine Bay (Figures 3.1a & 3.7). For example, the Sabine River sandur covers ~ 50 km^2, and another immediately to the north covers ~ 61 km^2. Each of these sandurs is occupied by two braided rivers, which comprise the active alluvial surface. The rivers have individual channels that are up to ~ 100 m wide at peak discharge when they transport coarse- to fine-grained pebbly sand. Adjacent terraces are kilometres in width, are separated from each other by escarpments ≥ 1 m high, and commonly display paleochannels.

The remainder of the mapped inactive alluvium occurs in the terraces of the rivers that have formed the prograding finger deltas on Sabine Peninsula (Figures 3.1b & c). During forced regression, these channels have become deeply incised and display little sinuosity or bifurcation (Figure 3.6; Forbes & Taylor 1998). The floodplains of these entrapped rivers are dominated by fine- to medium-grained sand and silt (Barnett *et al.* 1977), and are flanked by inactive sandy alluvium that forms slightly higher (≥ 1 m), vegetated terrace surfaces.

3.2.5 Colluvium

Gelifluction is the most active slope process in the study area, occurring on most moderately inclined slopes composed of unconsolidated sediment (felsenmeer, residuum, till veneer, raised marine sediments). On the east coast of Sabine Bay, gelifluction is particularly active on the steeper slopes of the Weatherall Fm (Figure 3.8), and elsewhere is pervasive on the residuum of Sabine Peninsula. Thaw flow slides are particularly abundant on Christopher Fm (central Sabine Peninsula, Figure 3.2) because of this formation's high clay content and the presence of partial vegetation cover, which lengthens the period of active layer saturation (Barnett *et al.* 1977; Hodgson 1982; Vincent 1983). Below marine limit, on Christopher, Kanguk, and Canyon Fiord fms, slopes (~ 2°) are considerably more prone to slumping than equivalent slopes in similar material above marine limit because of the increased moisture content (Barnett *et al.* 1977). Because slope processes producing colluvium are nearly ubiquitous on residuum, colluvium is not mapped on Figures 3.1a, b, and c. In high-relief regions, such as Barrow and Cape Colquhoun domes on Sabine Peninsula, slopes are mantled by talus cones and colluvial aprons derived from frost shattered bedrock. However, the small aerial extent of this colluvium does not permit representation at the scale shown in Figure 3.1c.

3.3 ICE COVERAGE AND DEGLACIATION

3.3.1 Style

Although their distribution is sparse, local erratics, till blankets, mega-flutings, moraines and deglacial landforms (lateral and proglacial meltwater channels and morainal banks) record the passage of ice that once crossed the highest terrain within the study area (50 - 275 m asl; Figures 3.1a, b, & c). Local erratics are pervasive within the field area, whereas till blankets are confined to the south coast of Sabine Bay and inland of Sherard Bay (Figures 3.1a & c). Mega-flutings were noted on the NW tip of Sabine Peninsula (Figures 3.1c & 3.9; cf., Fyles 1965). They are oriented SW-NE and occur below marine limit along the coastline up to ~ 5 km inland. They range in size from 2 - 5 km long, 100 - 200 m wide, and 10 - 30 m high. They form gently sloping surfaces and have been dissected by postglacial fluvial activity. Their composition is dominantly

sandy with a lag veneer of gravel and boulders. Abundant granite boulders (< 50 cm diameter) were observed on the surface of these mega-flutings (P. Lajeunesse, pers. comm. 2002).

The deglacial configuration of ice margins on NE Melville Island is recorded principally by lateral meltwater channels, which consistently display a pattern of retreat, at right angles to the coast, toward the interior of the island. At several sites, meltwater channels terminate at ice-contact or ice-fed deltas, or the upper limit of littoral fill, that mark Holocene marine limit (Figures 3.1a, b, c, 3.4, & 3.12). Discussion of the style of deglaciation of the study area will proceed from south to north.

Along the south coast of Sabine Bay, nested lateral meltwater channels record the successive retreat of valley glaciers to the south and southeast toward the interior of the island. In the same area proglacial meltwater channels occur where local bedrock ridges were breached as they emerged from the thinning ice. South of Nias Point, nested lateral meltwater channels mark a distinct southeastward retreat and terminate seaward at a break in slope interpreted to be marine limit (Site A, Figure 3.1a). This break in slope can be traced southward to Liddon Gulf, indicating that, at the time of deglaciation, the isthmus between Hecla and Griper Bay and Liddon Gulf was flooded by the sea, dividing Melville Island in two (Figure 1.1b; Hodgson *et al.* 1984). In the same vicinity of Nias Point, other meltwater channels can be traced to ice-fed deltas marking marine limit (~ 54 m asl, Site B, Figure 3.1a).

Between Reid Point and the head of Sabine Bay, a series of linear channels up to 6 km long are visible on air photos. These channels are not structurally controlled and upon close inspection, they appear to have small meanders and do not remain continuous for the entire 6 km. Thus, for the most part, they are interpreted to be segmented (< 1 km long) lateral meltwater channels that display strong parallelism over an area of low relief. Elsewhere along this stretch of coastline nested lateral meltwater channels grade to marine limit (Site D), and record up-valley retreat to the southeast towards the Edmund Lyons Hills. Inland of the head of Sabine Bay, two sinuous, low-amplitude morainal banks (Site E, Figure 3.1a) at similar elevations (< 42 m asl) occur within 2 km of each other. Lateral meltwater channels record southward and eastward retreat of ice lobes from these morainal banks.

Along the east coast of Sabine Bay, widespread lateral meltwater channels document southeast retreat inland from the coast (Figure 3.1a). Along a local bedrock ridge (> 260 m asl), lateral meltwater channels record progressive thinning of ice both to the north and to the south (Sites F & G, respectively, Figure 3.1a). Proglacial channels also mark sites where the ridge was breached by meltwater flowing northward as the ridge emerged from the thinning ice (Figure 3.10). On the northern side of the ridge, two erratic sandstone boulders (~ 5 m in diameter), lie atop a sinuous, low-amplitude morainal bank at < 61 m asl (Figure 3.11; Site H, Figure 3.1a). Ice retreated from this point southward toward the local bedrock ridge. On the south side of the ridge, lateral meltwater channels also record the retreat of ice up the Sabine River valley to the southeast (Site I; Figure 3.1a).

To the north, lateral meltwater channels document up-valley retreat of ice into the St. Arnaud Hills (Figure 3.1b). Through the isthmus connecting Eldridge and Sherard bays, ice retreated southward. Lateral meltwater channels mark the retreat of ice in a sequential fashion onto two southeast-facing cuestas (Site J, Figure 3.1b). On each of these cuestas (Sites K & L, Figure 3.1b), proglacial meltwater channels mark the points at which the cuestas were breached along the retreating ice margin. In the centre of the St. Arnaud Hills (Site M, Figure 3.1b), a series of lateral meltwater channels also marks the retreating western margin of ice onto higher topography (160 m asl). Along the south coast of Sherard Bay, sparse lateral meltwater channels depict similar retreat of valley glaciers into the interior (to the south and southwest; Sites N & O, Figure 3.1b).

Deglacial landforms are rare for most of northern Sabine Peninsula, north of Eldridge and Sherard bays, where the topography is dominated by dendritic drainage systems. In particular, they are almost entirely absent on bedrock that has weathered to a fine-grained residuum, such as the soft shale of the Christopher Fm, despite the fact that it outcrops both above and below marine limit (Figure 3.2). In contrast, deglacial landforms have been preserved on the felsenmeer sandstone and silty shales of the Hassel and Kanguk formations, respectively, which outcrop toward the centre and northern part of the peninsula (Figure 3.2). At the widest point of the peninsula (Sites P, Q, R & S, Figure 3.1c), nested lateral meltwater channels mark the retreat of small valley glaciers into the interior (> 100 m asl). West of Drake Point, lateral meltwater channels also mark

ice retreat up-valley to the south and eventually southwest (Site T, Figure 3.1c). Near the tip of Sabine Peninsula, lateral meltwater channels mark the southward retreat of ice onto Barrow Dome (≤ 275 m asl; Site U, Figure 3.1c). Northwest of the dome, a pair of lateral meltwater channels terminates at marine limit and is flanked by two ice-contact deltas (Site V, Figure 3.1c). A single pair of lateral meltwater channels (Site W, Figure 3.1c) documents eastward retreat of ice towards Cape Colquhoun Dome (≤ 209 m asl).

3.3.2 Elevation and Age of Marine Limit

At many sites, meltwater channels descend to marine limit where their sediments deposited ice-contact or ice-fed deltas (Figure 3.4). This relationship demonstrates that ice retreat and the establishment of marine limit occurred concurrently. Thus, dating marine limit implicitly establishes a chronology for deglaciation in most Arctic settings (Andrews 1970). Molluscs are abundant within the field area. However, samples could not always be tied to marine limit and thus these samples commonly provide a minimum estimate on the date of deglaciation.

In the field area, marine limit was recorded by the upper limit of littoral fill, ice-contact or ice-fed deltas, and washing limits. Littoral fill forms a blanket (> 2 m thick) of fine sediments along long stretches of coast (Figure 3.12). Because gelifluction is an active process throughout the study area, any marine limit elevation based on the upper limit of littoral fill records a minimum estimate on the height of the sea at deglaciation. However, given the fact that the upper limit of the fill is often uniform (cf., Figure 3.12), it is assumed to be within a few meters of the deglacial sea level. Ice-contact or ice-fed deltas occur only intermittently in the study area and were also formed at the ice margin. They consist of topset gravel and sand, coarse- to fine-grained foreset sand and silt, containing cobbles and pebbles, and bottomset silty-clay (Figure 3.13). Because Holocene fluvial processes have eroded and dissected these deltas, and in most cases removed the topset beds, any marine limit elevation based on the height of a delta is also a minimum estimate on the height of the sea at deglaciation. Washing limits are also sparse in the study area and also represent a minimum estimate on the height of the sea at the time of deglaciation because of overriding gelifluction deposits. Marine limits and associated deglacial dates are discussed from south to north.

Marine limit was surveyed at five locations along the south coast of Sabine Bay where littoral fill forms a uniform upper limit (Figure 3.12). South of Nias Point, the upper limit of fill marks marine limit at 54 m asl (Figure 3.14). Valves of *Hiatella arctica* were collected from sand and silt at 51 m asl, approximately 200 m seaward of marine limit, and dated 10,250 ± 80 BP (TO-9797, Table 3.1; Site 11, Figure 3.14). This sample is the oldest postglacial radiocarbon date along the south coast of Sabine Bay (collected in this study) and provides a minimum estimate on the date of deglaciation for the south coast of Sabine Bay. East of Reid Point, the summit of littoral fill marks marine limit at 55 m asl (Figure 3.14). Valves of *H. arctica* were collected at 46 m asl from fine sand and silt, 3 km to the northwest (seaward) (Site 14, Figure 3.14). This sample dated 10,080 ± 70 BP (Beta-162031, Table 3.1) and provides a minimum age estimate for the 55 m asl RSL, and hence for local deglaciation. Finally, near the head of Sabine Bay, two more marine limits were surveyed. The toe of a fan delta marks marine limit at 53 m asl (Figure 3.14), whereas farther east, a bench, approximately 50 m down-valley from lateral meltwater channels in a tributary valley of the Sabine River, marks marine limit at 42 m asl (Figure 3.14).

On the east coast of Sabine Bay, two measurements of marine limit indicate that the elevation of marine limit increases to the northeast. At one site, the uppermost washing limit reaches 57 m asl, whereas ~ 3 km east, the uppermost delta marks another marine limit at 61 m asl (Figures 3.14 & 3.13). Less than 2 km to the north of the delta, one valve of *H. arctica* was collected at 51 m asl from massive silty-clay (Site 18, Figure 3.14) and dated 9350 ± 70 BP (TO-9800, Table 3.1), providing a minimum estimate on the date of deglaciation for the east coast of Sabine Bay. Approximately 15 km to the north, paired valves of *H. arctica* were collected at 24 m asl and dated 9960 ± 70 BP (TO-9818, Table 3.1; Site 15, Figure 3.14). This sample was recovered from pebbly fine sand interpreted to be foreset beds. It is the oldest postglacial date along this coast and, although it can only be tied to a RSL of greater than 32 m asl, its age provides a better estimate on the date of deglaciation than TO-9800 (9.4 ka BP) collected 27 m higher.

Marine limit again increases to the northeast. Southeast of the head of Weatherall Bay (West Arm), the highest point on a truncated delta represents a minimum estimate on marine limit at 65 m asl. This (along with marine limit in Eldridge Bay) is the highest

surveyed marine limit in the study area (this study; Figure 3.14). Paired valves of *H. arctica* were collected in growth position from blue silty-clay within the delta and these sediments are considered to be distal foreset or proximal bottomset beds (Site 2, Figure 3.14). This sample dated 10,510 ± 90 BP (TO-9799, Table 3.1) and provides a minimum estimate on the date of deglaciation for the West Arm of Weatherall Bay.

No marine limit features were surveyed along the north coast of Sabine Bay, in the St. Arnaud Hills. However, paired valves of *H. arctica* were collected at 30 m asl from well-sorted sand containing pebbles (< 3 cm diameter) interpreted to be truncated foreset beds (Site 8, Figure 3.14). The sample dated 10,370 ± 70 BP (TO-9820, Table 3.1) and although it represents an unknown RSL of greater than 31 m asl, it is the best estimate on the date of deglaciation for the north coast of Sabine Bay.

Marine limit was surveyed at three locations along the east coast of Eldridge Bay. The upper limit of marine fill rises to 55 m asl (Figure 3.14). Less than 1 km seaward, paired valves of *H. arctica*, in growth position, were collected at 46 m asl (Site 3, Figure 3.14). The sample was recovered from clayey-silt with layers of sand representing distal foreset or bottomset beds. This sample dated 10,480 ± 70 BP (Beta-162033, Table 3.1) and represents a former RSL of > 47 m asl, likely 55 m asl (marine limit). Farther inland, the limit of littoral fill rises still higher marking marine limit at 65 m asl (Figure 3.14). Less than 2 km seaward, paired valves of *H. arctica* were collected at 36 m asl from fine silt in truncated foreset beds and dated 10,540 ± 80 BP (TO-9828, Table 3.1; Site 1, Figure 3.14). This sample is the oldest postglacial date in the study area and represents a RSL of > 41 m asl, and likely 65 m asl (marine limit), providing a minimum estimate on the date of deglaciation in Eldridge Bay. Finally, a washing limit marks marine limit at 60 m asl (Figure 3.14). Less than 1 km seaward, valves of *H. arctica* were collected at 52 m asl from well-sorted fine sand with pebbles (< 3 cm diameter) and dated 10,380 ± 80 BP (TO-9794, Table 3.1; Site 7, Figure 3.14). Three other samples of *H. arctica* (sites 4, 9, & 10, Figure 3.14, Table 3.1), not associated with specific RSLs but likely dating deglaciation in Eldridge Bay, were collected from the foreset beds of three deltas along this coast. One sample was collected at 36 m asl and dated 10,420 ± 70 BP (TO-9827, Table 3.1; Site 4, Figure 3.14). This sample represents a RSL of > 39 m asl, and likely 60 m asl (marine limit). The second sample was collected at 6 m asl and dated 10,360 ±

80 BP (TO-9791, Table 3.1; Site 9, Figure 3.14). This sample represents a RSL of > 10 m asl, and likely 65 m asl (marine limit). The final sample was collected at 37 m asl and dated 10,270 ± 90 BP (Beta-162034, Table 3.1; Site 10, Figure 3.14). This sample represents a RSL of > 37 m asl, and likely 55 m asl (marine limit).

In Sherard Bay, the summit of littoral fill marks marine limit at 64 m asl (Figure 3.14). Approximately 200 m downslope, valves of *H. arctica* were collected at 53 m asl from bedded sand with silty-clay layers, interpreted as distal foreset beds. This sample dated 10,240 ± 80 BP (TO-9801, Table 3.1; Site 12, Figure 3.14), thus providing a minimum estimate on the 64 m asl RSL. Approximately 2 km seaward, valves of *H. arctica* were collected from sand above foreset beds at 46 m asl, and dated 10,400 ± 70 (TO-9811, Table 3.1; Site 5, Figure 3.14). This is the oldest postglacial date in Sherard Bay and, although it cannot be tied to a specific RSL, its age provides a better estimate on the date of deglaciation of Sherard Bay than TO-9801 (10.2 ka BP, collected 7 m higher) and is also considered a better minimum age estimate on the 64 m asl marine limit.

Toward the tip of Sabine Peninsula, marine limit elevations decrease slightly. Southwest of Drake Point, the highest point on a thin veneer of deglacial sediments represents a minimum estimate on marine limit at 50 m asl (Figure 3.14). Paired valves of *H. arctica* were collected from silty-clay and dated 10,390 ± 80 BP (Beta-162035, Table 3.1; Site 6, Figure 3.14) thus providing a minimum estimate on the date of deglaciation for the east coast of Sabine Peninsula. North of Barrow Dome (near the tip of Sabine Peninsula), the highest point on an ice-contact delta marks marine limit at 59 m asl (Figure 3.14). Fragments of *H. arctica* were collected at 41 m asl within this delta from finely-bedded fine sand. The sample dated 10,180 ± 70 BP (TO-9829, Table 3.1; Site 13, Figure 3.14) and provides a minimum estimate on the date of deglaciation for the tip of Sabine Peninsula and a close age for the 59 m RSL.

3.4 RELATIVE SEA LEVEL HISTORY

This section presents the elevation and age of RSLs below marine limit on NE Melville Island. Following deglaciation, ongoing emergence of the coastline led to the formation of progressively lower RSLs marked by deltas and raised beaches.

Radiocarbon dating of widespread mollusc samples, complemented by driftwood and organic samples, collected from raised marine deposits have provided a chronological framework for the postglacial emergence of NE Melville Island. These dates are grouped into three areas: S. Sabine Bay, E. Sabine Bay, and Eldridge Bay. The advantage of presenting three separate areas is that this limits the effects of differential emergence across the entire area, allowing the construction of site-specific postglacial RSL curves (cf., Section 4.2.3).

3.4.1 S. Sabine Bay

Eleven samples of molluscs, driftwood, and organic material were collected along the south coast of Sabine Bay below marine limit (55 m asl) within a radius of 10 km. They range in age from 9.8 to 0.1 ka BP, and in elevation from > 31 m to < 1 m asl, and are presented in Table 3.2 and Figure 3.15. Three mollusc samples (*H. arctica*, *M. calcarea*, and *Astarte* sp.; Sites 17, 24, & 29) and one sample of organic material (Site 31) were collected from the foreset beds of four deltas consisting of interbedded sand and gravel. In the case of the mollusc samples, the delta surfaces have been eroded an unknown amount, therefore these samples date higher, unknown RSLs. The organic sample (Site 31) dates a 6 m asl RSL. Of the seven driftwood samples, one was collected embedded in the floodplain of an ephemeral stream at 9 m asl (Site 30), one was collected from a deflated surface above foreset beds and provides a maximum age for its elevation (Site 28), and another was collected from an embedded position within foreset beds and is assumed to have sunk, thus dating a higher, unknown RSL (Site 20). The other four driftwood samples were collected just above high tide, and below 2 m asl (Sites 33, 34, 35, & 37). Two of these samples (Sites 34 & 37) were collected above an erosional microcliff (< 20 cm high; Figure 3.16) that typifies many locations along this coastline and dated 760 ± 50 (Beta-162029, Table 3.2) and 110 ± 60 BP (UL-2580, Table 3.2). The microcliff separates the modern tidal flat from darker, lichen-covered terrain above and appears to be undergoing active erosion by the sea. Sample UL-2580 (Site 37) represents the youngest postglacial date in this study. However, because of fluctuations in the production of ^{14}C during the past 450 calendar years, a radiocarbon date within this time period cannot be assigned a single calendar age but rather has a range of possible

ages. Thus, sample UL-2580 (Site 37) could date anywhere from 0 - 155, 180 - 195, or 205 - 290 calendar years BP (cf., Bradley 1999).

3.4.2 E. Sabine Bay

Eight samples of molluscs and driftwood were collected along the east coast of Sabine Bay below marine limit (57 to 61 m asl) within a radius of 10 km. They range in age from 9.9 to 2.1 ka BP, and in elevation from > 36 m to 5 m asl, and are presented in Table 3.3 and Figure 3.17. One sample of *H. arctica* (Site 21, Figure 3.17) was collected from foreset sand, whereas two other samples of *H. arctica* (Sites 16 & 19) were collected from the bottomset beds of two deltas. In all three cases, the delta surfaces have been eroded an unknown amount, therefore these samples date higher, unknown RSLs. Two other mollusc samples (*M. calcarea* and unidentified fragments; Sites 22 & 23) were collected from massive deposits at 15 m asl and 22 m asl, respectively. Although related sea levels for these two samples are uncertain, the *M. calcarea* shells were paired and both samples were recovered with periostrichum intact and were thus determined not to have been disturbed. These samples also date higher, unknown RSLs. Two of the driftwood samples (Sites 26 & 27) were collected from surfaces above sandy foreset beds and provide maximum ages for their elevations, whereas the third driftwood sample (Site 32) was collected from an embedded position in a dry stream bed at 5 m asl. No driftwood was found below 1 m asl in this locality, as was the case both in S. Sabine Bay, and in Eldridge Bay.

3.4.3 Eldridge Bay

One sample of *M. calcarea* and one sample of driftwood were collected along the east coast of Eldridge Bay below marine limit (55 - 65 m asl). These two samples are presented in Table 3.4 and Figure 3.18, and, along with the six marine limit samples (Figure 3.14, Table 3.1), were collected within a radius of 5 km. The *M. calcarea* sample was collected from foreset beds at 19 m asl and dated 7780 ± 60 BP (TO-9792, Table 3.4; Site 25, Figure 3.18). As with the previous cases, the delta surface had been eroded an unknown amount, therefore this sample dates a higher, unknown RSL. The driftwood sample was collected < 6 m inland from high tide at < 1 m asl, and dated 160 ± 50 BP

(Beta-162032, Table 3.4; Site 36, Figure 3.18). Again, because of fluctuations in the production of ^{14}C during the past 450 calendar years, a radiocarbon date within this time period cannot be unequivocally assigned a single calendar age range but rather has several possible ages within its measured limit of one standard deviation. Thus, sample Beta-162032 (Site 36) could date anywhere from 0 - 30, 70 - 230, or 240 - 290 calendar years BP (cf., Bradley 1999).

3.4.4 Sherard Bay

One additional driftwood sample was collected in Sherard Bay below marine limit (64 m asl). This sample was collected from a deflation surface above foreset beds at 36 m asl and dated 8700 ± 70 BP (TO-9802, Site 18a). This sample will be used to draw isobases within the study area (cf., Section 4.2.4).

Legend for Figures 3.1a, b, & c.

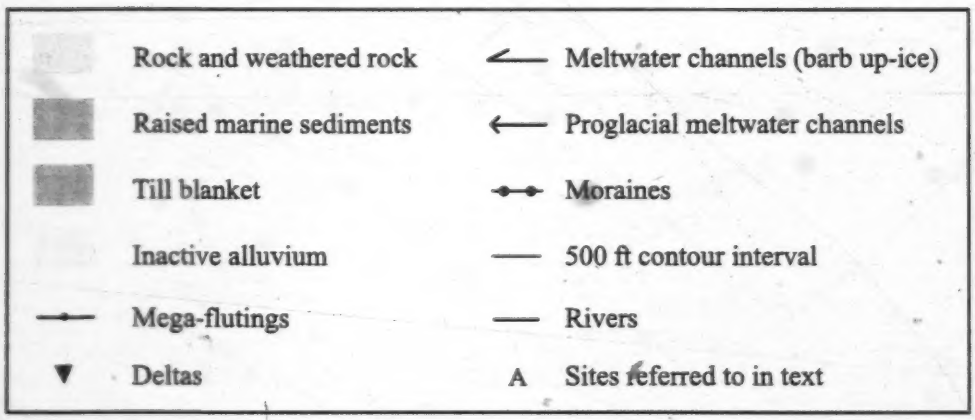

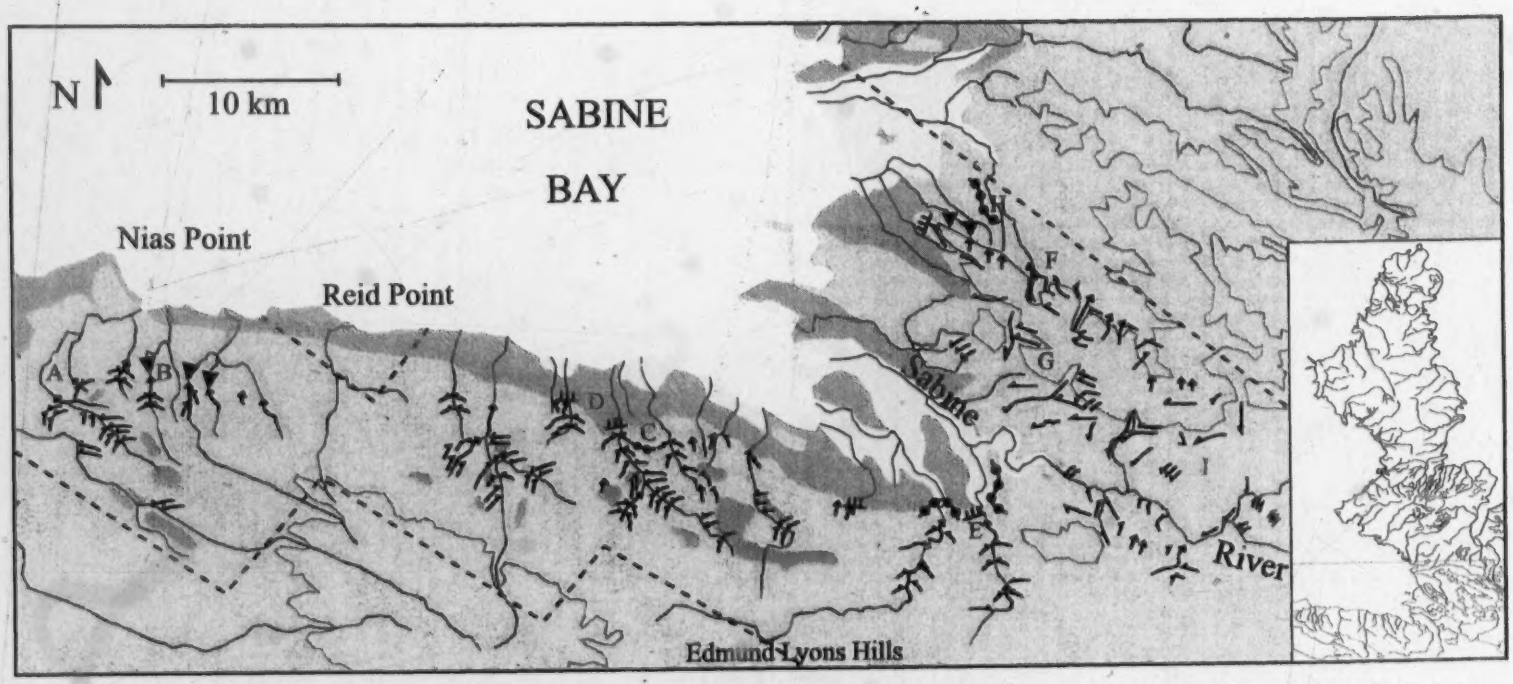

Figure 3.1a. Sabine Bay, showing distribution of surficial sediments and landforms discussed in text. Note that landforms were not mapped beyond the dashed line as this is the extent of the aerial photograph coverage. Surficial geology beyond this limit was mapped from the Landsat 7 image.

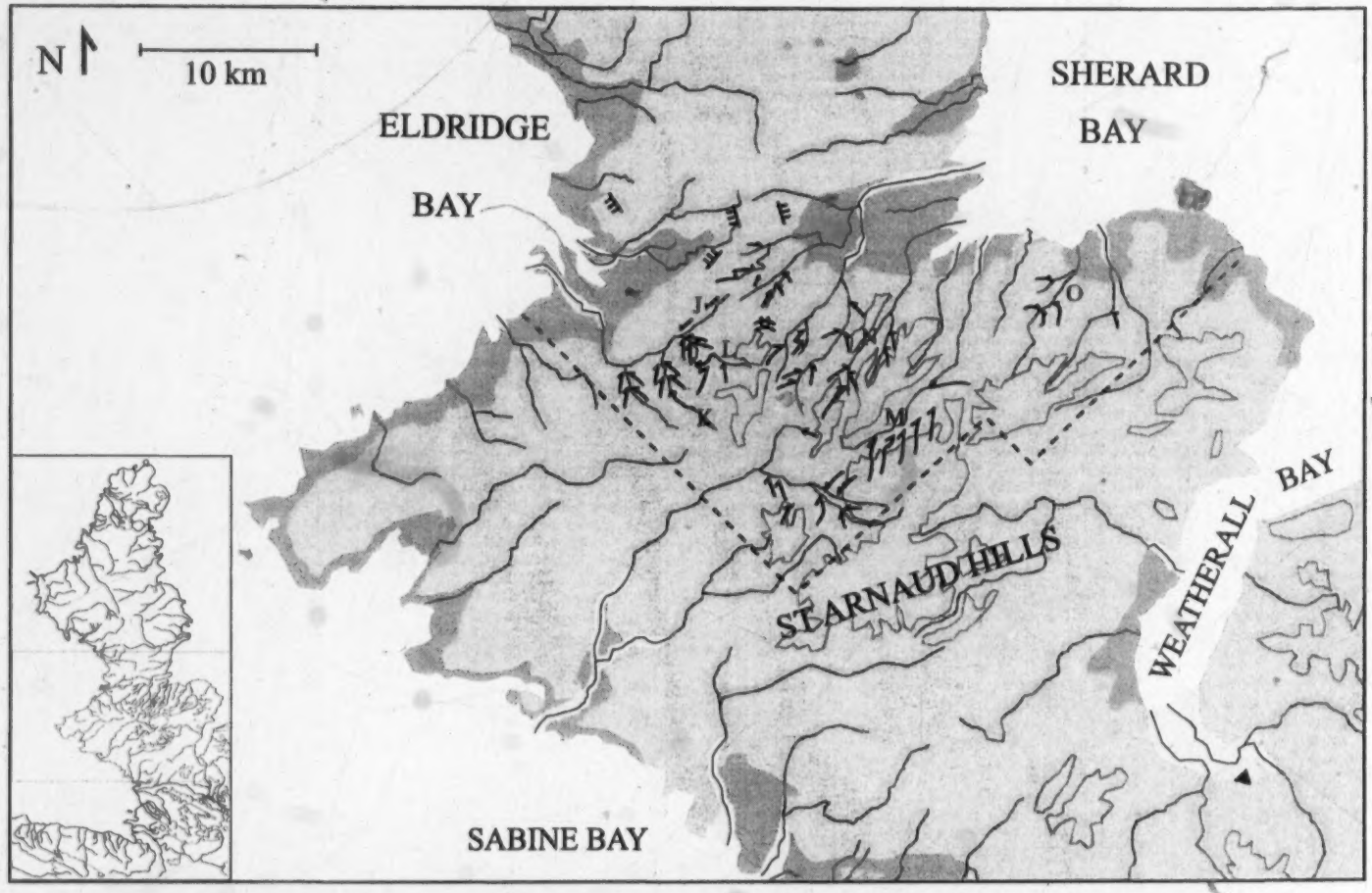

Figure 3.1b. Central Sabine Peninsula, showing distribution of surficial sediments and landforms discussed in text. Note that landforms were not mapped south of the dashed line as this is the extent of aerial photograph coverage. Surficial geology beyond this limit was mapped from the Landsat 7 image.

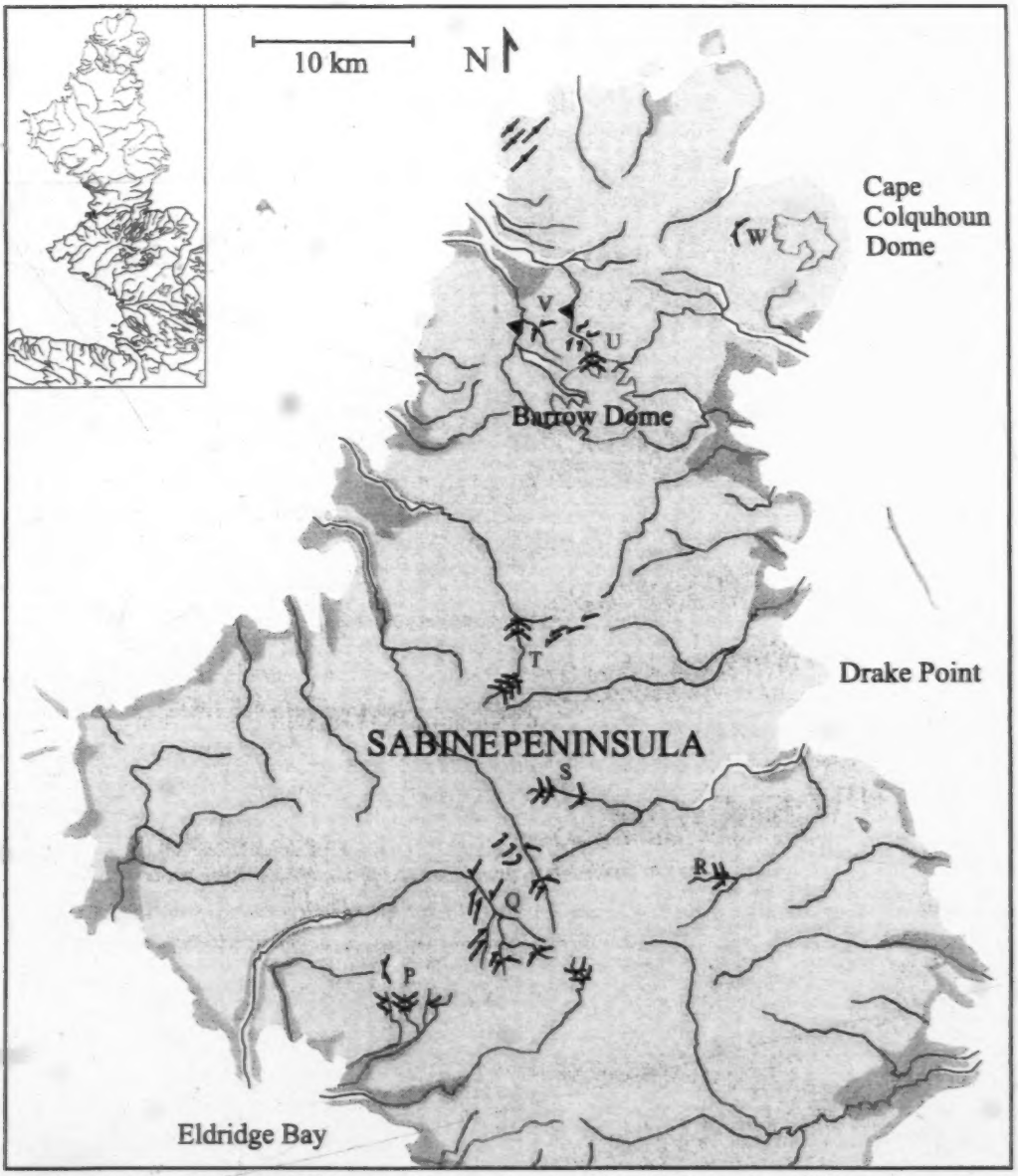

Figure 3.1c. Northern Sabine Peninsula, showing distribution of surficial sediments and landforms discussed in text.

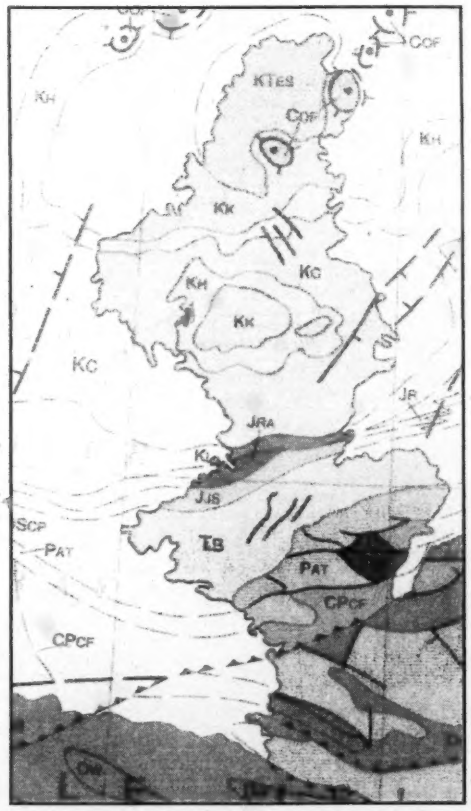

Figure 3.2. Bedrock formations of study area. (Source: Okulitch 1991).

Sverdrup Basin

KTES	Eureka Sound Group	PAT	Assistance & Trold Fiord fms
COF	Otto Fiord Fm	PBS	Belcher Channel & Sabine Bay fms
KK	Kanguk Fm	CPCF	Canyon Fiord Fm
KH	Hassel Fm		
KC	Christopher Fm		
KI & JRA	Isachsen Fm & Ringnes & Awingak fms		
JJS	Jameson Bay & Sandy Point fms		
TB	Bjorne Fm		

Franklinian mobile belt

DHB	Hecla Bay Fm
DGB	Griper Bay Fm
DW	Weatherall Fm

Figure 3.3. Periglacial stripes in weathered Hecla Bay Formation along the south coast of Sabine Bay. (Photo courtesy P. Lajeunesse.)

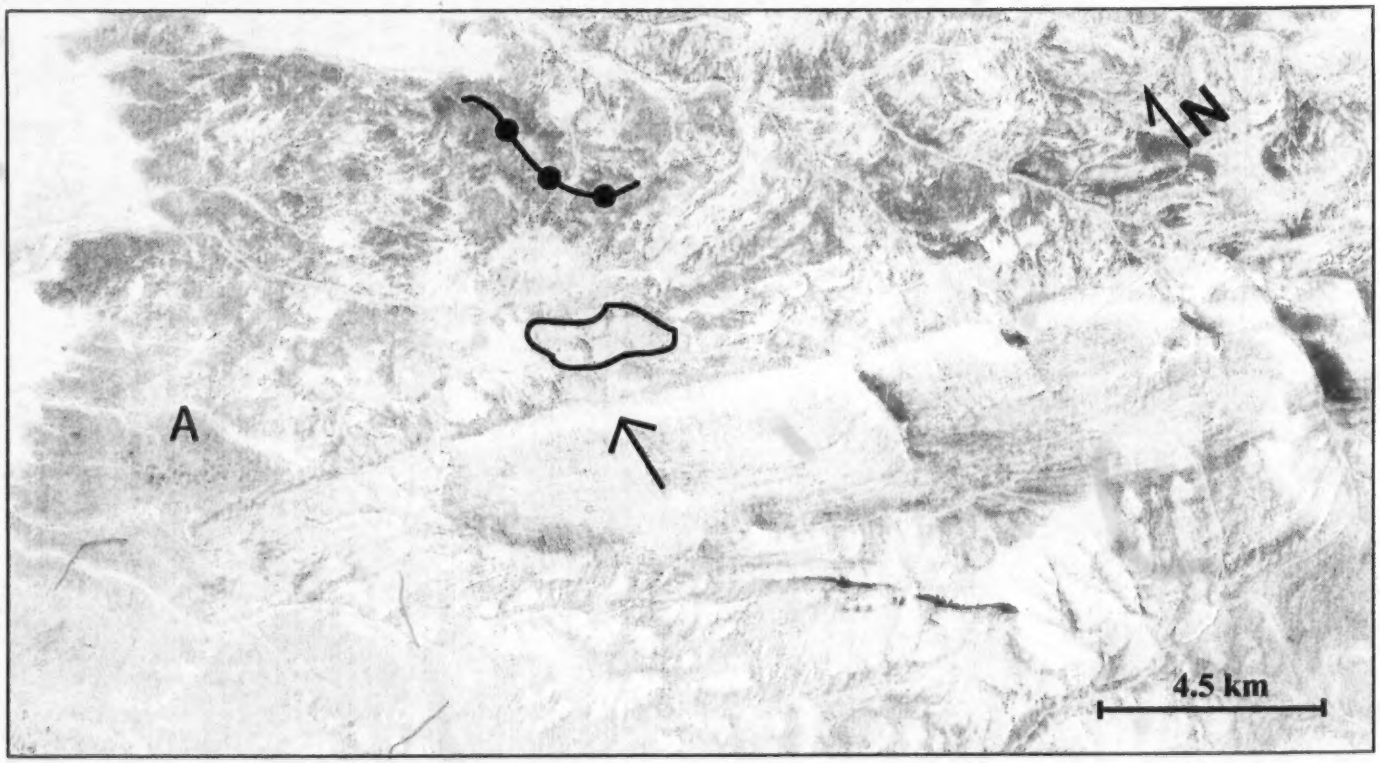

Figure 3.4. East coast of Sabine Bay showing morainal bank (dotted line), and proglacial meltwater channel (arrow) flowing northward off a local bedrock ridge to an ice-fed delta marking marine limit at > 61 m asl (highlighted area). Note also that poor drainage of nearshore sediments produces wet meadows (dark tones in left third of photograph) and low-centred polygons, which sometimes contain small ponds and lakes (site A).

Figure 3.5. Dissected delta on the south coast of Sabine Bay. Gently dipping foreset beds are visible on opposite side of stream. Samples 20 (black) and 24 (white) were collected from this site.

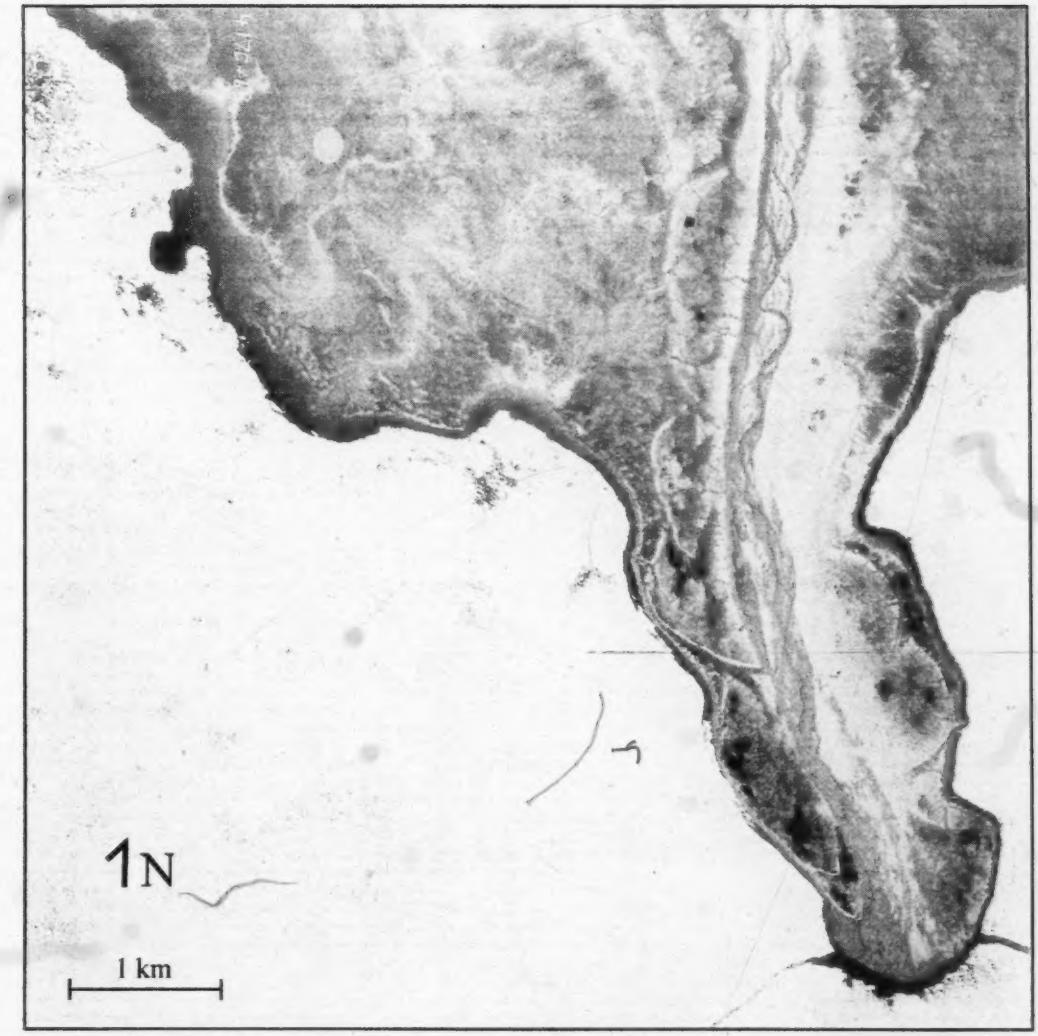

Figure 3.6. Telescoping finger delta at Chads Point, western Sabine Peninsula, recording progradation during postglacial emergence. Note polygonisation and snowmelt gullying on surfaces of former terraces and braided river confined to straight, incised channel.

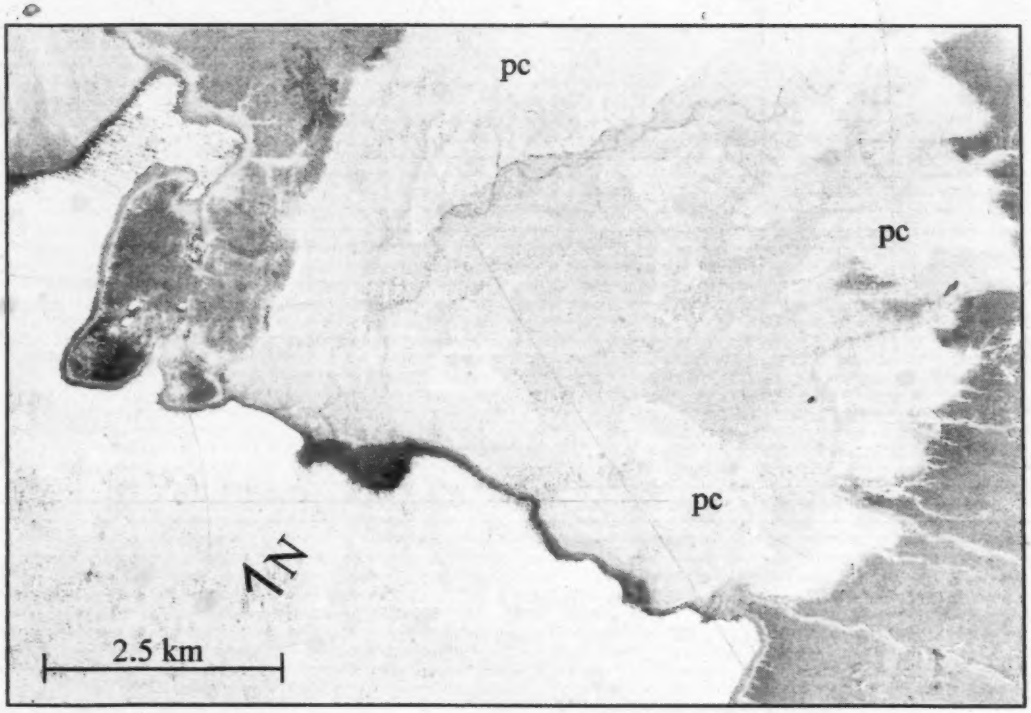

Figure 3.7. Modern sandur on the east coast of Sabine Bay. Note two braided streams that converge near the bay and paleochannels (pc) on former terrace levels (lighter toned) that are separated from the active channels by escarpments > 1 m high.

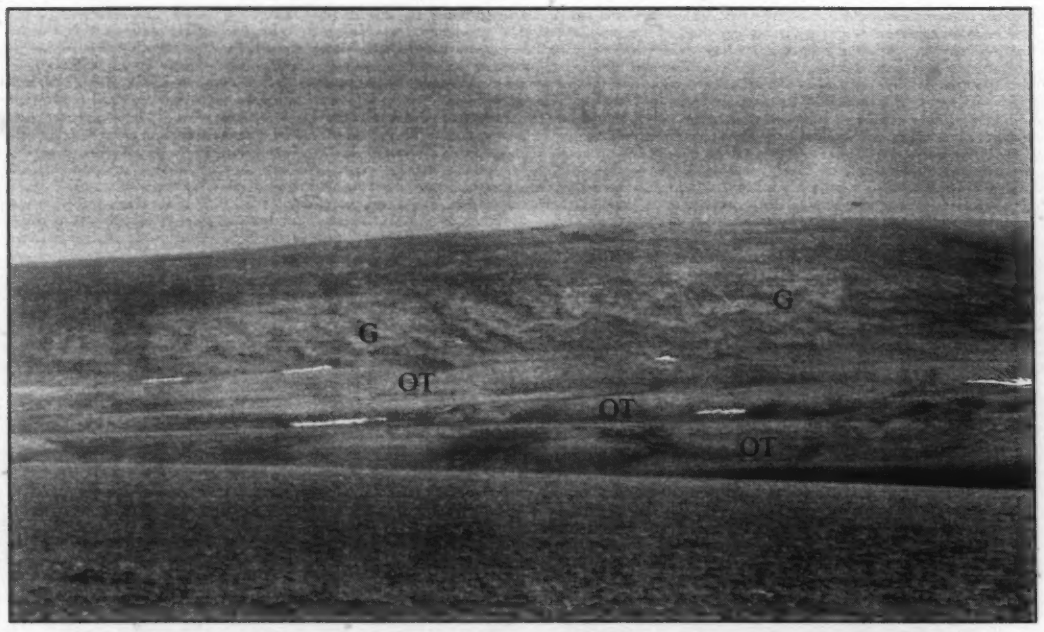

Figure 3.8. Gelifluction lobes (G) on exposed Weatherall Formation, east coast of Sabine Bay. Note outwash terraces (OT) in forefront, grading toward marine limit.

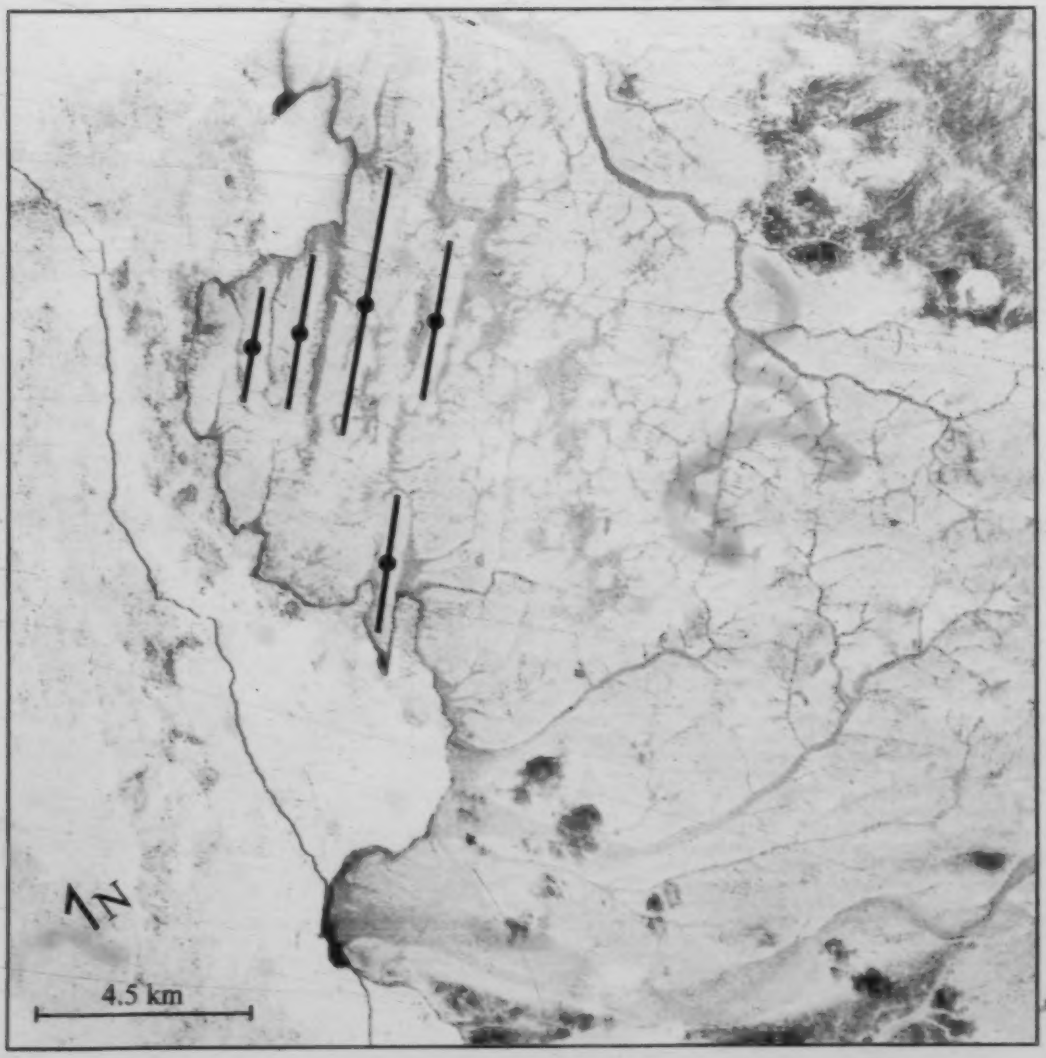

Figure 3.9. Mega-flutings trending SW-NE on NW Sabine Peninsula. The mega-flutings occur below marine limit and range in size from 2 - 5 km long, 100 - 200 m wide, and 10 - 30 m high.

Figure 3.10. Proglacial meltwater channel on the north side of a local bedrock ridge, east coast of Sabine Bay.

Figure 3.11. Sandstone erratics on a morainal bank, east coast of Sabine Bay.

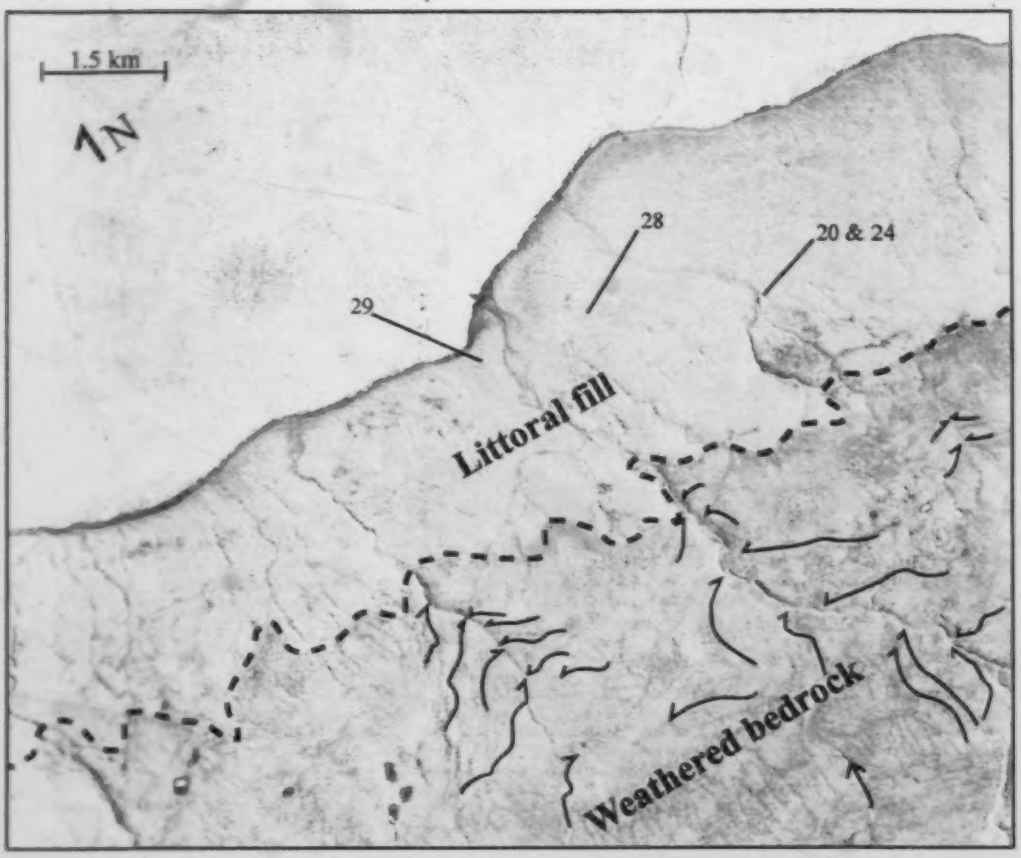

Figure 3.12. South coast of Sabine Bay showing littoral fill. These fine sediments form a blanket (< 2 m thick) with a uniform upper limit at ~ 55 m asl (marine limit) for a > 10 km stretch along this coastline and record a continuous ice margin inland of marine limit. Lateral meltwater channels (barb up-ice) show retreat of ice up-valley to the south. Locations of samples 20, 24, 28, & 29 are also shown.

Figure 3.13. Ice-fed delta marking marine limit (> 61 m asl) on the east coast of Sabine Bay. This delta has been eroded and dissected by postglacial fluvial processes. Topset beds are indistinct, whereas foreset beds consist of pebbly coarse sand and gravel.

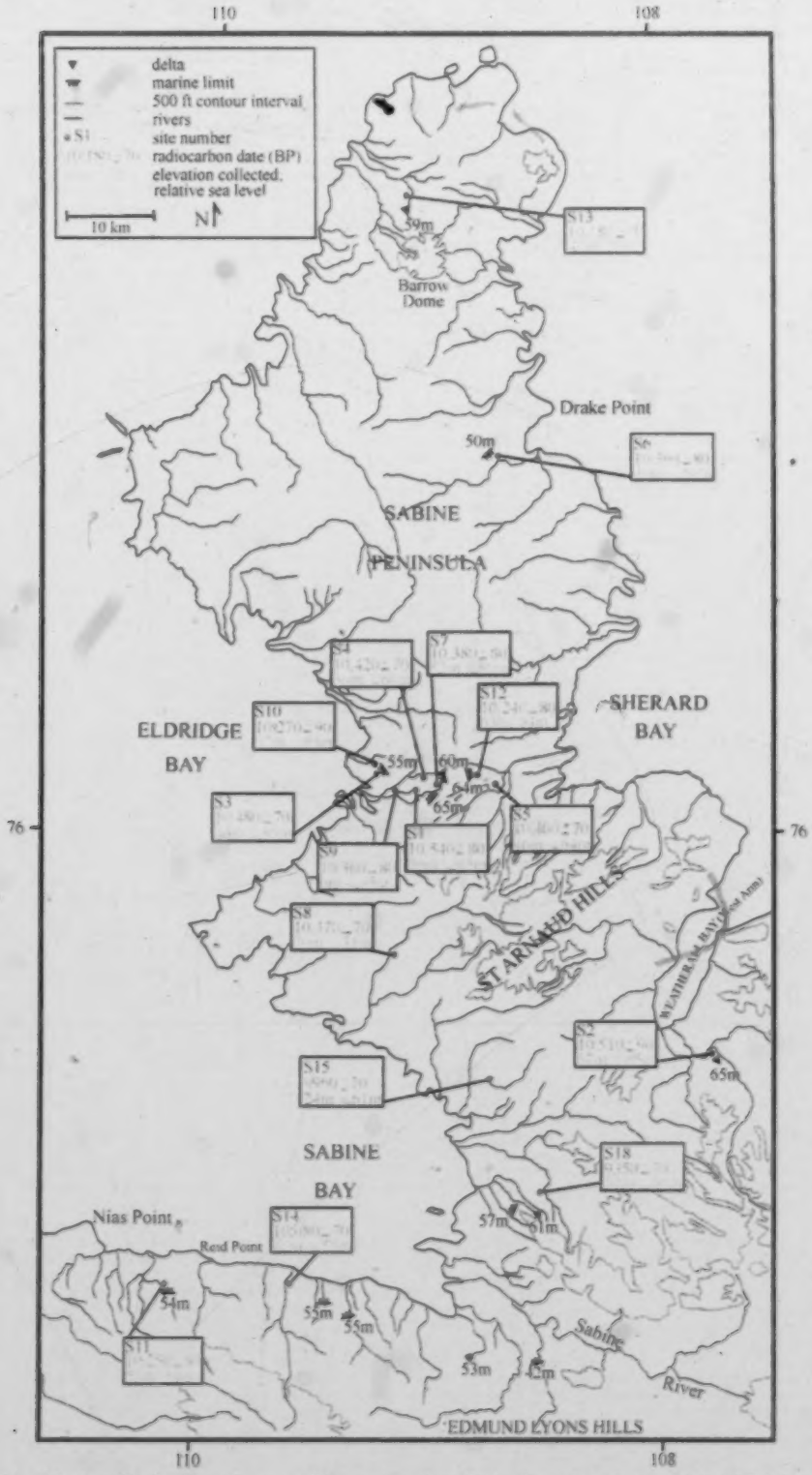

Figure 3.14. Marine limit elevations and associated radiocarbon dated-samples, NE Melville Island.

Table 3.1. Radiocarbon dates associated with marine limits, NE Melville Island. Location of sites displayed in Figure 3.14.

Site	Location	Laboratory Dating No.	Material	Age (radiocarbon years BP)	Description of Site	Enclosing Material	Sample Elevation (m asl)	Related RSL (m asl)	Latitude & Longitude
11	Nias Point	TO-9797	*H. arctica*	10,250 ± 80	deflation surface	sand & silt	51	54	N 75°30.755' W 110°18.013'
14	S. Sabine Bay	Beta-162031	*H. arctica*	10,080 ± 70	deflated surface on outside bend of large river	fine sand & silt	46	> 46 - = 55	N 75°31'08.3" W 109°35'24.7'
18	E. Sabine Bay	TO-9800	*H. arctica*	9350 ± 70	on flat surface affected by slumping and deflation	massive silty-clay w/ sand	51	> 51 - = 61	N 75°36'35.7" W 108°30'43.1"
15	E. Sabine Bay	TO-9818	*H. arctica*	9960 ± 70	deflation surface above foreset beds	fine sand & silt w/ pebbles (< 5 cm)	24	> 32 - = 61	N 75°43'51.0" W 108°44'15.6"
2	Weatherall Bay	TO-9799	*H. arctica*	10,510 ± 90	distal foreset beds or bottomset beds	blue silty-clay	57	> 65	N 75°45'01.8" W 107°45'51.3"
8	N. Sabine Bay	TO-9820	*H. arctica*	10,370 ± 70	foreset beds	well-sorted sand w/ pebbles (< 3 cm)	30	> 31	N 75°50'20.6" W 109°14'35.0"
3	Eldridge Bay	Beta-162033	*H. arctica*	10,480 ± 70	distal foreset beds or bottomset beds	clayey-silt with layers of sand	46	> 47 - = 55	N 76°04'02.1" W 109°12'46.9"
1	Eldridge Bay	TO-9828	*H. arctica*	10,540 ± 80	foreset beds	fine silt	36	> 41 - = 65	N 76°02'32.0" W 109°03'49.1"
7	Eldridge Bay	TO-9794	*H. arctica*	10,380 ± 80	deflation surface above foreset beds	well-sorted fine sand with pebbles (< 3 cm)	52	> 52 - = 60	N 76°03'01.0" W 109°02'28.5"
4	Eldridge Bay	TO-9827	*H. arctica*	10,420 ± 70	foreset beds	well-sorted fine sand w/ pebbles (< 1 cm)	36	> 39 - = 65	N 76°03'57.7" W 109°04'07.8"

Table 3.1. (continued) Radiocarbon dates associated with marine limits, NE Melville Island. Location of sites displayed in Figure 3.14.

Site	Location	Laboratory Dating No.	Material	Age (radiocarbon years BP)	Location	Enclosing Material	Sample Elevation (m asl)	Related RSL (m asl)	Latitude & Longitude
9	Eldridge Bay	TO-9791	*H. arctica*	10,360 ± 80	distal foreset beds	clayey-silt with layers of fine sand	6	> 10 - = 65	N 76°02'40.0" W 109°12'12.0"
10	Eldridge Bay	Beta-162034	*H. arctica*	10,270 ± 90	foreset beds	well-sorted fine sand	37	> 37 - = 64	N 76°04'13.6" W 109°13'48.8"
12	Sherard Bay	TO-9801	*H. arctica*	10,240 ± 80	distal foreset beds	bedded sand w/ silty-clay layers	53	64	N 76°03'04.7" W 108°51'09.2"
5	Sherard Bay	TO-9811	*H. arctica*	10,400 ± 70	surface above foreset beds	sand	46	> 46 - = 64	N 76°03'22.2" W 108°44'33.6"
6	Drake Point	Beta-162035	*H. artica*	10,390 ± 80	in slump block, ~ 1.5 m below initial surface	silty-clay	47	> 50	N 76°24'42.7" W 108°41'27.3"
13	Barrow Dome	TO-9829	*H. arctica*	10,180 ± 70	deflation surface above foreset beds	finely-bedded fine sand	41	> 59	N 76°41'08.8" W 109°07'38.7"

Table 3.2. Radiocarbon dates from S. Sabine Bay. Location of sites are shown in Figure 3.15.

Site	Laboratory Dating No.	Material	Age (radiocarbon years BP)	Description of Site	Enclosing Material	Sample Elevation (m asl)	Related RSL (m asl)	Notes	Latitude & Longitude
17	TO-9796	*H. arctica*	9820 ± 70	deflated surface above foreset beds	gravely sand	31	> 31 - < 55		N 75°31'00" W 109°32'00"
20	TO-9809	driftwood	8360 ± 90	above foreset beds	well-bedded fine sands	9	= 9	wet & partially decomposed	N 75°29'51.5" W 109°14'11.3"
24	Beta-162028	*M. calcarea*	7880 ± 60	foreset beds	well-bedded fine sands	13	> 13	with periostrichum	N 75°29'51.5" W 109°14'11.3"
28	TO-9826	driftwood	6130 ± 60	above foreset beds	bedded sands and silts	2	> 2		N 75°30.490' W 109°17.469'
29	TO-9795	*Astarte* sp.	6080 ± 60	deflated surface above foreset beds	sand	7	> 7		N 75°30'23.7" W 109°20'56.0"
30	Beta-162030	'driftwood	4420 ± 70	alluvial plain	sand	9			N 75°28.365' W 108°48.717'
31	TO-9815	terrestrial plant fragments	3660 ± 50	0.5 cm thick layer of organic material within foreset beds	fine sand and silt		6		N 75°28.483' W 108°48.119'
33	UL-2581	driftwood	870 ± 90	modern tidal flat	sand	< 2			N 75°31'57" W 109°50'44"
34	Beta-162029	driftwood	760 ± 50	above erosional microcliff ~10 m from coast	sand	< 1			N 75°29.468' W 108°59.560'
35	TO-9798	driftwood	650 ± 50	modern tidal flat	sand	< 1			N 75°32.165' W 109°43.393'
37	UL-2580	driftwood	110 ± 60	above erosional microcliff ~ 10 m from coast	sand	<1		embedded in vegetation	N 75°28'47" W 108°54'00"

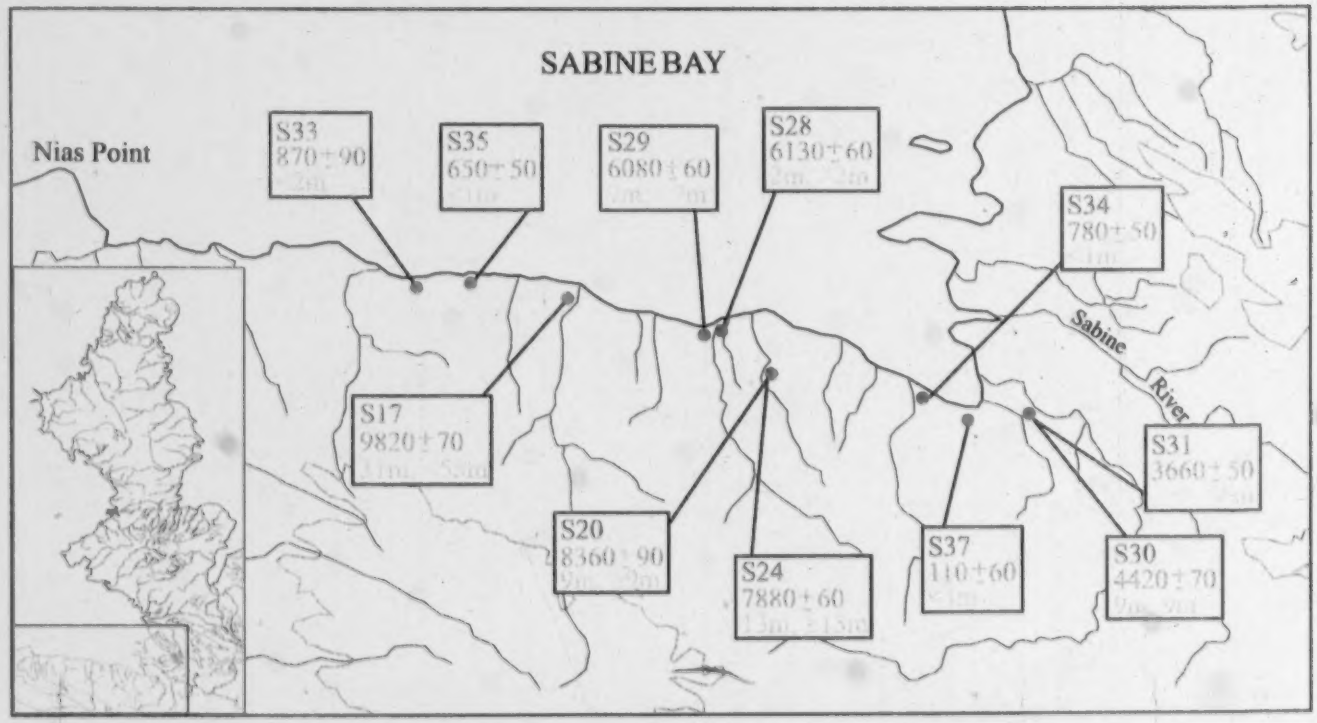

Figure 3.15. S. Sabine Bay, showing distribution of radiocarbon-dated samples cited in text.

Figure 3.16. Erosion microcliff along the south coast of Sabine Bay. The microcliff is < 20 cm high, and occurs at several sites along this coast. It separates the modern tidal flat from the darker, lichen-covered terrain above and appears to be undergoing erosion by the sea. Samples 34 & 37 were collected from such localities. (Photo courtesy P. Lajeunesse.)

Table 3.3 Radiocarbon dates from E. Sabine Bay. Locations of sites shown in Figure 3.17.

Site	Laboratory Dating No.	Material	Age (radiocarbon years BP)	Description of Site	Enclosing Material	Sample Elevation (m asl)	Related RSL (m asl)	Notes	Latitude & Longitude
16	TO-9808	*H. arctica*	9860 ± 80	pro-deltaic (bottomset) environment	massive silty-sand with pebbles	36	> 36 - < 61		N 75°43'26.2" W 108°43'20.6"
19	TO-9817	*H. arctica*	8470 ± 70	bottomset beds	blue-gray clay	33	> 33		N 75°38'41.5" W 108°34'12.2"
21	TO-9816	*H. arctica*	8170 ± 70	distal foreset beds	bedded silty-clay and fine sand	26	> 27		N 75°36'10.9" W 108°38'27.8"
22	TO-9819	*M. calcarea*	8100 ± 70	5 m high vegetated section	well-sorted fine sand	15	> 20	with periostrichum	N 75°36'04.4" W 108°44'24.5"
23	TO-9823	unidentified shell fragments	7890 ± 70	small section cut by stream	massive silty-clay	22	> 22	with periostrichum	N 75°36'41.3" W 108°39'14.3"
26	TO-9814	driftwood	6420 ± 60	deflation surface above foreset beds	bedded sand	19	19		N 75°29'41.6" W 108°34'26.6"
27	TO-9813	driftwood	6380 ± 60	deflation surface above foreset beds	bedded sand	15	> 15		N 75°33'16.7" W 108°47'23.5"
32	TO-9822	driftwood	2110 ± 50	dry braided stream bed	sand	5	5		N 75°37'22.6" W 108°42'48.1"

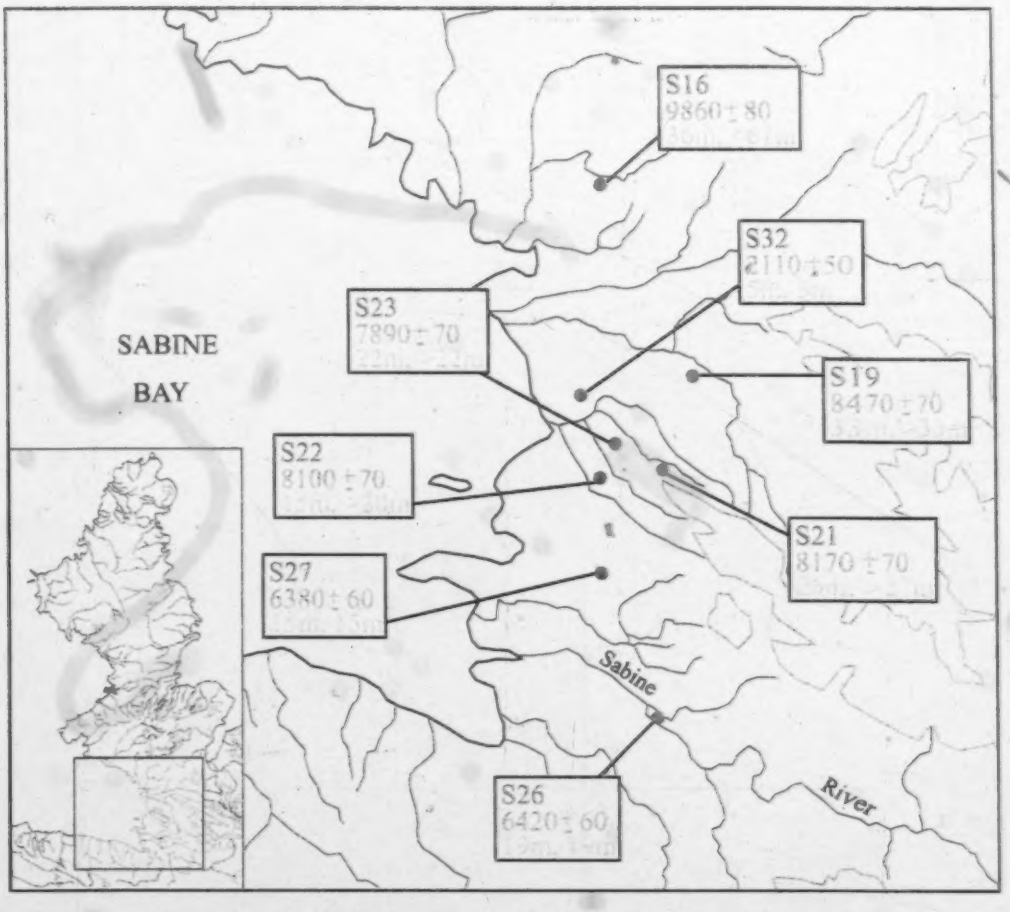

Figure 3.17. E. Sabine Bay, showing distribution of radiocarbon-dated samples cited in text.

Table 3.4 Radiocarbon dates from Eldridge Bay. Locations of sites shown in Figure 3.18.

Site	Laboratory Dating No.	Material	Age (radiocarbon years BP)	Description of Site	Enclosing Material	Sample Elevation (m asl)	Related RSL (m asl)	Latitude & Longitude
25	TO-9792	*M. calcarea*	7780 ± 60	foreset beds	interbedded silt & sand	19	> 19	N 76°04'52.0" W 109°15'42.2"
36	Beta-162032	driftwood	160 ± 50	vegetated surface 6 m from coast	sand	< 1		N 76°02'59.9" W 109°16'42.4"

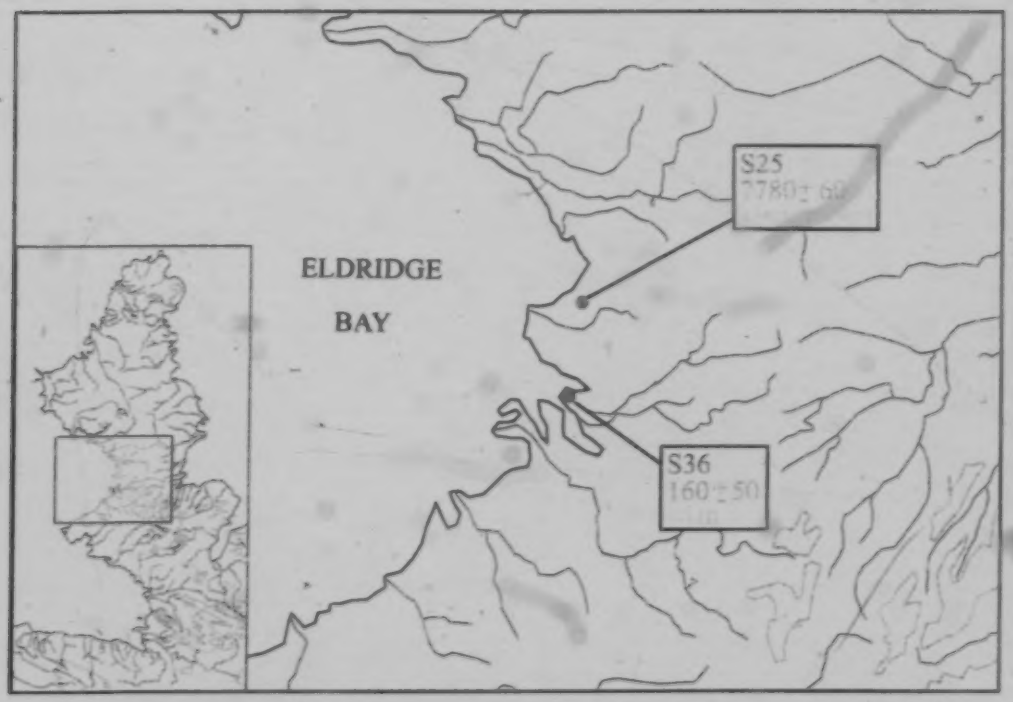

Figure 3.18. Eldridge Bay, showing distribution of radiocarbon-dated samples cited in text.

500 ft contour interval
rivers
• S1 site number
radiocarbon date (BP)
elevation of sample, relative sea level
10 km
N

Table 3.5. Radiocarbon date from Sherard Bay.

Site	Location	Laboratory Dating No.	Material	Age (radiocarbon years BP)	Description of site	Enclosing Material	Sample Elevation (m asl)	Related RSL (m asl)	Latitude & Longitude
18a	Sherard Bay	TO-9802	driftwood	8700 ± 70	deflation surface above foreset beds	well-sorted sand	36	36	N 76°02'58.7" W 108°40'58.5"

CHAPTER 4: DISCUSSION, REGIONAL SYNTHESIS AND FUTURE RESEARCH

4.1 INTRODUCTION

The objectives of this thesis, introduced in Chapter 1, were:

1) To determine the style of glaciation and deglaciation of NE Melville Island with respect to three potential sources of ice (the LIS, the IIS, and local island-based ice caps);
2) To determine the magnitude and timing of postglacial emergence across NE Melville Island with respect to these former ice masses, including the direction of dominant glacial unloading following the LGM; and,
3) To further clarify the form of the RSL curves from marine limit to modern sea level.

This chapter builds upon the results presented in Chapter 3, placing the style of and chronology of glaciation and deglaciation, as well as the nature of postglacial emergence and submergence across NE Melville Island, into a regional context. It concludes by addressing unresolved questions that have arisen from this thesis.

4.2 DISCUSSION

4.2.1 Late Quaternary Ice Coverage

Currently, the chronology of Late Wisconsinan ice build-up on NE Melville Island remains undetermined, as sub-till organics or ice-transported mollusc samples suitable for radiocarbon dating were not found. The existence of till blankets, moraines, mega-flutings, and erratics, as well as deglacial landforms such as morainal banks and meltwater channels, however, attests to pervasive glaciation of the study area. That some of these landforms extend to Holocene marine limit demonstrates coverage during the Late Wisconsinan when ice extended an unknown distance offshore into Hecla and Griper Bay and into Byam Martin Channel. Most significantly, the lack of far-traveled erratics (of either Laurentide or Innuitian provenance) above marine limit indicates that

the study area was glaciated by local island-based ice during the Late Wisconsinan. Although Laurentide till is widespread ~ 60 km to the south on Dundas Peninsula (Figure 1.6; Fyles 1967; Hodgson *et al.* 1984), there is no evidence that Laurentide ice extended to Hecla and Griper Bay. In the absence of ice flow indicators (striae), the pattern of ice advance is assumed to be opposite to the pattern of ice retreat (indicated primarily by lateral meltwater channels; cf., Section 4.2.2; Hodgson 1992; Bednarski 1998). If correct, the advance of ice across NE Melville Island was the product of radial outflow, at right angles to the coast, supplied from several coalescing ice centres located over interior uplands (Edmund Lyons Hills, St. Arnaud Hills, central Sabine Peninsula, and Barrow and Cape Colquhoun domes; Figure 1.1b).

Neither the till blankets nor the mega-flutings described in Chapter 3 (Figures 3.1a & c) can be strictly constrained to the Late Wisconsinan. The mega-flutings below marine limit on the northern tip of Sabine Peninsula (Figure 3.9) are oriented transversely to the most probable (offshore) direction of local ice flow during the last glaciation. Because they also contain abundant granite erratics, they are the only landforms in the study area attributed to non-local ice. It is considered unlikely that the granites were deposited by Innuitian ice because mapped granite dispersal trains from the Canadian Shield of SE Ellesmere Island (underlying the Prince of Wales Icefield, ~ 700 km NE of Melville Island; Trettin 1991) do not occur on Ellef Ringnes Island (> 200 km to the NE; Figure 1.1a), which lies across the flowline that would extend from the Shield to Melville Island (Atkinson 2003). Therefore, the granite erratics, and associated mega-flutings, presumably record a Laurentide ice advance from mainland Canada. Whether this ice advance is Late Wisconsinan or older has yet to be determined. However, an expansive late Wisconsinan, Laurentide ice shelf is recognised along southern Melville Island (Hodgson & Vincent 1984; Dyke & Prest 1987). A second ice shelf of similar size may also have advanced from the M'Clintock Ice Divide, extending through Byam Martin Channel along the island's east coast. If so, it could have reached the northern end of Sabine Peninsula and deposited the mega-flutings (J. England, pers. comm. 2002).

Conspicuous dendritic drainage (in particular on the Christopher Fm) and unaltered residuum characterise most of the study area. The paucity of glacial landforms (both erosional and depositional) and sediments, as well as far-traveled erratics (above

marine limit), indicate minimal erosion, transport and deposition by ice. This can be attributed to the widespread occurrence of protective, cold-based ice (cf., Dyke 1993) or to the fact that poor lithification of the bedrock (in particular within Sverdrup Basin) promotes rapid weathering that inhibits both the original formation and/or subsequent preservation of glacial landforms. Cold-based thermal regimes exist where the duration and thickness of ice cover are insufficient to promote the removal of pre-existing permafrost by geothermal heat and strain heat flow (Dyke 1993). Sparse till blankets along the south coast of Sabine Bay (Figure 3.1a) are likely the product of isolated warm-based thermal regimes. For example, most of these till blankets occur on the stoss side of local bedrock ridges where seaward ice flow would have undergone compression resulting in increased ice deformation and strain heating. This could have raised basal ice temperatures to the pressure melting point, causing the subsequent deposition of till blankets at these sites. Thus, for the most part, evidence indicates that the ice cover on NE Melville Island during the last glaciation was predominantly cold-based. If a warm-based thermal regime did exist during the last glaciation, it was likely confined to the localities where till blankets were noted.

4.2.2 Deglaciation and the Profile of Marine Limit

During deglaciation, two former seaways connected Hecla and Griper Bay to Liddon Gulf, and Eldridge Bay to Sherard Bay, dividing Melville Island into at least three smaller islands (Tozer & Thorsteinsson 1964; Hodgson *et al.* 1984). Lateral meltwater channels, morainal banks, and both ice-contact and ice-fed deltas (Figures 3.1a, b, & c) record the pattern of ice retreat. Although not preserved on all types of bedrock, lateral meltwater channels show ice retreat into the interior of the island, at right angles to the coast, toward several dispersal centres.

From the south coast of Sabine Bay, ice retreated southward and southeastward toward a former dispersal centre located in the Edmund Lyons Hills (south of the study area; cf., Hodgson *et al.* 1984). Once this ice had retreated from the sea, it stabilised on local bedrock ridges, before continuing to retreat southeastward. At Nias Point, proglacial meltwater channels breach a local bedrock ridge and extend to ice-fed deltas marking marine limit (Site B, Figure 3.1a). Further east along the same coast, the upper

limit of littoral fill forms an expansive and prominent marine limit at approximately 55 m asl (Figure 3.12). The uniform height of this fill, extending > 10 km along this coast, suggests that a continuous ice margin stood immediately inland of marine limit. Furthermore, morainal banks near the head of Sabine Bay (Site E, Figure 3.1a) mark the grounding lines of two former glaciers that temporarily stabilised in the sea before retreating both southward onto higher land and southeastward up the Sabine River valley, respectively. On the east coast of Sabine Bay, ice retreated southeastward, toward the interior of the island, to an unidentified ice centre outside of the study area. Another morainal bank records a grounding line during an interval of ice margin stability. During subsequent ice retreat from the coast, ice again stabilised on a local bedrock ridge and ice-fed deltas were deposited, marking marine limit at 61 m asl. The fact that morainal banks were noted near the head and along the east coast of Sabine Bay is likely due to the proximity of higher topography, which facilitated temporary stillstands during retreat from the sea.

Along the length of Sabine Peninsula, ice retreated radially from the coast onto local uplands where it eventually separated into several small ice caps before melting completely. Four 'late centres' of ice retreat are recorded on Sabine Peninsula: St. Arnaud Hills (> 200 m asl), central Sabine Peninsula (at its widest point; ≤ 152 m asl), and Barrow and Cape Colquhoun domes (≤ 275 m asl and ≤ 209 m asl, respectively). North of the Barrow Dome, lateral meltwater channels outlining a former glacier are flanked by two ice-contact deltas that mark marine limit. The lower topography on Sabine Peninsula, combined with its small area, likely favoured more rapid retreat than elsewhere on NE Melville Island.

The abundance of lateral meltwater channels throughout most of the study area indicates that cold-based ice was widespread during retreat (cf., Dyke 1993). Lateral meltwater channels are well-preserved on formations more resistant to weathering, such as the sandstone of the Franklinian mobile belt and the Hassel Fm, but are conspicuously lacking from fine-grained residuum such as that produced by weathering of the soft shale of the Christopher Fm. This difference might be attributed to more rapid postglacial weathering on lithologies such as the Christopher Fm (which is particularly prone to mass-wasting, cf., Section 3.2.5), or it might be indicative of subglacial processes

operating differently on specific lithologies (cf., Hodgson 1985, 1992). The morainal banks near the head and along the east coast of Sabine Bay are landforms often associated with well-developed subglacial drainage and relatively high sedimentation rates (cf., Ó Cofaigh *et al.* 1999). However, the low amplitude of the morainal banks implies that small amounts of debris had been entrained which could imply that they are products of cold-based ice which remained stable for an extended period of time (cf., Regimes 2 & 6, Powell 1984; Evans 1990).

Marine limits surveyed in this study range from 42 m asl (head of Sabine Bay) to 65 m asl (West Arm of Weatherall Bay and Eldridge Bay; Figure 4.1). In previous studies, marine limits were reported up to 82 m asl between Sherard and Weatherall bays (Figure 4.1; Henoch 1964; Tozer & Thorsteinsson 1964; McLaren & Barnett 1978). Across the study area, marine limit show a systematic rise to the northeast, from ~ 55 m asl along the south coast of Sabine Bay to between 65 and 82 m asl west of Weatherall Bay (Tozer & Thorsteinsson 1964; Figure 4.1). From this point, marine limit decreases northward to 50 m asl at Drake Point and 59 m asl near the tip of Sabine Peninsula (Figure 4.1). Assuming that marine limit across the study area is similar in age, this pattern would suggest that greater emergence has occurred to the east, between Weatherall and Sherard bays, a pattern that could not record isostatic recovery from local ice caps alone. Henoch (1964) was the first to suggest that this could be explained by glacioisostatic unloading from a non-local ice load over the QEI to the NE, now recognised as the IIS (Blake 1970). If, however, the IIS is not responsible for a rise in marine limit to the NE, then a tectonic contribution may have occurred. A swarm of earthquake epicentres occurs in Byam Martin Channel, off the eastern coast of Sabine Peninsula, and this area coincides with diapiric structures and dykes extending northeastward from northern Sabine Peninsula (cf., Section 1.2; Basham *et al.* 1977; Hasegawa 1977).

Near the head of Sabine Bay, two marine limits, at 42 m asl (this study) and 43 m asl (Tozer & Thorsteinsson 1964) are ~ 10 m lower than marine limit at 53 m asl (this study) surveyed less than 5 km away. Because of their proximity, it is unlikely that these discordant marine limits are the result of different ice load histories. Although no radiocarbon-dated samples are currently available, the lower marine limits (~ 42 m asl)

must represent later deglaciation in that part of the valley (cf., Andrews 1970), thus recording prolonged restrained rebound, and delayed entry of the sea. A later date of deglaciation would be in keeping with the relatively high topography at the head of Sabine Bay (≥ 240 m asl) and the proposed ice centre in the Edmund Lyons Hills.

4.2.3 Age of Marine Limit and Relative Sea Level Curves

The minimum age for entry of the sea across the study area ranges between 10.5 and 10.0 ka BP, indicating that marine limit is somewhat diachronous. Weatherall and Eldridge bays are the first sites to undergo deglaciation at 10.5 ka BP (Sites 1, 2, & 3, Figure 3.14). These dates also coincide with the highest marine limits observed within the field area (65 m asl). Elsewhere, deglaciation was widely underway by 10.4 ka BP, e.g., in Sherard Bay (Site 5, Figure 3.14), on Sabine Peninsula (Drake Point; Site 6, Figure 3.14), in the St. Arnaud Hills (Site 8, Figure 3.14), and along the south coast of Sabine Bay (Nias Point; GSC-338; Blake 1972; Hodgson *et al.* 1984). Deglaciation was underway at the northern tip of Sabine Peninsula by 10.2 ka BP, (Site 13, Figure 3.14), whereas deglaciation was delayed on the east coast of Sabine Bay until 10.0 ka BP (Site 15, Figure 3.14). The subdued topography and smaller areal extent of ice on central Sabine Peninsula likely lead to the earlier breakup of ice there, whereas areas of higher topography, such as the east coast of Sabine Bay (> 260 m asl) and Barrow and Cape Colquhoun domes (≤ 275 m asl and ≤ 209 m asl, respectively) supported late-lying ice for several centuries longer.

Postglacial RSL curves in and near glaciated regions can take three forms: continuous postglacial emergence, initial emergence followed by submergence, or continuous submergence (Clark *et al.* 1978; Quilan & Beaumont 1981; Dyke & Peltier 2000). The elevation of marine limit is largely dictated by the date of deglaciation and former ice thickness (Andrews 1970), but, near the former ice limit, additional factors come into play such as the migration of the peripheral forebulge, as well as eustatic and hydroisostatic effects (Clark *et al.* 1978; Quinlan & Beaumont 1981; Tushingham 1991; Dyke & Peltier 2000). In this thesis, only RSL change is presented, and issues such as forebulge migration are inferred from the shape of the curves. No attempt is made to

identify the specific contribution of eustatic sea level rise or hydroisostatic deformation to the shape of these curves (cf., Mörner 1976; Clark *et al.* 1978; England 1992).

Three new RSL curves have been constructed across the study area: S. Sabine Bay, E. Sabine Bay, and Eldridge Bay (Figures 4.2 - 4.4; Table 4.1). All radiocarbon-dated samples are listed in Tables 3.1 - 3.4 and locations of the samples are shown in Figures 3.14, 3.15, 3.17, and 3.18. Three separate curves were constructed in order to avoid inaccuracies that would inevitably result if all emergence across the study area were combined on a single curve (i.e., it limits the effects of differential emergence across the study area). Consequently, the dated samples for each curve fall within a radius of $\leq$ 10 km. In all three curves, mollusc samples fall below the curve because the dated organisms lived at some depth below their related RSLs. Where molluscs were collected from identifiable foreset beds, they are assigned to the best estimate of the former delta surface to which those beds rise. However, not all mollusc samples can be tied to specific RSLs and thus their elevation commonly represents a minimum estimate on the height of their corresponding sea level (especially in the case of outliers of deep-water rhythmites). In terms of driftwood samples, sea-ice push can cause small amounts of displacement upslope, whereas wave pitching of wood is minimal due to the brief open-water seasons and short wave fetches in this region (cf., Dyke 1998). Thus, in most cases, driftwood samples were assumed to fall within a few metres of the curve. Nonetheless, several driftwood samples (Sites 20 & 28, Figure 3.15; Site 27, Figure 3.17) are considered to lie below their associated RSL and are assumed to have sunk or been redeposited downslope. The sole organic sample (Site 31, Figure 4.2) was collected from foreset beds and its age is likely associated with a higher RSL. All radiocarbon-dated samples are plotted with two standard errors and are associated with a specific RSL where applicable.

Using the best samples from each of the three sites, an exponential curve of the form $y = ae^{bx}$ was fit to the data, where y is the elevation in metres, x is the age in ka years, a is a constant, and b is the proportionality constant (cf., Andrews 1970; Table 4.1). The coefficients of determination (R^2) for all three curves are above 0.98 (Table 4.1) indicating high correlation fits of the points to the curves. However, as the number of samples used to construct the curves is small (5 or 6), the coefficients of determination

become less significant. Nonetheless, by most standards, these curves represent a comparable level of control compared to sites reported elsewhere in Arctic Canada or Europe (cf., Forman *et al.* 1997; Dyke 1998). Keeping this in mind, the derivative of the equation for each RSL curve was used to calculate rates of emergence, and $(\log_e 2)/b$ (cf., Andrews 1970; Dyke 1998; Dyke & Peltier 2000) was used to calculate the half-lives (Table 4.1).

4.2.3.1 S. Sabine Bay

Six radiocarbon dates were used to construct the RSL curve for S. Sabine Bay extending from 10.4 ka BP to 0.9 ka BP (Figure 4.2). Local marine limit at 55 m asl and its age are well constrained at this site by two concordant dates of 10,380 ± 160 ka BP (GSC-338; Blake 1972; Hodgson *et al.* 1984) on *H. arctica* collected at 44 m asl near Nias Point, and 10.3 ka BP (Site 11). The shape of the curve from 10.4 ka BP to 0.9 ka BP is expressed by the equation $y = 1.40e^{0.36x}$, and is constrained by samples GSC-338, 11, 14, 30, 31, and 33 (Tables 3.1 & 3.2) as these samples are closely associated with their assigned RSLs. Between 4.5 and 9.5 ka BP, the curve is not well constrained due to the absence of dated samples that can be assigned to a specific RSL. Despite this, samples 17, 24, and 29 generally support the shape of the curve. Samples 20 and 28 are driftwood samples that must either have been redeposited downslope or they sank below their associated RSLs. Driftwood samples 34, 35, and 37 were not used to estimate the shape of the curve because they suggest that wood of a wide range of ages has collected near modern high tide since 0.9 ka BP and thus shape of the curve is different after 0.9 ka BP (see below).

The RSL curve for S. Sabine Bay (Figure 4.2) indicates the rate of initial emergence (at 10.4 ka BP) to be 2.1 m/century, and that this subsequently slowed to 0.30 m/century by the mid-Holocene after most of the ice had disappeared (cf., Walcott 1972). The half-life of this curve from 10.4 ka BP to 0.9 ka BP is calculated to be 1.9 ka. This exponential curve was not extended from 0.9 ka BP to present because the driftwood samples indicate that sometime after 0.9 ka, submergence of the coastline began to occur. For example, four driftwood samples, at < 1.5 m asl, range in age from 110 to 870 years BP (Sites 33, 34, 35, & 37). Within this sample population are pieces of modern wood,

evidently manufactured. If sample 33 accurately dates its contemporary shoreline, then sometime after 870 years BP, sea level reached a lowstand at an unknown depth from which it has transgressed to its modern position. This transgression could refloat and redeposit wood of intervening ages (0.9 ka BP to present) at the modern shoreline, which is consistent with the radiocarbon dating.

4.2.3.2 E. Sabine Bay

Five radiocarbon-dated samples were used to construct the RSL curve for E. Sabine Bay, which displays continuous emergence from 10.0 ka BP to at least 2.1 ka BP. The shape of the curve is expressed by the equation $y = 2.5e^{0.33x}$. Local marine limit (57 to 61 m asl) is constrained by samples 15, 16, and 18 (Tables 3.1 & 3.3). Although sample 18 is considerably younger (~ 0.5 ka) than samples 15 and 16, it is most likely associated with the 61 m asl marine limit delta because it was collected < 2 km away, whereas samples 15 and 16 were collected ~ 15 km away and could possibly be associated with a higher, unreported marine limit. Samples 26 and 32 constrain the central and lower parts of the curve, respectively. No samples are available to constrain the curve between 2.2 and 6.3 ka BP, whereas all the remaining samples between 6.5 and 9.3 ka BP fall below the curve. However, samples 19, 21, 22, and 23 are mollusc samples that date higher, unknown RSLs, generally supporting the shape of the curve. Sample 27 is a driftwood sample that is clearly a maximum age for its current elevation, and may also have been redeposited downslope or sunk below its RSL.

Initial emergence (at 10.0 ka BP) is calculated as 2.2 m/century, whereas by the mid-Holocene emergence had slowed to 0.43 m/century (Table 4.1). Ongoing emergence at 2.1 ka BP is calculated to have been 0.16 m/century (Table 4.1). The half-life of this curve is calculated as 2.1 ka (Table 4.1). Currently, it is unknown whether the modern coastline in this area is undergoing emergence or submergence as no samples younger than 2.1 ka BP were collected. Unlike S. Sabine Bay, low elevation driftwood (< 1 m asl) was not recovered along this coast.

4.2.3.3 Eldridge Bay

Six radiocarbon dates were used to construct the RSL curve for Eldridge Bay, which extends from 10.5 ka BP to the 0.2 ka BP (Figure 4.4). The shape of the curve is expressed by the equation $y = 0.46e^{0.47x}$. Samples 1, 3, and 7 (Tables 3.1 & 3.4) constrain the age of marine limit (55 to 65 m asl) between 10.5 and 10.4 ka BP. Samples 25 and 36 constrain the central and lower parts of the curve, respectively. Although the molluscs of sample 25 represent a higher, unknown RSL and thus should fall somewhere below the curve, they were used in this case because without them the curve falls significantly below the sample, and departs from the other two curves in this area (Figures 4.2 & 4.3). Thus, (after the establishment of marine limit) this curve is considered to represent a minimum slope for RSL during the past 10.5 ka. Unfortunately, samples were not found to better constrain the curve between 1 and 7.5 ka BP or between 8 and 10.2 ka BP.

Initial emergence at Eldridge Bay began ~ 10.5 ka BP and is calculated to be 3.0 m/century, whereas by the mid-Holocene emergence had slowed to 0.23 m/century (Table 4.1). The half-life of this curve is calculated to be 1.5 ka (Table 4.1). Because only one sample was collected near present sea level (< 1 m asl), it is unknown whether this coastline has experienced continuous emergence since deglaciation, or whether submergence has recently commenced as it has on S. Sabine Bay. However, if the isobases drawn from this study are correct (cf., Section 4.2.4; Figure 4.7), then this site must be undergoing submergence as well, as it is located down-isobase from S. Sabine Bay and thus should have began submergence first (assuming the migration of a crustal forebulge from west to east, parallel to the isobases). Consequently, if this coastline is undergoing submergence, this would require alteration of the curve presented here.

4.2.3.4 Synthesis

Figure 4.5 compares all three curves showing that the E. Sabine Bay curve is positioned above and to the left of both the S. Sabine Bay and Eldridge Bay curves. This indicates that E. Sabine Bay has experienced a greater amount of postglacial emergence. The younger age of marine limit at E. Sabine Bay also indicates that this site was deglaciated later than the other two sites. Given the proximity of E. Sabine Bay to higher topography, it is likely that it may also have been located closer to a local ice dispersal

centre. Its greater emergence would be consistent with greater glacial unloading compared with the other two sites. In comparison, the Eldridge Bay curve shows that it was the first site to be deglaciated, and that it has had the slowest overall emergence rate, indicating that it experienced the least amount of glacial unloading (Table 4.1). Although the evidence remains to be found, Eldridge Bay should also have undergone submergence before the other two sites.

Initial rates of postglacial emergence displayed by all three RSL curves are 2.1 m/century (S. Sabine Bay), 2.2 m/century (E. Sabine Bay), and 3.0 m/century (Eldridge Bay; Table 4.1). These rates are noticeably slower than rates reported from other localities in the Canadian High Arctic located closer to the axis of the Innuitian uplift (e.g. 5 to 7 m/century; cf., Dyke 1983; Blake 1975, 1992; Lemmen *et al.* 1994; Ó Cofaigh 1999). Initial emergence in Eldridge Bay appears more rapid than at the other two sites and this is likely an artifact of poorer stratigraphic control. Eldridge Bay has the oldest marine limit (hence earliest deglaciation) and its overall emergence through time shows the least amount of glacial unloading per unit time.

The half-lives calculated for the three RSL curves were 1.5 ka (Eldridge Bay), 1.9 ka (S. Sabine Bay), and 2.1 ka (E. Sabine Bay; Table 4.1). This suggests that curve half-lives decrease towards the ice margin, i.e., in the direction of the least amount of glacial unloading (as shown by the three curves; Figure 4.5). These half-lives are dissimilar to those reported in recent papers by Dyke (1998) and Dyke and Peltier (2000) for sites spanning the former geographic extent of the IIS. For example, they predicted half-lives of 2 ka at heavily loaded sites within the limits of the former IIS (e.g., Grinnell Peninsula, Devon Island; Dyke 1998), which decreased to 1 ka near its former ice margin. According to Dyke and Peltier (2000), curves within the study area on NE Melville Island should have half-lives of 1.25 to 1.5 ka, consequently, all three half-lives calculated here are greater than expected (with the possible exception of Eldridge Bay, the least constrained of the three curves). This discrepancy between the predicted and observed half-lives for the NE Melville Island curves may be due to inherent uncertainties of curves based predominantly on few samples and on radiocarbon-dated mollusc samples, whereas Dyke (1998) based his conclusions on a series of 14 curves constructed from multiple samples consisting mostly of driftwood on raised beaches.

At least two of these curves (S. Sabine Bay and Eldridge Bay) can likely be classified as Type B curves according to Quinlan and Beaumont (1981) or the Transition between Zones I and II of Clark *et al.* (1978). These curves display an initial period of emergence caused by isostatic rebound that is greater than eustatic sea level rise, followed by submergence as the crest of the peripheral forebulge passes through the site later in the Holocene. This type of curve is now widely recognised for areas located at, and beyond, the Late Wisconsinan ice limit (cf., Liverman 1994; Barnhardt *et al.* 1995). Thus, a record of a late Holocene lowstand (followed by recent and ongoing submergence) along S. Sabine Bay, and the likelihood of even earlier submergence in Eldridge Bay, is consistent with the eastward passage of a peripheral forebulge through the study area. Currently, the geomorphic evidence for a late Holocene transgression in the study area is subtle. The most recognisable landform is a decimetre-high microcliff found at the shoreward limit of high tide along the south coast of Sabine Bay (Figure 3.16). The microcliff has a maturely vegetated surface, which appears to be undergoing truncation by wave erosion and sea-ice push.

Figure 4.6 displays the three new RSL curves compared to Henoch's (1964) curve for eastern Melville Island, as well as McLaren and Barnett's (1978) curves for the eastern and southern coasts of Melville Island. Unfortunately, there is limited usefulness in comparing these six curves because the three previously published curves are based on data collected over much larger areas (radii of 70 - 90 km). Thus, the earlier curves inherently contain a sizeable amount of differential emergence (i.e., they unavoidably amalgamate what ought to be multiple emergence curves). Henoch's (1964) curve also puts deglaciation in Weatherall Bay at 9.1 ka BP, some 1.4 ka later (younger) than the dates now available from this study, resulting in a conspicuously steeper curve. Similarly, Hodgson *et al.* (1984) emphasised that the upper portion of McLaren and Barnett's (1978) 'Winter Harbour' curve (> 9.6 ka BP) is unreliable because they suggest that a date of 10.9 ka BP was obtained on ice-transported shells. Therefore, new curves from this study are considered to take precedence over these earlier curves because they offer better stratigraphic control and a tighter geographic base.

4.2.4 Isobases

Isobases have been drawn in order to assess differential emergence within the study area (Figure 4.7). The 8.5 ka BP shoreline was chosen in order to build upon a well-established database of postglacial shoreline displacement of the same age available from the eastern and central Arctic (Ó Cofaigh 1999; Morrison 2000; Atkinson unpublished data). Although samples dating exactly 8.5 ka BP were not collected in the study area, the RSL curves discussed above have adequate control to calculate the elevation of the 8.5 ka BP shoreline. Based on these curves, the three elevations used for the 8.5 ka BP isobases are: > 25 m asl for Eldridge Bay; 30 m asl for S. Sabine Bay; and 40 m asl for E. Sabine Bay (Figure 4.7). The elevation for the 8.5 ka BP shoreline in Sherard Bay is taken to be ~ 33 m asl and was based on a date of 8.7 ka BP (TO-9802; Table 3.5) for a 36 m asl RSL. This value was calculated by subtracting the emergence that would have occurred between 8.7 and 8.5 ka BP, based on the Eldridge Bay RSL curve (20 km away). A final control point for the 8.5 ka BP isobases was used from the West Arm of Weatherall Bay where a date of 8.3 ka BP was obtained on *H. arctica* at 54 m asl (I(GSC)-21; Henoch 1964). Consequently, the 8.5 ka BP shoreline there would be > 54 m asl. Isobases drawn on the 8.5 ka BP shoreline derived from the three RSL curves are consistent with the two external control points, suggesting that the direction and gradient of shoreline tilt is meaningful. The resulting isobases trend NNE-SSW through the study area and rise in elevation towards the ESE, in the direction of the highest marine limit reported on the island (101 m asl, south of Towson Point; Figure 4.1). The 8.5 ka BP isobases indicate that the study area was glacioisostatically-dominated by a non-local ice source to the ESE. Since the IIS was located to the NE of the study area and the M'Clintock Ice Divide of the LIS was located SSE of the study area, the tilt of these isobases likely reflects a transition zone between the glacial unloading of these two ice sheets. During the last glaciation, NE Melville Island was likely located in the peripheral depression of both of these regional ice sheets. To the north of the study area, isobases are possibly deflected in a northward direction reflecting glacioisostatic dominance by the IIS, whereas to the south (Dundas Peninsula), isobases are likely deflected to the southwest reflecting glacioisostatic dominance by the LIS.

4.3 REGIONAL IMPLICATIONS AND FUTURE RESEARCH

4.3.1 Last Glaciation

As already demonstrated, the landscape of NE Melville Island was entirely glaciated by several coalescent local ice caps during the last glaciation. This is consistent with the style of glaciation of other areas in the western Canadian Arctic. For example, western Melville Island and Prince Patrick Island were both glaciated by local ice caps during the Late Wisconsinan (Dyke & Prest 1987; Hodgson 1992; Hodgson *et al.* 1994). Furthermore, to the south of the study area, Hodgson *et al.* (1984) also proposed northward retreat of local ice into the Edmund Lyons Hills. It remains to be demonstrated whether any of this local ice coalesced with regional ice, especially whether local Melville Island ice coaslesced with the grounded margin of the Viscount Melville Sound Ice Shelf that repeatedly impinged upon the south coast of Dundas Peninsula (Hodgson *et al.* 1984; Hodgson 1992). To date, evidence is lacking for similar overriding of the NE extremity of the study area by the IIS, which this fieldwork suggests is unlikely. Therefore, the style of ice proposed for the study area necessitates a revision of the EPILOG paper (Dyke *et al.* 2002), which hypothetically extended the IIS onto eastern Melville Island while indicating local ice caps farther to the west (Figure 1.2).

4.3.2 Deglaciation

Deglaciation on NE Melville Island occurred as local ice retreated into the interior at right angles from the coast, occupying several residual dispersal centres. This pattern of retreat is consistent with that reported from western Melville Island (Hodgson 1992) and southern Melville Island (Edmund Lyons Hills; Hodgson *et al.* 1984). Marine limits surveyed within the study area rise to the NE across the island (cf., Section 1.5.2.2). However, the number of sites has substantially increased and many new radiocarbon dates refine the chronology of ice retreat. Still farther east, marine limit continues to increase eastward to 150 m asl on Bathurst Island, and farther north, to 91 m asl on Lougheed Island (Hodgson 1989). Collectively, this regional pattern indicates greater unloading by ice in the direction of the 'lowland sector' of the IIS (Dyke *et al.* 2002).

Deglaciation on NE Melville Island was underway between 10.5 and 10.0 ka BP. In Eldridge Bay, six samples of *H. arctica* dating deglaciation range in age from 10.5 to 10.3 ka BP and were collected at elevations between 6 and 52 m asl (Figure 3.14 & Table 3.1). This abundance of molluscs dating from deglaciation suggests that during deglaciation, conditions were conducive to mollusc growth, whereas the paucity of mollusc samples of younger ages in this bay indicates that favourable growth conditions diminished soon afterwards and have persisted throughout most of the Holocene (cf., Hodgson *et al.* 1984, 1994). If so, it seems possible that the increased meltwater flux that characterised the deglacial environment likely led to more productive and seasonally open water compared to present, as recognised for bowhead whale populations and other marine fauna along the retreating LIS farther south (Dyke *et al.* 1996, 1997). However, increased meltwater is accompanied by an increase in sedimentation rates, which is usually a factor in reducing mollusc productivity (cf., Gulliksen *et al.* 1985). Possible explanations include the fact that increased sedimentation might have provided increased nutrients (cf., Hodgson 1992) and likely enhanced the preservation potential of these molluscs (cf., Dyke *et al.* 1996).

Deglacial dates on NE Melville Island of 10.5 to 10.0 ka BP are consistent with the pattern of deglaciation across the archipelago as originally proposed by Blake (1972). By ~ 11 ka BP, molluscs had first reached the SW coast of Prince Patrick Island recording the earliest retreat from the Archipelago (Blake 1972; Dyke *et al.* 1996). By 10.5 ka BP, water had penetrated from SE Prince Patrick Island to the west coast of Melville Island and into Hecla and Griper Bay (Blake 1972; Hodgson *et al.* 1984, 1994; Dyke *et al.* 1996). By 10 ka BP, deglaciation was underway on the eastern coast of Melville Island and on Lougheed Island (Lowdon & Blake 1987). Subsequently, Hassel Sound (separating Amund and Ellef Ringnes islands; Figure 1.1a) became ice-free between 9.7 and 9.2 ka BP (Atkinson 2003) and by 9.0 ka BP, most major waterways in the archipelago were open (Blake 1972; Dyke *et al.* 1996). The last major marine channel to become ice-free was Nares Strait (between Ellesmere Island and Greenland; England 1999; England & Atkinson 2003). This regional pattern of deglaciation indicates rapid and progressive retreat across the western archipelago from west to east. There, favoured by low topography and expansive marine channels, eustatic sea level rise

from the melting of the LIS prior to 9.2 ka BP would have progressively undermined the lowland sector of the IIS (cf., Tushingham & Peltier 1991; England 1992, 1999; Lemmen *et* al. 1994; Dyke 1998, 1999; Ó Cofaigh 1998; Ó Cofaigh *et al.* 1999). Once the IIS retreated eastward to its alpine sector, retreat would have slowed due to elevated topography and narrow waterways (Dyke 1998; Ó Cofaigh 1998; England 1999).

4.3.3 Postglacial Emergence and Submergence

This thesis presented 38 new radiocarbon dates for NE Melville Island, from which three new RSL curves were constructed. The amount of emergence recorded on NE Melville Island since deglaciation ranges between 42 and 65 m asl. Taking into account an estimated 55 m of eustatic sea level rise since 11 ka BP (Fairbanks 1989; Tushingham & Peltier 1991), this data indicates that between 97 and 120 m of isostatic uplift might have occurred on NE Melville Island since deglaciation. Within the study area, and on Melville Island as a whole, a rise of paleoshorelines to the ESE demonstrates that NE Melville Island is likely located in a transition zone between the glacioisostatic dominance of the IIS to the NE and the LIS to the SSE.

Submergence of the western part of the study area indicates the eastward migration of the peripheral forebulge through the study area, at least to S. Sabine Bay. This is the first report of submergence anywhere on Melville Island, despite the fact that repeated surveys of the Quaternary geology have been made on Dundas Peninsula and western Melville Island (Tozer & Thorsteinsson 1964; Hodgson *et al.* 1984; Hodgson 1992), as well as on eastern Melville Island (Henoch 1964; Tozer & Thorsteinsson 1964; McLaren & Barnett 1978). In fact, McLaren and Barnett (1978) concluded that ongoing emergence was still occurring on the east coast of Melville Island at rate of ~ 0.35 cm/a. This is a conspicuously rapid rate, and equivalent to mid-Holocene emergence rates reported from the curves presented in this study (Table 4.1). Evidence for submergence elsewhere on Melville Island has been derived from archeological research that complements the results of this study. For example, west of the study area (McCormick Inlet; Figure 1.1b) a date of 1.7 ka BP (I-840; Henoch 1964) was obtained on peat under a Dorset dwelling at 1.8 m asl. This indicates that less than 1.8 m of emergence has occurred in the past 1.7 ka (a rate that does not accord with the rapid ongoing emergence

proposed for eastern Melville Island, McLaren & Barnett 1978). Indeed, this evidence suggests that McCormick Inlet likely began to submergence sometime after 1.7 ka BP. Furthermore, to the south of the study area (north of Winter Harbour; Figure 1.1b), a date of 0.6 ka BP (I-842; Henoch 1964) on driftwood at 1.6 m asl represents a maximum sea level for that time and suggests either near equilibrium conditions or possible submergence of the south coast. Approximately 300 km to the west of NE Melville Island, Hodgson *et al.* (1994) reported submergence on the western coast of Prince Patrick Island, but suggested that emergence continued on the island's eastern coast. The evidence presented here for submergence along S. Sabine Bay, and more broadly in Hecla and Griper Bay to the north (below), would require that all of Prince Patrick Island is currently submerging.

The most conservative approach to separating areas of net submergence from areas of net emergence in the western archipelago is to draw the modern position of the zero isobase. This currently trends NNE-SSW through the study area, east of S. Sabine Bay (this study). Hence, the zero isobase needs to be repositioned well east of where it has previously been designated (cf., Section 1.5.2.2; Walcott 1972; Andrews 1989; Hodgson *et al.* 1994). Recent reports for submergence on the SE coast of Melville Island now include: drowned gullies, tundra vegetation and oil exploration tracks from the 1970s, as well as inland migration of beaches. All of these features suggest that the forebulge has migrated east of the study area, and is now located off the east coast of Melville Island (Lajeunesse *et al.* 2003).

4.3.4 Conclusions and Future Research

The most significant results of this thesis include: (1) the clarification of the style of the last glaciation on NE Melville Island, demonstrating the passage of local ice during the Late Wisconsinan; (2) an improved deglacial chronology for this area based on numerous radiocarbon-dated marine limits, coincident with the radial retreat of local ice; and (3) the establishment of three well-controlled RSL curves which were used to determine the half-lives for glacioisostatic recovery and to show the displacement of the 8.5 ka shoreline which rises across the study area to the ESE. An important aspect of the RSL curves, both from a theoretical and applied standpoint, is the recognition that

submergence within the study area is both recent and ongoing. This apparently represents the eastward migration of a peripheral forebulge. Further clarification of the history, magnitude and migration of this submergence will contribute detailed geological evidence on the collapse of peripheral forebulges that characterise the entire perimeter of North American and European ice sheets and which warrant improved geophysical modeling. Such evidence would also clarify the impact of recent submergence on coastal processes in the western Arctic archipelago, and would be relevant to planning and management of increased human activity in this region. Currently, the depth and timing of the lowstand along S. Sabine Bay and elsewhere (e.g., Eldridge Bay) needs to be more tightly constrained, and one possible avenue to explore would be to core coastal estuaries that may contain drowned lacustrine sediments suitable for radiocarbon dating. In terms of the late Quaternary history, the origin and age of the mega-flutings on northern Sabine Peninsula should also be clarified. These landforms may record the passage of a former Laurentide ice shelf that currently is only identified in M'Clure Strait, along Melville Island's south coast (J. England, pers. com. 2002). The thorough documentation of former Laurentide ice shelves is central to the understanding of the NW part of this ice sheet, and warrants further research. Finally, it also remains to be determined whether local Melville Island ice interacted with either of the regional ice sheets.

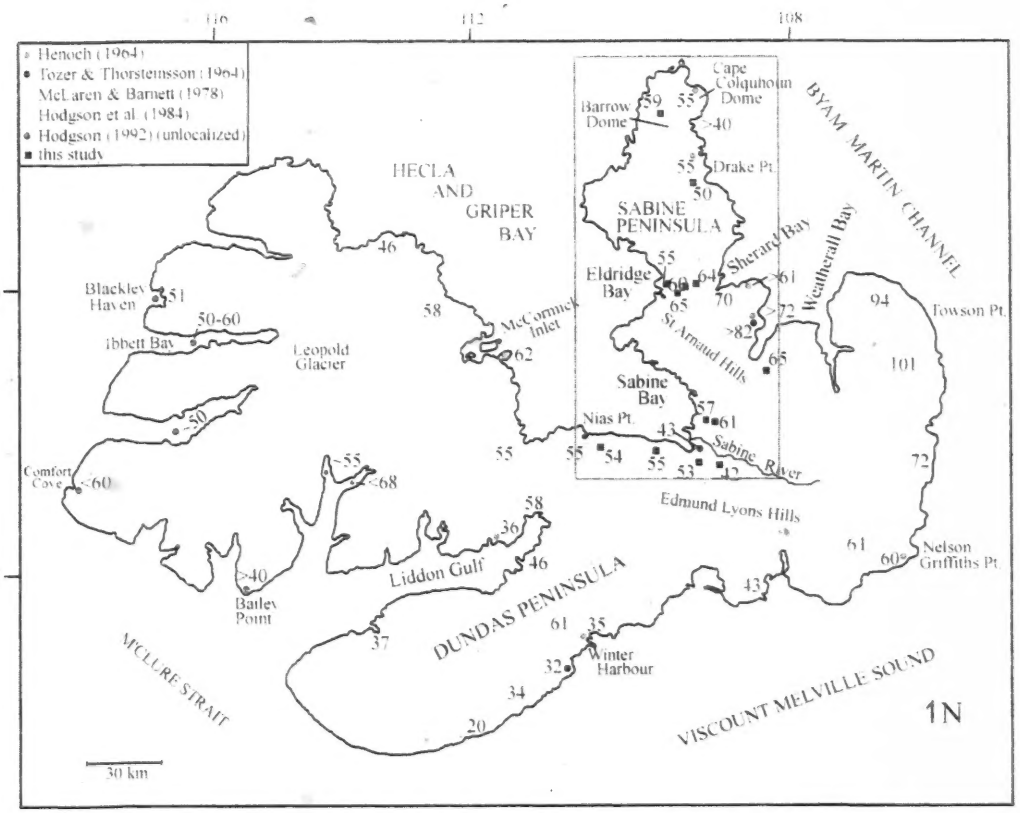

Figure 4.1. Previously surveyed marine limits and marine limits surveyed in this study on Melville Island (elevation in metres above sea level). Marine limit elevations rise across Melville Island from southwest to northeast. Within the study area, marine limits rise towards the peninsula between Sherard and Weatherall bays.

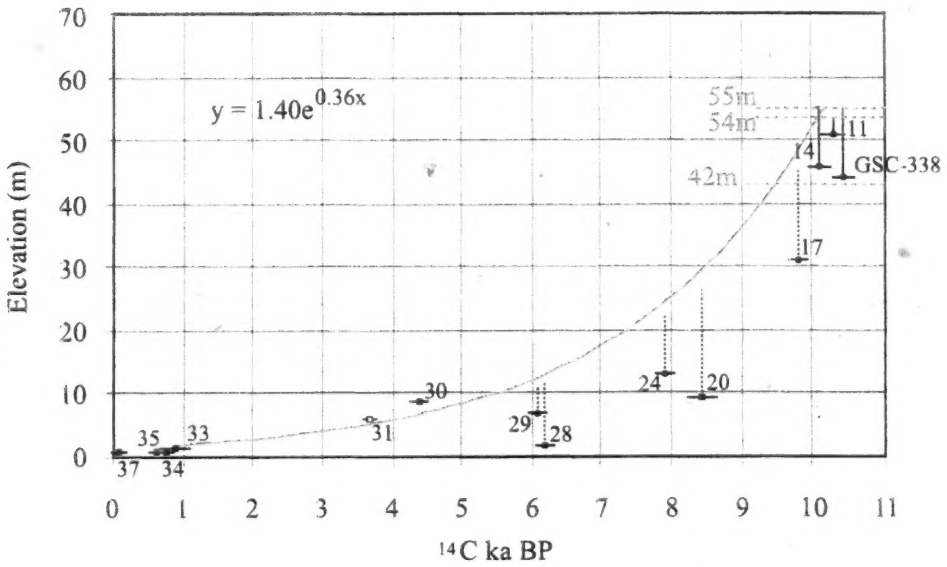

Figure 4.2. Relative sea level curve for S. Sabine Bay. Samples are plotted with two standard errors.

•	mollusc sample
▪	driftwood sample
▫	organic sample
65m	marine limit elevation
—	associated relative sea level
.....	unknown relative sea level

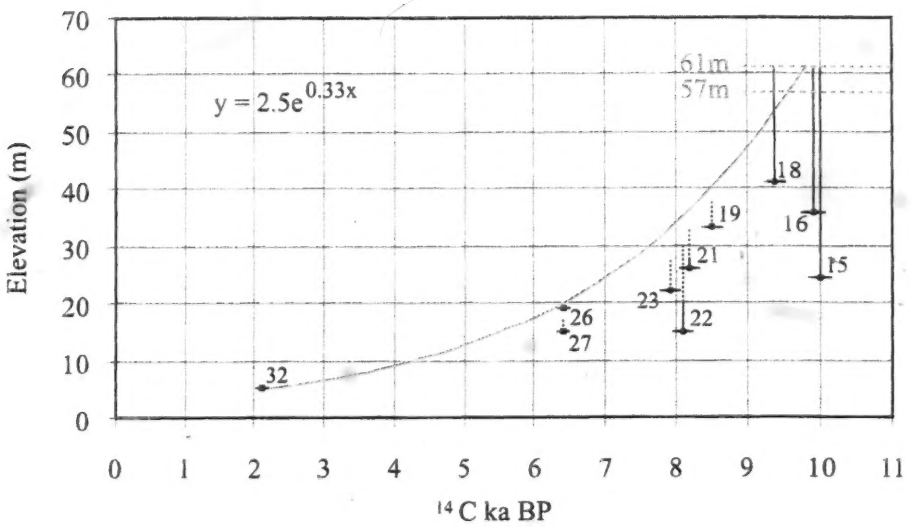

Figure 4.3. Relative sea level curve for E. Sabine Bay. Samples are plotted with two standerd errors.

•	mollusc sample
▪	driftwood sample
65m	marine limit elevation
—	associated relative sea level
.....	unknown relative sea level

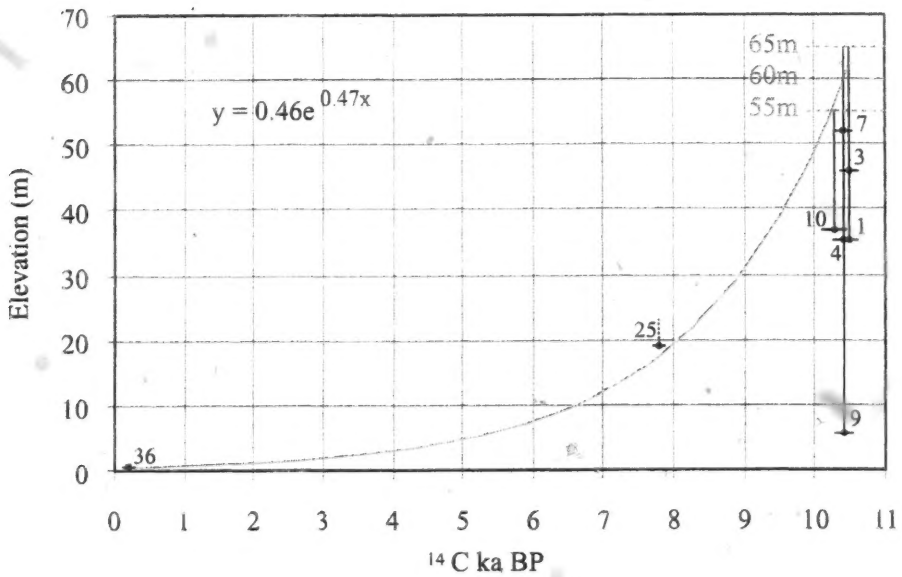

Figure 4.4. Relative sea level curve for Eldridge Bay. Samples are plotted with two standard errors.

•	mollusc sample
▪	driftwood sample
65m	marine limit elevation
—	associated relative sea level
.....	unknown relative sea level

Table 4.1. Equations, emergence rates, and half-lives of RSL curves.

Site	RSL curve	No. of samples	R^2	Derivative	Initial emergence rate (m/century)	Mid-Holocene emergence rate (m/century)	Half-life
S. Sabine Bay	$y = 1.40e^{0.36x}$	6	0.986	$y' = 0.36(1.40e^{0.36x})$	2.1 @ 10.4 ka BP	0.30 @ 5 ka BP	1.9 ka
E. Sabine Bay	$y = 2.50e^{0.33x}$	5	0.995	$y' = 0.33(2.50e^{0.33x})$	2.2 @ 10.0 ka BP	0.43 @ 5 ka BP	2.1 ka
Eldridge Bay	$y = 0.46e^{0.47x}$	6	0.999	$y' = 0.47(0.46e^{0.47x})$	3.0 @ 10.5 ka BP	0.23 @ 5 ka BP	1.5 ka

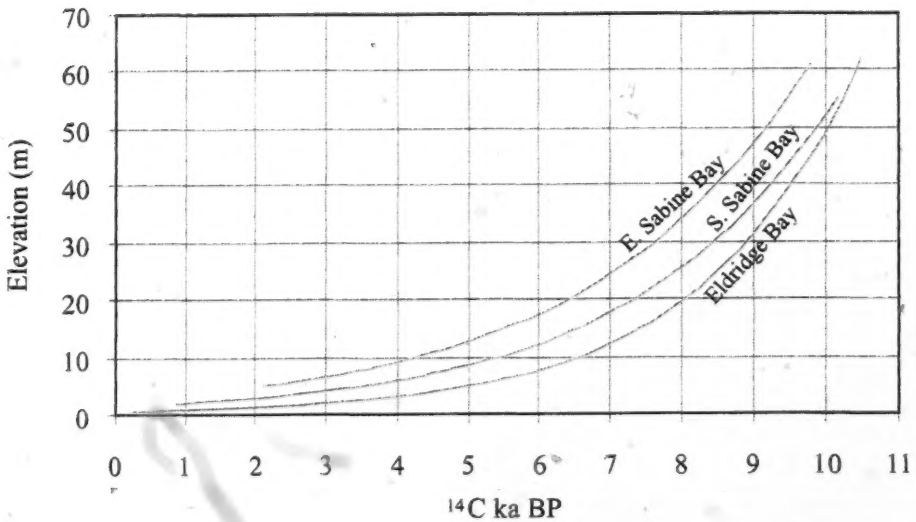

Figure 4.5. Three relative sea level curves for NE Melville Island.

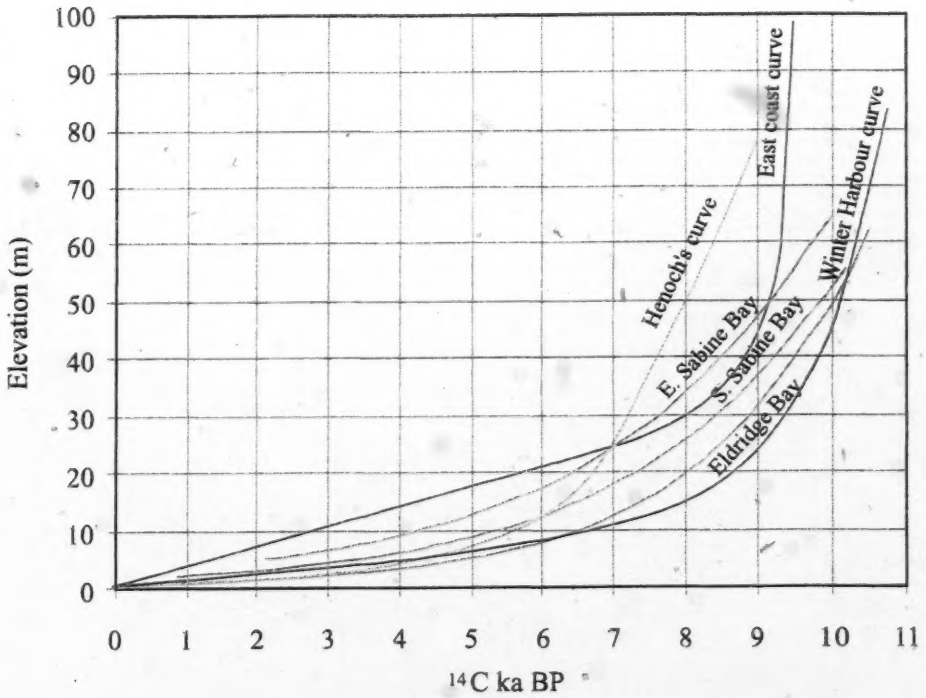

Figure 4.6. The three relative sea level curves for NE Melville Island, along with Henoch's (1964) curve, and McLaren & Barnett's (1978) curves for Winter Harbour and the east coast of Melville Island.

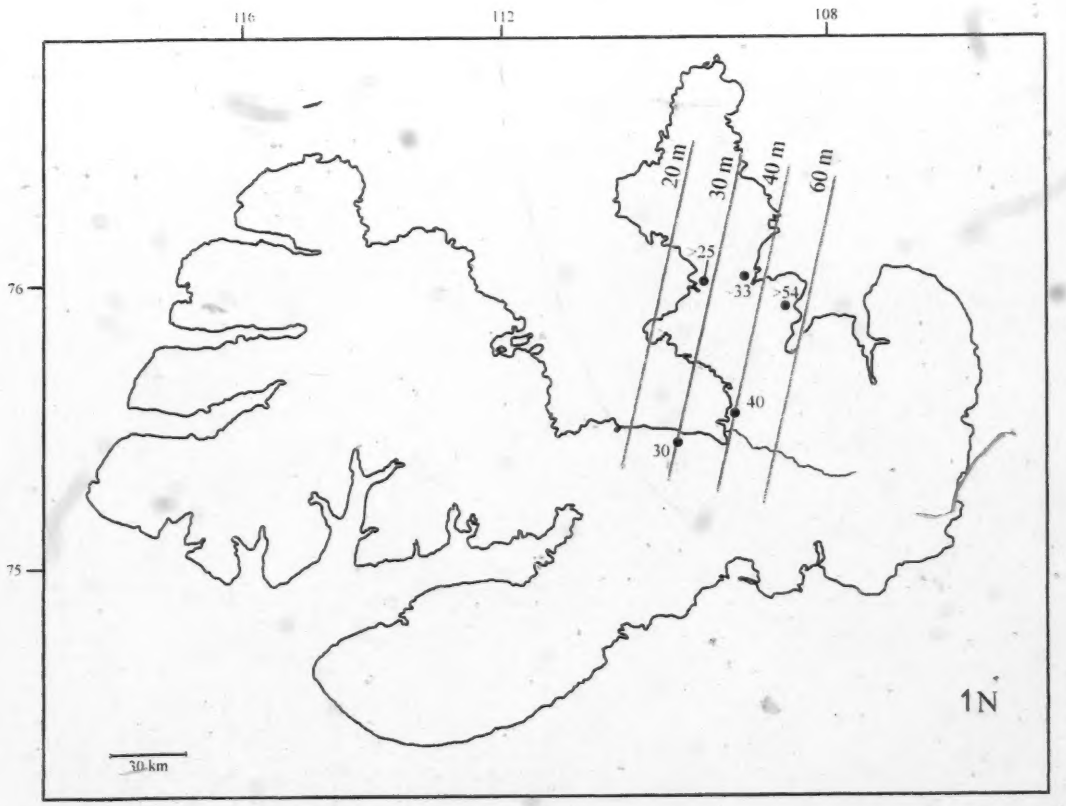

Figure 4.7. Isobases drawn on the 8.5 ka shorelines for the study area using control points referred to in text. Note that E. Sabine Bay (40 m asl) is the site furthest up-isobase, and Eldridge Bay (> 25 m) is the site furthest down-isobase (cf. Figure 4.5).

REFERENCES

Andrews, J.T. 1969. The pattern and interpretation of restrained, post-glacial and residual rebound in the area of Hudson Bay. *In* Earth Science Symposium on Hudson Bay, P.J. Hood (ed.). Geological Survey of Canada, Paper 68-53, 49-62.

Andrews, J.T. 1970. A geomorphological study of post-glacial uplift with particular reference to Arctic Canada. Institute of British Geographers, Special Publication Number 2, London, 67-96.

Andrews, J.T. 1986. Elevation and age relationships: raised marine deposits and landforms in glaciated areas: examples based on Canadian Arctic data. *In* Sea-level Research: a manual for the collection and evaluation of data, O. van de Plassch (ed.), Amsterdam, 618p.

Andrews, J.T. 1989. Postglacial emergence and submergence. *In* Chapter 8, Quaternary Geology of Canada and Greenland, R.J. Fulton (ed.). Geological Survey of Canada, Geology of Canada, no. 1.

Atkinson, N. 2003. Late Wisconsinan glaciation of Amund and Ellef Ringnes islands, Nunavut: evidence for the configuration, dynamics, and deglacial chronology of the northwest sector of the Innuitian Ice Sheet. Canadian Journal of Earth Sciences **40**, 351-363.

Barnett, D.M. 1972. Surficial geology and geomorphology of Melville Island, District of Franklin. Geological Survey of Canada, Paper 72-1, Part A, 152-153.

Barnett, D.M., Edlund, S.A., and Dredge, L.A. 1977. Terrain Characterization and Evaluation: An Example from Eastern Melville Island. Geological Survey of Canada, Paper 76-23.

Barnhardt, W.A., Gehrels, W.R., Belknap, D.F., and Kelley, J.T. 1995. Late Quaternary relative sea-level change in the western Gulf of Maine: evidence for a migrating glacial forebulge. Geology **23**, 217-230.

Basham, P.W., Forsyth, D.A., and Wetmiller, R.J. 1977. The seismicity of northern Canada. Canadian Journal of Earth Sciences **14**, 1646-1667.

Bednarski, J. 1998. Quaternary history of Axel Heiberg Island bordering Nansen Sound, Northwest Territories, emphasising the Last Glacial Maximum. Canadian Journal of Earth Sciences **35**, 520-533.

Belknap, D.F., Shipp, R.C., and Kelley, J.T. 1986. Depositional setting and Quaternary stratigraphy of the Sheepscot Estuary, Maine: a preliminary report. Géographie physique et Quaternaire **40**, 55-69.

Bell, T. 1992. Glacial and sea level history of western Fosheim Peninsula, Ellesmere Island, Arctic Canada. PhD thesis, University of Alberta, Edmonton, Alberta.

Bishof, J.F., and Darby, D.A. 1999. Quaternary ice transport in the Canadian Arctic and extent of Late Wisconsinan glaciation in the Queen Elizabeth Islands. Canadian Journal of Earth Sciences **36**, 2007-2022.

Blake, W. Jr. 1970. Studies of glacial history in Arctic Canada. I. Pumice, radiocarbon dates, and differential postglacial uplift in the eastern Queen Elizabeth Islands. Canadian Journal of Earth Sciences **7**, 634-664.

Blake, W. Jr. 1972. Climatic implications of radiocarbon-dated driftwood in the Queen Elizabeth Islands, arctic Canada. *In* Climatic Changes in Arctic Areas During the Past Ten-Thousand Years, Y. Vasari, H. Hyvarinen, and S. Hicks (eds.). Acta Universitatis Ouluensis, 77-104.

Blake, W. Jr. 1975. Radiocarbon age determination and postglacial emergence at Cape Storm, southern Ellesmere Island. Geografiska Annaler **57A**, 1-71.

Blake, W. Jr. 1992. Holocene emergence at Cape Herschel, east-central Ellesmere Island, Arctic Canada: implications for ice sheet configuration. Canadian Journal of Earth Sciences **29**, 1958-1980.

Bradley, R.S. 1999. Paleoclimatology: Reconstructing Climates of the Quaternary. Harcourt Academic Press, San Diego, 613p.

Bryson, R.A., and Hare, F.K. 1974. Climates of North America. Elsevier Scientific Publishing Company, New York.

Clark, J.A., Farrell, W.E., and Peltier, W.R. 1978. Global changes in postglacial sea level: a numerical calculation. Quaternary Research **9**, 265-287.

Craig, B.G., and Fyles, J.G. 1960. Pleistocene geology of Arctic Canada. Geological Survey of Canada, Paper 60-10.

Dawes, P.R., and Christie, R.L. 1991. Geomorphic Regions. *In* Chapter 3, Geology of the Innuitian Orogen and Arctic Platform of Canada and Greenland, H.P. Trettin (ed.). Geological Survey of Canada, Geology of Canada, no. 3.

Dyke, A.S. 1983. Quaternary Geology of Somerset Island, District of Franklin. Geological Survey of Canada, Memoir 404.

Dyke, A.S. 1987. A reinterpretation of glacial and marine limits around the northwestern Laurentide Ice Sheet. Canadian Journal of Earth Sciences **24**, 591-601.

Dyke, A.S. 1993. Landscapes of cold-centred Late Wisconsinan ice caps, Arctic Canada. Progress in Physical Geography **17**, 223-247.

Dyke, A.S. 1998. Holocene delevelling of Devon Island, Arctic Canada: implications for ice sheet geometry and crustal response. Canadian Journal of Earth Sciences **35**, 885-904.

Dyke, A.S. 1999. The last glacial maximum and the deglaciation of Devon Island: support for an Innuitian Ice Sheet. Quaternary Science Reviews, **18**, 393-420.

Dyke, A.S., and Prest, V.K. 1987. Late Wisconsinan and Holocene history of the Laurentide Ice Sheet. Géographie physique et Quaternaire **41**, 237-263.

Dyke, A.S., Morris, T.F., and Green, D.E.C. 1991. Postglacial Tectonic and Sea Level History of the Central Canadian Arctic. Geological Survey of Canada, Bulletin 397.

Dyke, A.S., Morris, T.F., Green, D.E.C., and England, J. 1992. Quaternary geology of Prince of Wales Island, Arctic Canada. Geological Survey of Canada, Memoir 433.

Dyke, A.S., Dale, J.E., and McNeely, R.N. 1996. Marine molluscs as indicators of environmental change in glaciated North America and Greenland during the last 18 000 years. Géographie physique et Quaternaire **50**, 125-184.

Dyke, A.S., England, J., Reimnitz, E., and Jetté, H. 1997. Changes in driftwood delivery to the Canadian Arctic Archipelago: the hypothesis of postglacial oscillations of the Transpolar Drift. Arctic **50**, 1-16.

Dyke, A.S., and Peltier, W.R. 2000. Forms, response times, and variability of relative sea-level curves, glaciated North America. Geomorphology **32**, 315-333.

Dyke, A.S., Andrews, J.T., Clark, P.U., England, J.H., Miller, G.H., Shaw, J., and Veillette, J.J. 2002. The Laurentide and Innuitian ice sheets during the Last Glacial Maximum. Quaternary Science Reviews **21**, 9-31.

Edlund, S.A. 1985. Lichen-free zones as neoglacial indicators on western Melville Island, District of Franklin. Geological Survey of Canada, Paper 85-1A, 709-712.

Edlund, S.A. 1993. The distribution of plant communities on Melville Island, Arctic Canada. *In* The Geology of Melville Island, Arctic Canada, R.L. Christie and N.J. McMillan (eds.). Geological Survey of Canada, Bulletin 450, 247-255.

Edlund, S.A., and Alt, B.T. 1989. Regional congruence of vegetation and summer climate patterns in the Queen Elizabeth Islands, Northwest Territories, Canada. Arctic **42**, 3-23.

England, J. 1987. Glaciation and the evolution of the Canadian high arctic landscape. Geology **15**, 419-424.

England, J. 1992. Postglacial emergence in the Canadian High Arctic: integrating glacioisostasy, eustasy, and late deglaciation. Canadian Journal of Earth Sciences **29**, 984-999.

England, J. 1998. Support for the Innuitian Ice Sheet in the Canadian High Arctic during the Last Glacial Maximum. Journal of Quaternary Science **13**, 275-280.

England, J. 1999. Coalescent Greenland and Innuitian ice during the Last Glacial Maximum: revising the Quaternary of the Canadian High Arctic. Quaternary Science Reviews **18**, 421-456.

England, J., and Ó Cofaigh, C. 1998. Deglacial sea level history along Eureka Sound: the effects of ice retreat from a central basin to alpine margins [abstract]. Geological Association of Canada, Québec City, A-52.

England, J., Smith, I.R., and Evans, D.J.A. 2000. The last glaciation of east-central Ellesmere Island, Nunavut: ice dynamics, deglacial chronology, and sea level change. Canadian Journal of Earth Sciences **37**, 1355-1371.

England, J., and Atkinson, N. 2003. Recent developments on the configuration, surface topography, and dynamics of the Late Wisconsinan, Innuitian Ice Sheet [abstract]. 33rd Annual Arctic Workshop, Norway, 37.

Evans, D.J.A. 1990. The effect of glacier morphology on surficial geology and glacial stratigraphy in a high arctic mountainous terrain. Zeitschrift für Geomorphologie **34**, 481-503.

Fairbanks, R.G. 1989. A 17,000 year glacio-eustatic sea level record: influence of glacial melting rate on the Younger Dryas event and deep ocean circulation. Nature **342**, 637-642.

Forbes, D.L., and Taylor, R.B. 1994. Ice in the shore zone and the geomorphology of cold coasts. Progress in Physical Geography **18**, 59-89.

Forbes, D.L., and Taylor, R.B. 1998. Progradation and architecture of Holocene finger deltas under forced regression in a High-Arctic setting [abstract]. Geological Association of Canada, Québec City, A-56.

Forman, S.L., Weihe, R., Lubinski, D., Tarasov, G., Korsun, S., and Matishov, G. 1997. Holocene relative sea-level history of Franz Josef Land, Russia. USA Bulletin 109, 1116-1133.

Fyles, J.G. 1965. Surficial geology, western Queen Elizabeth Islands. Geological Survey of Canada, Paper 65-1, 3-5.

Fyles, J.G. 1967. Winter Harbour Moraine, Melville Island. Geological Survey of Canada, Paper 67-1, Part A, 8-9.

Fyles, J.G. 1990. Beaufort Formation (Late Tertiary) as seen from Prince Patrick Island, Arctic Canada. Arctic **43**, 393-403.

Gulliksen, B., Holte, B., and Jakola, K.-J. 1985. The soft bottom fauna in Van Mijenfjord and Raudfjord, Svalbard. *In* Marine Biology of Polar Regions and Effects of Stress on Marine Organisms, J.S. Gray, and M.E. Christiansen (eds.). John Wiley, 199-211.

Harrison, J.C. 1993. A summary of the structural geology of Melville Island, Canadian Arctic Archipelago. *In* The Geology of Melville Island, Arctic Canada, R.L. Christie and N.J. McMillan (eds.). Geological Survey of Canada, Bulletin 450, 257-283.

Harrison, J.C. 1994. Melville Island and Adjacent Smaller Islands, Canadian Arctic Archipelago, District of Franklin, Northwest Territories. Geological Survey of Canada, Map 1844A, scale 1:250,000.

Harrison, J.C. 1995. Melville Island's Salt-Based Fold Belt, Arctic Canada. Geological Survey of Canada, Bulletin 472.

Hasegawa, H.S. 1977. Focal parameters of four Sverdrup Basin, Arctic Canada, earthquakes in November and December of 1972. Canadian Journal of Earth Sciences **14**, 2481-2494.

Henoch, W.E.S. 1964. Postglacial marine submergence and emergence of Melville Island, N.W.T. Geographical Bulletin **22**, 105-126.

Hill, P.R., Mudie, P.J., Moran, K., and Blasco, S.M. 1985. A sea-level curve for the Canadian Beaufort shelf. Canadian Journal of Earth Sciences **22**, 1383-1393.

Hill, P.R., Héquette, A., and Ruz, M.H. 1993. Holocene sea-level history of the Canadian Beaufort shelf. Canadian Journal of Earth Sciences **30**, 103-108.

Hillaire-Marcel, C. 1980. Les faunes des mers post-glaciaires du Québec: quelques considérations paléoécologiques. Géographie physique et Quaternaire **34**, 3-59.

Hodgson, D.A. 1981. Surficial geology, Lougheed Island, northwest Arctic Archipelago. Geological Survey of Canada, Paper 81-1C, 27-34.

Hodgson, D.A. 1982. Surficial Materials and Geomorphological Processes, Western Sverdrup and Adjacent Islands, District of Franklin. Geological Survey of Canada, Paper 81-9.

Hodgson, D.A. 1985. The last glaciation of west-central Ellesmere Island, Arctic Archipelago, Canada. Canadian Journal of Earth Sciences **22**, 347-368.

Hodgson, D.A. 1989. Quaternary stratigraphy and chronology (QEI). *In* Chapter 6, Quaternary Geology of Canada and Greenland, R.J. Fulton (ed.). Geological Survey of Canada, No. 1, 452-459.

Hodgson, D.A. 1990. Were erratics moved by glaciers or icebergs to Prince Patrick Island, western Arctic Archipelago, Northwest Territories. Geological Survey of Canada, Paper 90-1D, 67-70.

Hodgson, D.A. 1992. Quaternary Geology of Western Melville Island, Northwest Territories. Geological Survey of Canada, Paper 89-21.

Hodgson, D.A., and Vincent, J.-S. 1984. A 10,000 yr BP extensive ice shelf over Viscount Melville Sound, Arctic Canada. Quaternary Research **22**, 18-30.

Hodgson, D.A., Vincent, J.-S., and Fyles, J.G. 1984. Quaternary Geology of Central Melville Island, Northwest Territories. Geological Survey of Canada, Paper 83-16.

Hodgson, D.A., Taylor, R.B., and Fyles, J.G. 1994. Late Quaternary sea level changes on Brock and Prince Patrick islands, western Canadian Arctic Archipelago. Géographie physique et Quaternaire **48**, 69-84.

Kerr, J.Wm. 1981. Evolution of the Canadian Arctic Islands: A Transition between the Atlantic and Arctic Oceans. *In* The Ocean Basin Margin, Volume 5, The Arctic Ocean, A.E.M. Nairn, M.Jr. Churkin, and F.G. Stehli (eds.). Plenum Press, New York, 105-199.

Lajeunesse, P., England, J., and Hanson, M. 2003 (in prep). Modern relative sea level rise on eastern Melville Island, Canadian Arctic Archipelago: evidence, products, and implications.

Lamoureux, S.F., and England, J.H. 2000. Late Wisconsinan Glaciation of the central sector of the Canadian High Arctic. Quaternary Research **54**, 182-188.

Lemmen, D.S., Aitken, A.E., and Gilbert, R. 1994. Early Holocene deglaciation of Expedition and Strand fiords, Canadian High Arctic. Canadian Journal of Earth Sciences **31**, 943-958.

Liverman, D.G.E. 1994. Relative sea-level history and isostatic rebound in Newfoundland, Canada. Boreas **23**, 217-230.

Lowdon, J.A., and Blake, W. Jr. 1987. Geological Survey of Canada Radiocarbon Dates VI. Geological Survey of Canada, Paper 87-2B.

MacLean, B., Sonnichsen, G., Vilks, G., Powell, C., Moran, K., Jennings, A., Hodgson, D., and Deonarine, B. 1989. Marine Geological and Geotechnical Investigations in Wellington, Byam Martin, Austin, and Adjacent Channels, Canadian Arctic Archipelago. Geological Survey of Canada, Paper 89-11.

Marshall, S.J., and Clarke, G.K.C. 1999. Ice sheet inception: subgrid hypsometric parameterization of mass balance in an ice sheet model. Climate Dynamics **15**, 533-550.

Maxwell, J.B., 1981. Climatic regions of the Canadian Arctic Islands. Arctic **34**, 225-240.

Mayewski, P.A., Denton, G.H., and Hughes, T.J. 1981. Late Wisconsin Ice Sheets in North America. *In* The Last Great Ice Sheets, Denton, G.H., and Hughes, T.J. (eds.) John Wiley & Sons, New York, 67-178.

McLaren, P., and Barnett, D.M. 1978. Holocene emergence of the south and east coasts of Melville Island, Queen Elizabeth Islands, Northwest Territories, Canada. Arctic **31**, 415-427.

Mörner, N.-A. 1976. Eustasy and geoid changes. Journal of Geology **84**, 123-151.

Morrison, C.A. 2000. Late Quaternary Glacial and Sea Level History of west-central Axel Heiberg Island, High Arctic Canada. MSc thesis, University of Alberta, Edmonton, Alberta.

Ó Cofaigh, C. 1998. Geomorphic and sedimentary signatures of early Holocene deglaciation in High Arctic fiords, Ellesmere Island, Canada: implications for deglacial ice dynamics and thermal regime. Canadian Journal of Earth Sciences **35**, 437-452.

Ó Cofaigh, C. 1999. Holocene emergence and shoreline delevelling, southern Eureka Sound, High Arctic Canada. Géographie physique et Quaternaire **53**, 235-247.

Ó Cofaigh, C., Lemmen, D.S., Evans, D.J.A., and Bednarski, J. 1999. Glacial landform-sediment assemblages in the Canadian High Arctic and their implications for late Quaternary glaciation. Annals of Glaciology **28**, 195-201.

Ó Cofaigh, C., England, J., and Zreda, M. 2000. Late Wisconsinan glaciation of southern Eureka Sound: evidence for extensive Innuitian ice in the Canadian High Arctic during the Last Glacial Maximum. Quaternary Science Reviews **19**, 1319-1341.

Okulitch, A.V. (compiler). 1991. Geology of the Canadian Archipelago and North Greenland; Figure 2. *In* Innuitian Orogen and Arctic Platform: Canada and Greenland, H.P. Trettin (ed.). Geological Survey of Canada, Geology of Canada, No. 3, scale 1:2,000,000.

Peltier, W.R. 1994. Ice Age paleotopography. Science **265**, 195-201.

Perry, R.K., Fleming, H.S., Weber, J.R., Kristofferson, Y., Hall, J.K., Grantz, A., Johnson, G.L., and Cherkis, N.Z. 1987. Bathymetry of the Arctic Ocean; Geological Society of America, scale 1:6,000,000.

Powell, R.D. 1984. Glaciomarine processes and inductive lithofacies modeling of ice shelf and tidewater glacier sediments based on Quaternary examples. Marine Geology **57**, 1-52.

Quinlan, G., and Beaumont, C. 1981. A comparison of observed and theoretical postglacial relative sea level in Atlantic Canada. Canadian Journal of Earth Sciences **18**, 1146-1163.

Reeh, N. 1984. Reconstruction of the glacial ice covers of Greenland and the Canadian Arctic islands by three-dimensional, perfectly plastic ice-sheet modeling. Annals of Glaciology **5**, 115-121.

Sim, V.W. 1960. Maximum post-glacial marine submergence in northern Melville Peninsula. Arctic **13**, 178-193.

Tozer, E.T., and Thorsteinsson, R. 1964. Western Queen Elizabeth Islands, Arctic Archipelago. Geological Survey of Canada, Memoir 332.

Trettin, H.P. 1991. Tectonic Framework. *In* Chapter 4, Geology of the Innuitian Orogen and Arctic Platform of Canada and Greenland, H.P. Trettin (ed.). Geological Survey of Canada, Geology of Canada, No. 3, 59-66.

Tushingham, A.M. 1991. On the extent and thickness of the Innuitian Ice Sheet: a postglacial-adjustment approach. Canadian Journal of Earth Sciences **28**, 231-239.

Tushingham, A.M., and Peltier, W.R. 1991. Ice-3G: A new global model of Late Pleistocene deglaciation based upon geophysical predictions of post-glacial relative sea level change. Journal of Geophysical Research **96**, 4497-4523.

Vincent, J.-S. 1983. La géologie du Quaternaire et la géomorphologie de l'Île Banks, Arctique Canadien. Geological Survey of Canada, Memoir 405.

Vincent, J-S. 1984. Quaternary stratigraphy of the western Canadian Arctic Archipelago. *In* Quaternary Stratigraphy of Canada – A Canadian Contribution to IGCP Project 24, R.J. Fulton (ed.). Geological Survey of Canada, Paper 84-10, 87-100.

Wadhams, P., Squire, V.A., Ewing, J.A., and Pascal, R.W. 1986. The effect of the marginal ice zone on the directional wave spectrum of the ocean. Journal of Physical Oceanography **16**, 358-376.

Wadhams, P., Squire, V.A., Goodman, D.J., Cowan, A.M., and Moore, S.C. 1988. The attenuation rates of ocean waves in the marginal ice zone. Journal of Geophysical Research **93**, 6799-6818.

Walcott, R.I. 1972. Late Quaternary vertical movements in eastern North America: quantitative evidence of glacio-isostatic rebound. Reviews of Geophysics and Space Reviews **10**, 849-884.